Diplomarbeit

Raman Spectra Fiber Optic Distributed Temperature Sensing in Avalanche Research

Ausgeführt zur Erlangung des akademischen Grades Dipl. –Ing. für Kulturtechnik und Wasserwirtschaft an der Universität für Bodenkultur

Unter der Leitung von

Prof. Dipl. –Ing. Dr. Johannes Hübl

Mitbetreuer

Dipl. –Ing. Dr. Alexander Prokop

Ausgeführt von
Michaela Wörndl
H0221206

Institut für Alpine Naturgefahren
Universität für Bodenkultur

Wien, 1. Juni 2010

Dank geht an das gesamte Institut für Alpine Naturgefahren, für die Unterstützung in jeglicher Hinsicht und für das kollegiale Arbeitsklima.

Dank geht auch an zahlreiche Studienkollegen und Arbeitskollegen, von denen mir einige immer zur Seite standen.

Danke an meine Eltern, und an Freunde, die mich auf meinem Weg durch dieses Studium begleitet und unterstützt haben.

ZUSAMMENFASSUNG

Die räumliche Verteilung von Schneeeigenschaften kann sich schnell über die Zeit ändern und/oder ihre Entwicklung über die Zeit kann an verschieden Orten unterschiedlich ablaufen. Geeignete Mess- und Monitoringmethoden, die es erlauben dieses komplexe Verhalten, bei angemessenem finanziellen Aufwand und Arbeitsaufwand, zu Beobachten/Analysieren, sind schwer zu finden. Raman Spectra Fiber Optic Distributed Temperature Sensing (DTS) ist eine Laser-basierte Methode, mit der Temperaturen gleichzeitig und kontinuierlich in zahlreichen Punkten und über Zeiträume mehrerer Wochen oder länger, entlang eines Fiberglaskabels gemessen werden können. Die Anschaffung der Kabel ist mit geringen Kosten verbunden. Die Instrumente sind in der Anschaffung teuer und ihre Handhabung erfordert ein hohes Niveau an Fachkenntnis und Erfahrung. In Verbindung mit ähnlich räumlich und zeitlich verteilten Messungen weiterer Schneeeigenschaften oder in Kombination mit Schneedeckenmodellen können Schneetemperaturmessungen verwendet werden um die Schneefestigkeit und deren Verteilung abzuschätzen. In einer Feldstudie in Mammoth Mountain, CA, U.S.A. wurde ein DTS System installiert um Schneetemperaturen entlang eines 2 km langen Kabels zu messen. Verschiedene Teile des Kabels maßen Temperaturen an der Basis und in unterschiedlichen Tiefen der Schneedecke, mit einer räumlichen Wiederholpräzision von 0.06 °C und einer zeitlichen Wiederholpräzision von 0.04 °C und besser. Beobachtete Temperaturen variierten räumlich um mehrere °C. Unterschiedliche zeitliche Entwicklungen der thermischen Verhältnisse in verschiedenen Teilen der Schneedecke und an verschiedenen Punkten des Untersuchungsgeländes wurden gemessen und dokumentiert. Unterschiedliche Schneetiefen und Änderungen des Geländes und der Vegetation wurden als Hauptursachen der für die räumliche Variabilität vermutet. Zeitliche Änderungen der Schneetemperaturen deckten sich teilweise mit Änderungen der Umgebungstemperatur oder der Schneeoberflächentemperatur und der Schneetiefe. Erfahrungen bei der Anwendung eines DTS Systems in Schnee und die Anwendbarkeit der Methode für die Lawinenforschung werden diskutiert. Eine Einleitung in die Methodik des Ramans Spectra Fiber Optic Distributed Temperature Sensing ist enthalten.

ABSTRACT

Snowpack properties can vary spatially on scales smaller than slopes and temporally within hours or less. The pattern of spatial variability can vary in time and the character of temporal variability can vary in space. It is difficult to find appropriate monitoring techniques that allow covering this complex behavior at reasonable expenditures of human resources, time and money. Raman spectra fiber optic distributed temperature sensing (DTS) is a laser-light based measurement technology measuring temperatures. Temperatures can be measured simultaneously and continuously in a multitude of sample spots along a fiber-optic cable over several weeks or longer. The cables are cheap but the instruments are expensive and their handling requires a high level of expertise and experience. Snow temperature measurements in combination with other distributed measurements or models can help derive estimates of snow stability and its distribution. A field study was conducted on Mammoth Mountain, CA, U.S.A, using the DTS technology in a snow environment. Temperatures were measured along a 2 km cable, during four distinct measurement sessions over several days. Parts of the cable were deployed at the soil snow interface, and in two different snow depths. Relative accuracies of 0.06 °C in space (spatial repeatability) and of 0.04 °C in time (temporal repeatability) could be achieved. Horizontal spatial temperature variations in the range of several °C at the base of the snowpack and within the snow cover could be detected. Differences in the evolution of temperatures in different snow depths and different locations across the study field could be successfully monitored. Variations in snow depths and changes in terrain features seemed to be the major driving forces for spatial temperature variations. The temporal evolution of the snow's thermal settings corresponded either to changes in ambient air temperatures or in snow surface temperatures and depth of the snow cover. Experiences with a DTS system in a snow environment and its applicability in avalanche research are discussed. A general introduction to Raman Spectra Fiber Optic Temperature Sensing is provided.

Outline

PART C: RESULTS

PART D: REFERENCES AND APPENDICES

1. INTRODUCTION

Avalanches are the result of numerous processes that act over large ranges of different spatial and temporal scales (Hägeli, 2004, 12). They are influenced by weather effects on synoptic scales and also by micro-scale snow-metamorphic processes. Raman spectra fiber optic distributed temperature sensing (DTS) is a measurement method, which can provide spatially and temporally resolved temperature data over different scales, from a few meters up to 30 km. The goal of this work is to identify this measurement technology's potential in contributing to a better understanding of avalanche processes and accordingly to improvements in avalanche modeling, -warning and -forecasting. In the first part the relevance of studying snow temperature variations in avalanche research is assessed. An overview is given on recent research on snow cover variability and on studies of temperature settings in alpine snow packs. Briefly common measurement and modeling methods of temperatures in snow and their assets and drawbacks are discussed. The second part provides an introduction to Raman Spectra Distributed Temperature Sensing with respect to applications in snow environments and the method is discussed in the context of a field study that was carried out on Mammoth Mountain, CA, U.S.A., during the winter 2008/2009. The field study aimed at detecting possible small temperature variations at the base of the snow pack and at observing temperature variations in different snow depths. The conclusions highlight experiences with the application of a DTS system when studying snow temperatures; examine the quality of the results gained from the field study and outline possible improvements and future applications.

PART A: THEORETICAL BACKGROUND

2. SNOW AVALANCHES – AN ALPINE NATURAL HAZARD

Natural hazards in alpine regions threatening humans and their properties are typically caused by flowing water or by snow, soil, rock or ice in motion (Hübl et al, 2006). In the Austrian "Naturgefahren Steckbrief" (characterizations of natural hazards) avalanches are defined as a rapidly moving mass of snow that come off mountain slopes and are gliding or falling towards the valley bottoms (Rudolf-Miklau, 2009). They are one of the dominant hazardous processes in mountainous terrain (Hübl et al., 2006). Other alpine natural hazards or mountain hazards are mudflows, torrents, floods and rockfall. All these processes, including avalanches, can also be referred to as gravitational natural hazards as they mostly occur in strongly inclined terrain (Hübl et al., 2006). Rudolf-Miklau (2009) lists avalanches in second place of Austria's most important natural hazards. They are the only natural process in the Alps that still causes fatalities on a regular basis (Rudolf-Miklau, 2009). Only floods pose a higher risk to Austria's population, mainly because of their potential to result in severe property damage and in region wide catastrophes. Avalanches rank high as well in terms of threats to property and in their potential to cause catastrophes but what is most important is that they are the largest risk to individuals and their lives in Austrian Alps today (Rudolf-Miklau, 2009). From 1984 to 2005 in average 31 people died in avalanches per year in Austria (Rudolf-Miklau, 2009), about a hundred individuals are killed each year in the entire European Alps (www.slf.ch[4]), causing avalanches to be the most life threatening natural hazard in the region.

Hazards exist when life and property are exposed to harmful impacts of natural processes (Rudolf-Miklau, 2009), as for example avalanches. Densely populated regions in the European Alps have always been areas of high exposure to gravitational hazards. Risks for communities or individuals exist when their exposure to a natural process may result in a loss of property or lives (Rudolf-Miklau, 2009). In the 1950ies many people died in Austria and Switzerland when avalanches hit their residences. Also later, in the 1970ies a series of avalanche occurrences caused deaths and severe property damage in the Alps, this time in France and Switzerland (McClung and Schaerer, 1999). 1835 people were killed in Switzerland between 1937 and 2010, 30 % of which had been hit either on transport axes or in settlements. Since 1970 the share of people killed in traffic or in settlements decreased. While before 1970 about 12 people were killed in settled areas per year, after 1970 only 4 victims a year were counted on roads and in permanently inhabited locations in Switzerland (www.tec21.ch/pdf_anzeigen.php?pdf=tec21_0820063199.pdf). Strong efforts were made during the second half of the 20th century to reduce risks for settlements and infrastructure in the Alps, mostly through permanent technical protection measures and other permanent solutions, such as protective forests and adapted land use planning (www.slf.ch[1]).

2.1 SNOW AVALANCHE PROTECTION

2.1.1 Permanent Protection Measures

Permanent technical protections are designed to continuously provide a certain level of security throughout the entire calculated life span of a structure (Bergmeister et al., 2009). Land use restrictions or protective forests provide protection as long as a system is not subjected to significant changes, which could be caused, for example, as a result of climate change or deforestation. Typically, dimensions of technical structures and extents of restricted areas for settlements are defined based on analyses of past events (historical data) and process simulations (McClung and Schaerer, 1993). Databases, witness reports, experiences and numerical and physical models are employed to identify so called design events of a certain magnitude and impact that are related to a specific probability of occurrence (Bergmeister et al., 2009). Then protection structures are planned to withstand a design event of a chosen probability of occurrence, which usually relates to an object's or a community's need for protection (Schutzbedarf) (Bergmeister et al., 2009). They are designed to last for a certain life span, which often is a period of 100 years. Process simulations typically use data about the slope's topography, the starting zone's areal extent and the expected size of the avalanche crown (Kulterer, 2004) to render information about the extent, the flow path and the expected impact of an avalanche of a certain magnitude. As long as natural processes are smaller or equal to the size of a design event, settlements and roads remain protected.

The significant decline of victims in intensively used regions in the European Alps during the second half of the last century indicated that efforts in permanently protecting settlements and traffic lines were highly effective. However, permanent protection has its limits as structures and land use zoning are always based on a design event with a certain probability of occurrence. There always remains the residual risk that an event occurs, which is larger than the design event. Further safety, which can be achieved through permanent protection, is limited to certain areas in the mountains and cannot be provided in the backcountry. Figure 1 displays a technical avalanche protection in the starting zone of an avalanche, constructed to protect the village of Ischgl and an avalanche dam, which aims to minimize impacts of an avalanche on a farmhouse in Galtuer. Both villages are located in the Austrian Alps.

Fig. 1: permanent technical protection measures against avalanches in the Austrian Alps

2.1.2 Temporary Protection Measures

Often temporary protection is used to complement permanent measures (Bergmeister et al., 2009), for example, when a natural hazardous process exceeds the magnitude or intensity of the permanent measures' design event(s). They also are employed when permanent solutions would be too expensive (www.slf.ch[1]), as for example to protect skiing resorts or remote traffic lines. Temporary protection against avalanches can be either active protection, as the use of explosives to trigger controlled avalanching and to remove potentially dangerous snow masses; or passive protection, as temporary closure or evacuation of roads, slopes or entire regions. In both cases warnings and continuous monitoring of the snow pack's stability status are necessary to identify dangerous situations. Figure 2 shows examples of how to apply explosives to unstable, snow covered slopes - a helicopter and a "Lawinenorgel" that can shoot explosive charges to the avalanche prone terrain; further it shows a group of skiers traveling safely in avalanche terrain, after the avalanche had been triggered by an explosion.

Fig. 2: Helicopter and "Lawinenorgel" for applying explosive charges to unstable slopes and skiers in front of an avalanche triggered by explosives.

Temporary measures are adapted to the snow's stability and characteristics at a specific location and at a certain point in time (www.slf.ch[1]; www.noezsv.at). Referring to Adams (1995), McClung (2002a) distinguishes two categories of avalanche risk analyses. In an engineering approach formal statistical principles are employed for the design of permanent solutions, as for example for land-use planning in avalanche prone terrain.

The second approach is more dynamic, subjective and time dependent (Adams, 1995 in McClung, 2002a), and would for example be applied for temporary solutions and in the backcountry.

Many regions and skiing resorts employ so called avalanche committees (safety services), who are in charge of assessing the snow pack's current stability and of the decision-making of whether or not to set temporary actions (http://lawine.tirol.gv.at/uploads/media/05_Die_Arbeit_der_Lawinenkommissionen.PDF) to protect villages, traffic lines and tourist facilities (Bründl et al., 2003). In Tyrol (Austria) currently 224 avalanche committees (safety services) are employed to protect 153 villages and several skiing resorts (http://lawine.tirol.gv.at/organisation/lawinenkommission).

2.1.3 Today's limits of Avalanche Protection

In the early 1970ies a new trend in avalanche fatalities was detected. In Europe and also in the mountain ranges of the United States, Canada and Japan an increase in avalanche caused fatalities in the backcountry and out of bounds of skiing resorts was noticed (McClung and Schaerer, 1999). Starting in the early 1970ies until the early 1990ies the number of people killed by avalanches during backcountry recreational activities rose significantly. Between 1974 and 1989 the rate of recreational fatalities in Canada tripled (McClung and Schaerer, 1999). From 1977 to 2006 703 people were killed in avalanches in Switzerland during recreational activities, either in the backcountry or off-piste close to skiing resorts (Harvey and Zweifel, 2008).

Permanent protection initiatives complemented with temporary measures could successfully reduce risks in settled areas (www.slf.ch[1]) but at the same time increasing popularity in backcountry recreational activities lead to a new rise in avalanche risks.

Avalanche committees, backcountry recreationalists and off-piste skiers and snowboarders are strongly dependent on knowledge about a snow pack's current stability at a certain point in time and at a certain location and they need this information for comparatively small scales (in the order of slopes).

In their decision-making they are often supported by avalanche warnings or avalanche danger reports. Starting in the mid 1990ies agencies in the Alps reacted on increasing demands for timely and spatially more precise avalanche warnings, and improved their warning-, information- and also education services (Bründl et al., 2003). In Switzerland avalanche warnings developed from weekly bulletins to comprehensive information services (Bründl et al., 2003) that are today updated twice a day and that are easily available to the public.

2.1.4 Recent Year's Achievements

The very recent years showed a further increase in backcountry recreationalists in Europe, Canada and the United States (www.erstespur.de; http://www.avalanche-center.org/Incidents/statistics/; www.bergrettung.at; www.tec21.ch) It is estimated that the number of winter-backcountry-recreationalists in the Tyrol was five times higher in 2008 than it was about fifteen years earlier (Mueck, 2008). Most avalanche victims in the last ten years were caught on their skis, snowboards or snowmobiles in the backcountry or just out of the bounds of skiing resorts (http://www.avalanche-center.org/Incidents/statistics/; www.bergrettung.at). They often were killed in avalanches, which they triggered themselves (www.slf.ch[4], McClung, 2002a). In 2008 Harvey and Zweifel, however, could show that, even though more people were travelling on ski-tours or in off-piste terrain in Switzerland, fatalities did not increase. They concluded that recreationalists' knowledge about avalanche dangers had developed and that prevention, rescue training, avalanche warning and access to information about current hazard situations had improved. They assumed that a combination of all these factors could contribute to reduce individuals' risks in avalanche prone terrain. More avalanche accidents were reported since the late 1990ies, but fatalities did not increase compared to the late 1970ies. This may be explained by the fact that, due to rising public awareness, generally more avalanche occurrences were reported in recent years, also more harmless ones, but it is also mentioned that rescue techniques, equipment and know-how in companion rescue have improved (Harvey and Zweifel, 2008). They also noted a significant change in the ratio of fatalities in guided and non-guided activities. The number of accidents that happened during guided tours did decrease (Harvey and Zweifel, 2008). According to Harvey and Zweifel (2008) this indicates that better education and a higher level of professionalism of guides and leaders could reduce avalanche risks for guided individuals and groups. Education and training in rescue but also in avalanche risk assessment seem to have helped reduce the ratio between the number of individuals exposed to avalanche hazards and the number of fatalities.

However, numbers show that there is still need of further improvement in order to minimize injuries and fatalities caused by avalanches (Harvey and Zweifel, 2008). Even though there was no catastrophic occurrence in this particular winter, which would have affected many individuals in one event, 48 individuals died in avalanche accidents in the Austrian Alps during the winter in 2004/2005. The accidents took place in the backcountry and in skiing resorts and were caused by a multitude of distinct avalanche events (www.bergrettung.at). Hägeli mentions in his work (2004), referring to the Canadian Avalanche Association, that in Canada annual fatalities were still increasing and avalanches today are the leading source of fatalities caused by natural hazards (Hägeli, referring to CAA). Citing Bhudak Consultants Ltd., 2003, Hägeli (2004) calls for public avalanche safety programs, which include public avalanche warnings, public awareness programs and public education, in order to help improve the situation in Canada. The most promising approaches to mitigate avalanche risks in the future seem to be the improvement of avalanche warnings and the creation of a broad public awareness as well as widespread education about the hazard amongst winter-backcountry-recreationalists. As opposed to engineering structures and other permanent protection solutions this requires detailed knowledge about the spatial and temporal distribution of snow pack properties on small spatial and temporal scales. Schweizer et al. (2003) defined the questions of where and when does what kind of avalanche potentially occur, as the key questions for backcountry travelers, avalanche committees (snow safety managers) and accordingly for avalanche forecasters.

2.2 SNOW STABILITY EVALUATION AND AVALANCHE WARNING

Time spans between clear warning signs and the actual occurrence of natural hazards in alpine regions are typically short (Bergmeister et al., 2009). Avalanche occurrences, for example, can be preceded by so-called "Whoomp"-sounds but they usually can only be heard close to the avalanching slope and very shortly before the snow pack collapses (Munter, 2003). Therefore avalanche committees and decision makers who control temporary protection measures (Mueck, 2008, McClung, 2002), backcountry skiers, and in some areas also lumberjacks and agricultural workers (www.noeszv.at) often have to rely on issued avalanche warnings based on short-term forecasts and on their individual judgment based on the gathered information and individual know-how.

2.2.1 Snow Avalanche Formation

Avalanche formation is the result of complex interactions between terrain, snow pack and meteorological conditions (Schweizer et al., 2003). Avalanches form when stresses applied on the snow pack are large enough to overcome its resistance. In avalanche research and forecasting it is tried to assess both, the stresses that have to be expected and the snow pack's stability behavior (stability evaluation). Generally stresses on the snow pack result from the down-slope component of its weight. Additional loads may be applied through new snowfall, skiers and also through rock fall, falling ice or smaller avalanches. How much stress a snow pack at a certain point and at a certain time can withstand is determined by its actual stability, which is depending on the current local snow conditions. There are different mechanisms causing a snow pack to fail and they initiate different types of avalanches.

2.2.2 Types of Snow Avalanches and of Failure Mechanisms

Four major types of avalanches, depending on the physical properties of the collapsing snow pack can be distinguished. There are dry loose-snow-avalanches, wet loose-snow-avalanches and dry and wet slab-avalanches. The three types are the result of different failure mechanisms and are indicated by different physical conditions, mainly depending on the snow's density, hardness, temperature, rate of deformation, and quality of binding between adjacent layers (McClung and Schaerer, 1993). Loose snow avalanches differ from slab avalanches in their type of release. Loose snow avalanches start in a point with little cohesion in surface layers of dry or wet snow. Slabs consist of cohesive snow and are released over a plane of weakness (Schweizer et al., 2003).

Three general types of failure can be distinguished. Either a snow pack fails as cohesion and friction between snow particles are overcome by down-slope forces, mostly due to its own weight (loose snow avalanches); or shear forces within a weak layer or bonds between two layers are overcome by shear stresses due to the load it carries (dry slab avalanches, often triggered by skiers); or friction at confined layers within the snow pack or at the ground is reduced due to free water accumulations and the snow starts to glide (wet slab avalanches). The moisture content of avalanches influences their flow paths and their extent and impact. Wet avalanches travel with higher friction and more closely follow terrain features. Loose dry snow tends to travel in straight lines. In case of slab avalanches the snow's hardness determines how far fractures may propagate and therefore controls the size of slabs that may release.

Information about the character of probable avalanches is important for engineers when planning and designing permanent protection structures and measures, for skiers when choosing travel routes in the backcountry; and for decision-makers when, for example, choosing the right timing for the application of explosives.

2.2.3 Assessment of Snow Avalanche Dangers

Stability conditions can vary significantly, in space with terrain, and in time and as there are various complex failure mechanisms. Often it is hard to gather data from avalanche starting zones as the hazard prevents access to the area. Direct stability measurements, as for example Rutschblock-tests or Extended-Column-Tests often are too time consuming, and usually they only test a small area of the snow pack. Figure 3 shows the conduction of an extended column test and of a Rutschblock test, to assess the snow pack's stability in a distinct point and to draw conclusions about the stability in other locations with similar characteristics.

Fig. 3: Assessing the snow pack's stability through an extended column test and a Rutschblock test

Therefore measurements of other factors that are indirectly influencing stability and extrapolations are often the only basis for areal stability assessment on snow and for according decision-making (McClung and Schaerer 1993). Which factors are monitored on which spatial and temporal scales often not so much depends on the direct significance for snow stability but more on available measurement technologies and on possibilities to gather the data at locations of interest. However, McClung and Schaerer (1993) stress the fact that a holistic approach is crucial in stability evaluations, as a snow pack's mechanical properties are the result of complex interactions of a handful of physical properties that may evolve differently, in space and in time. Even if one factor can be measured at high temporal and spatial distribution, uncertainties remain and only a combination of many measurements and detailed knowledge about their variability can render a clear picture of the snow's most likely behavior. Therefore, in order to assess actual and future stability conditions, which are the basis for any decision-making process when moving in avalanche prone terrain, the actual condition and evolution of many factors should be considered.

The snow pack and meteorological conditions have to be monitored, they have to be related to terrain features, signs of instability have to be identified and consequences that have to be expected have to be assessed in order to allow decision-making, risk reduction and protection of properties and lives (McClung and Schaerer, 1999; Munter, 2003).

2.2.4 Snow Avalanche Forecasting

As defined by McClung (2002a) avalanche forecasting is the prediction of current and future instabilities in space and in time relative to a given triggering load, which would for example be the weight of a skier or a snow-mobile. He further introduces the term of applied avalanche forecasting, which also includes the decision-making, following the prediction (McClung, 2002a). As a snow pack's condition is a result of its evolution throughout a winter-season continuous monitoring of its evolution and metamorphism, from the first snowfall of the season to the melting of the snow pack, is necessary in order to estimate its stability at a certain point in time (McClung, 2002a). Compared to warnings for other natural hazardous processes, avalanche warning usually requires a higher degree of detail. Information about the exact timing and location of individual events on the smallest scales is needed (Hägeli, 2004) in order to protect, for example, individual backcountry travelers. Backcountry travelers are, as described earlier (chapters 2.1.3. and 2.1.4.), mostly responsible for avalanche risks today.

Warning services (Lawinenwarndienste) and also some members of avalanche committees gather information from weather stations, some of them placed right at avalanche starting zones, and from observations in the field (http://lawine.tirol.gv.at/uploads/media/05_Die_Arbeit_der_Lawinenkommissionen.PDF), as for example stability tests (Rutschblocktest, Extended Column Test), to assess the snow pack's properties. The Swiss avalanche-warning agency at the SLF and forecasters in France also employ models to assess the snow pack's layering properties and get estimates on it stability behavior and on avalanche dangers (www.slf.ch[2], Hägeli, 2008). However, due to the inhomogeneous topography of mountainous terrain and complex interactions between terrain features and weather effects, such as precipitation, radiation and wind, annual alpine snow packs are highly variable in time and in space (www.slf.ch[3]). According to McClung (2002a) a fundamental physical uncertainty in avalanche forecasting resides in usually unknown temporal and spatial variations in the snow cover and their links to terrain. Figure 4 displays the avalanche safety service's office in at the skiing resort of Ischgl, Austria and two weather stations, used for snow and avalanche research.

Fig. 4: avalanche committee (safety service) and two weather stations used for snow- and avalanche research

As only a limited number of points can be monitored or modeled the variability of the snow's properties in time, in space and differences in their temporal evolution in different locations cause major insecurities about a snow pack's stability behavior and exhibit major challenges for forecasters and decision-makers. Extrapolation of snow properties across slopes or even mountain ranges often proves to be difficult, as they may vary strongly, even on small scales. As the goal is to identify possible locations of avalanche trigger points, very detailed point – to point extrapolations of measurements, observations and model results would be necessary (Hägeli, 2004).

Mainly the similarity of two locations with respect to the investigated properties determines whether an extrapolation would be licit or not. Therefore basic knowledge about scale characteristics of snow pack stability and of its influencing parameters is fundamental for the development of appropriate monitoring networks and useful forecasting models (Hägeli, 2004), but information is limited so far. Avalanche forecasting and decision-making (applied avalanche forecasting) about snow stability and safety in avalanche terrain are exacerbated by the complexity of a snow pack's failure mechanisms and its various influencing factors and by the high spatial and temporal variability of snow pack properties in the backcountry.

Harvey and Zweifel (2008) showed in their work that, when a danger level of "considerable" was issued more accidents seemed to occur than during times with "high" avalanche hazards. The European avalanche hazard scale lists the following for a danger level of "considerable": "Triggering is possible, sometimes even with low additional loads, particularly in the steep slopes that are indicated in the bulletin. In certain conditions some medium but also few large sized natural avalanches are possible." (http://www.avalanches.org/basics/degree-of-hazard/). The danger level of "high" is described as: "Triggering is probable, even with low additional loads, on numerous steep slopes. In some conditions frequent medium or several large sized natural avalanches are possible." (http://www.avalanches.org/basics/degree-of-hazard/). At the high danger level, the issued description claims entire mountains to be dangerous. The level is defined as considerable when the snow pack's stability situation is highly variable and only specific expositions are indicated as dangerous in the bulletin. It seems that the considerable situation causes more people to take the risk and go out in the backcountry where they then might misjudge the stability of a distinct slope or part of a slope and get caught in an avalanche. Avalanche forecasting services today can reliably issue occurrence probabilities for certain regions, but, as snow, as a highly porous material close to its melting point, has a highly variable character, they currently cannot predict timing and locations of single avalanche events (Schweizer et al., 2003). McClung (2002b) mentions that the major cause of avalanche accidents is a failure of human perception, when people think that the snow's stability is something other than it actually is (McClung, 2002).

More detailed information in avalanche bulletins about the timing and location of snow pack instabilities and better understanding of their spatial and temporal variability and how they relate to and can be identified through observed terrain features, as well as associated public education, seem to be the major goals when trying to reduce avalanche caused fatalities in the future. Figures 5, 6 and 7 show the classification of avalanche dangers in Europe, in Canada and in the United States. Figure 8 displays how an avalanche bulletin is created at the Swiss SLF (www.slf.ch[5]).

Degree of hazard

Degree of hazard	Icon	Snowpack stability	Avalanche Probability	Colouring
1 - Low		The snowpack is generally well bonded or loose and stressless.	Triggering is generally possible only with high additional loads 2 on a few locations in steep extreme terrain. Only a few sluffs and small natural avalanches are possible.	green: 204, 255, 102 (RGB)
2 - Moderate		The snowpack is moderately well bonded on some steep slopes [1], otherwise generally well bonded.	Triggering is possible in particular with high additional loads 2, particularly on the steep slopes indicated in the bulletin. Large natural avalanches are not likely.	yellow: 255, 255, 000 (RGB)
3 - Considerable		The snowpack is moderately to weakly bonded on many steep slopes.	Triggering is possible, sometimes even with low additional loads 2 particularly in the steep slopes that are indicated in the bulletin. In certain conditions, some medium but also few large sized natural avalanches are possible.	orange: 255, 153, 000 (RGB)
4 - High		The snowpack is weakly bonded on most steep slopes.	Triggering is probable even with low additional loads 2 on numerous steep slopes. In some conditions, frequent medium or several large sized natural avalanches are likely.	red: 255, 000, 000 (RGB)
5 - Very high		The snowpack is generally weakly bonded and largely unstable.	Numerous large natural avalanches are likely, even on moderately steep terrain.	red: 255, 000, 000 (RGB) / black squared

Fig. 5: classification of avalanche hazards, Europe (www.avalanches.org/basics/degree-of-hazard)

WHAT Danger Level (& Colour)	WHY Avalanche Probability, Triggers	WHAT TO DO Recommended Action in the Backcountry
LOW (green)	Natural avalanches very unlikely. Human triggered avalanches *unlikely.*	Travel is generally safe. Normal caution is advised.
MODERATE (yellow)	Natural avalanches unlikely. Human triggered avalanches *possible.*	Use caution in steeper terrain on certain aspects (defined in accompanying statement).
CONSIDERABLE (orange)	Natural avalanches possible. Human triggered avalanches *probable.*	Be increasingly cautious in steeper terrain.
HIGH (red)	Natural and human triggered avalanches *likely.*	Travel in avalanche terrain is not recommended.
EXTREME (red w/ black border)	Widespread natural or human triggered avalanches *certain.*	Travel in avalanche terrain should be avoided and travel confined to low angle terrain well away from avalanche path run-outs.

Fig. 6: avalanche danger levels, Canada (http://www.avalanche-center.org/Education/danger/cadanger.php)

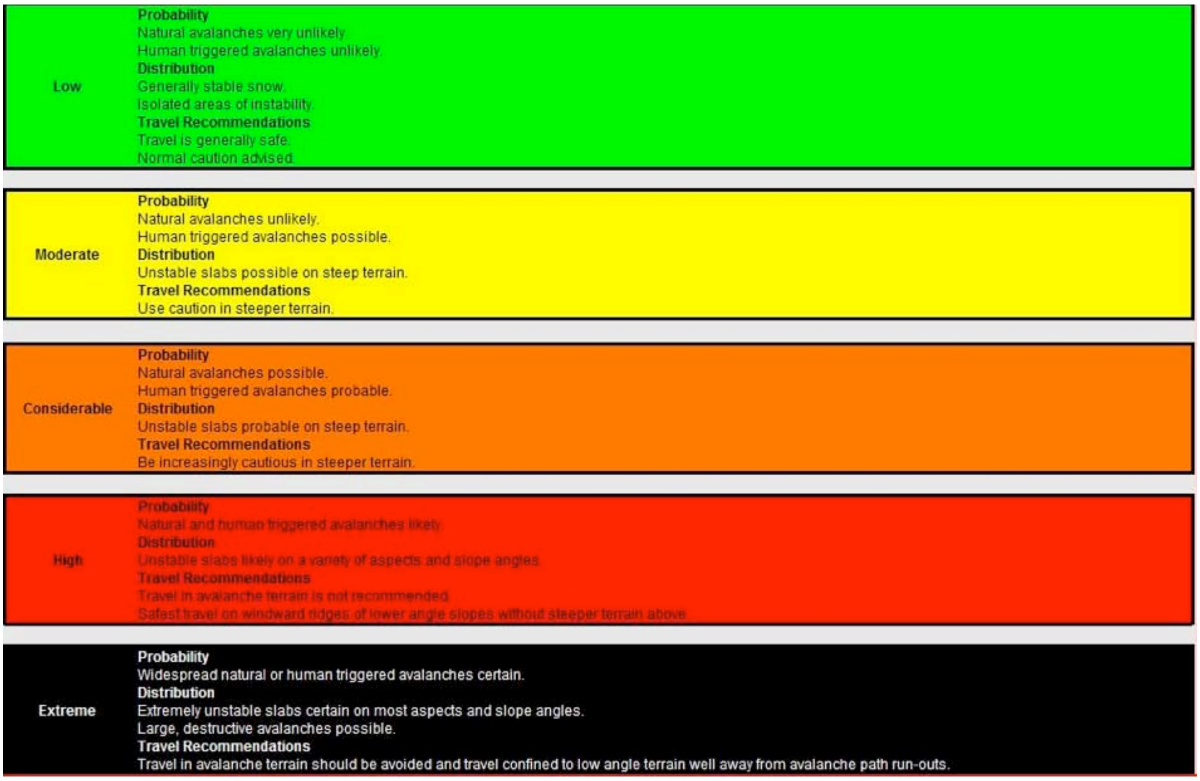

Low	**Probability** Natural avalanches very unlikely. Human triggered avalanches unlikely. **Distribution** Generally stable snow. Isolated areas of instability. **Travel Recommendations** Travel is generally safe. Normal caution advised.
Moderate	**Probability** Natural avalanches unlikely. Human triggered avalanches possible. **Distribution** Unstable slabs possible on steep terrain. **Travel Recommendations** Use caution in steeper terrain.
Considerable	**Probability** Natural avalanches possible. Human triggered avalanches probable. **Distribution** Unstable slabs probable on steep terrain. **Travel Recommendations** Be increasingly cautious in steeper terrain.
High	**Probability** Natural and human triggered avalanches likely. **Distribution** Unstable slabs likely on a variety of aspects and slope angles. **Travel Recommendations** Travel in avalanche terrain is not recommended. Safest travel on windward ridges of lower angle slopes without steeper terrain above.
Extreme	**Probability** Widespread natural or human triggered avalanches certain. **Distribution** Extremely unstable slabs certain on most aspects and slope angles. Large, destructive avalanches possible. **Travel Recommendations** Travel in avalanche terrain should be avoided and travel confined to low angle terrain well away from avalanche path run-outs.

Fig. 7: avalanche danger levels, USA (www.mtavalanche.com)

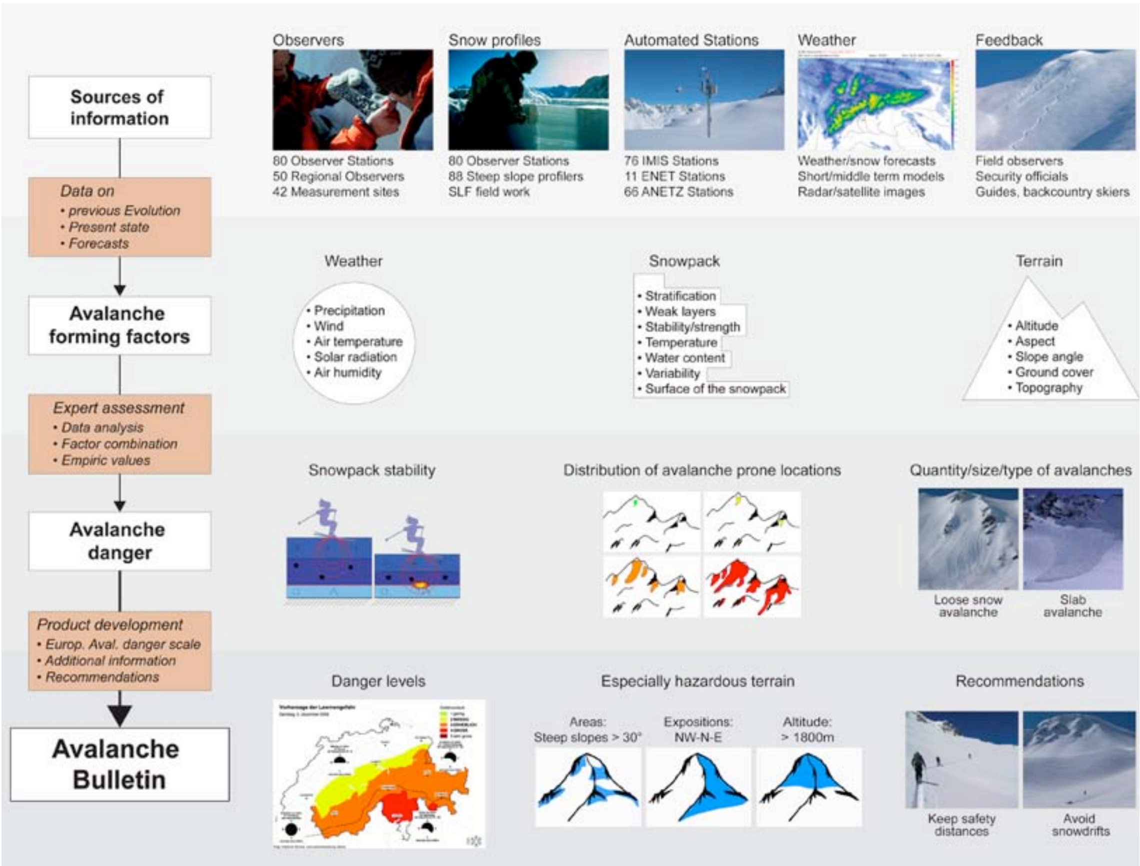

Fig. 8: Development of an avalanche bulletin at the SLF in Switzerland (http://www.slf.ch/lawineninfo/zusatzinfos/howto/entstehung_bulletin_gross_e.jpg)

3. SNOW- AND AVALANCHE RESEARCH

3.1 SNOW PHYSICAL BACKGROUND WITH AN EMPHASIS ON TEMPERATURE INFLUENCED PROCESSES

Temperature settings, i.e. temperatures and temperature gradients in a seasonal snow pack are the result of ambient air temperatures, heat exchange at the snow surface and heat transport within the snow cover and the soil, and are also determined by the actual snow depth and actual snow conditions (albedo, density) at a certain location. Temperatures and temperature gradients, especially in the upper parts of a snow cover and on the snow surface are mainly controlled by energy fluxes based on the balance between incoming short wave and long wave radiation and outgoing long wave radiation. Temperatures and temperature gradients control snow metamorphic processes and strongly influence its mechanical properties, significantly determining a seasonal snow pack's stability evolution in time. They are strongly influencing snow hardness and brittleness, which are important for the formation of slab avalanches and they are important for snowmelt processes and the destabilization of snow covers due to high water contents. Blowing snow, terrain features, the general snow distribution as a result of variable precipitation patterns and the spatial and temporal variations in a snow pack's temperature settings are responsible for variations in avalanche hazards at the scale of a single slope (McClung and Scherer, 1993).

3.1.1 Heat Transport within an Alpine Seasonal Snow pack

Whether heat is added to the snow pack or lost depends on the difference between snow surface temperatures and ambient air temperatures. Warmer surfaces loose heat to the surrounding air; colder surfaces are warmed. Conduction, convection and radiation are the three processes that allow heat to enter or leave the surface. However, the influence of conduction in air is negligible. A snow pack can also get warmed or cooled through falling snow of a warmer or colder temperature, though only to a limited extent (McClung and Schaerer, 1993).

Several processes drive heat transport within the snow pack, which together determine its so-called effective conductivity (Wiesinger, 1988). Heat can be transported through conduction between ice crystals and through conduction and convection and in form of radiation energy and vapor diffusion in the pore space. The thermal diffusivity of snow is generally low and depends on its density. Generally conduction between ice crystals is more important than the processes in the pore space as its capacity is much higher. However, in low-density snow (<100kg/m^3) crystal structures are rather discontinuous and vapor-diffusion can be responsible for a third of the snow's effective conductivity (Wiesinger, 1988). As a result, due to the temperature's impact on the rate of vapor diffusion, heat transport therefore becomes even less efficient as temperatures decrease (McClung and Schaerer, 1993). As saturated warm air can hold more water vapor than saturated cold air heat flow by condensation goes from warmer to colder parts of the snow cover. Given the case that some other requirements are fulfilled (large enough pore space, not too cold ambient temperatures) water vapor flux may contribute to the formation of faceted crystals and surface- and depth hoar, which are major causes for weaknesses within a snow pack. Buried surface hoar- and depth hoar layers promote fracture propagation and easily collapse when shear stresses are applied (McClung and Schaerer, 1993).

The overall effective conductivity of low-density snow is about a 1/25 that of ice but it gets ten times higher when density increases to about 600kg/m^3 and when conduction through ice crystals dominates heat transport. Typically snow at densities from

100kg/m^3 to 400kg/m^3 is relevant for avalanche formation and conduction and diffusion both play a role in heat transport (McClung and Schaerer, 1993).

The extent of heat fluxes within the snow pack depends on convection, on the snow's effective thermal conductivity and also on the current temperature gradient. Heat fluxes cause high instability of temperature settings within a snow pack (Wiesinger, 1988) in space and in time. Temperature gradients establish as a result of temperature differences between the two boundaries of a snow pack – the ground and the atmosphere – and are themselves variable in time and also in space. Temporal changes in temperature gradients are mostly the result of changing atmospheric conditions. While ground temperatures typically remain stable, and close to the melting point, air temperatures may vary strongly in time and can reach values much higher and much lower than 0 °C. Usually temperature gradients in a snow cover are largest early in the season, when snow packs are shallow, and they are generally stronger and more variable in the upper 30 cm of a snow cover. The extent of temporal temperature variations during a winter season depends on the variability of meteorological conditions, such as air temperature, precipitation, clouds and radiation. When air temperatures increase during springtime, the snow warms up and the temperature gradient decreases towards an isothermal state. Considerable snowmelt does not occur until a snow pack reaches the state of being isothermal.

Gradients are stronger in continental snow climates (smaller snow depths, colder air temperatures and less clouds) than they are in maritime snow climates. Gradients in regions with large amounts of snow precipitation are smaller but local extremes can develop when, due to wind drift or previous avalanching, snow depths are small at certain spots and when air temperatures are cold (McClung and Schaerer, 1993). Spatial gradient variations can be caused by differences in snow depth, terrain and vegetation, exposure and elevation. Horizontal temperature gradients may develop, for example, near rock outcrops (McClung and Schaerer, 1993).

Different temperature gradients and also differences in general temperature settings (also different snow climates) encourage growth of different crystal forms, and do strongly affect the character and the timing of avalanches that develop. For example, depth hoar crystals form when, due to a strong temperature gradient and sufficient supply of moisture, vapor flux is high and when pore spaces are large enough to allow extensive growth of faceted crystals. The result is a highly unstable layer within the snow pack. Typically depth hoar can form early in the season, especially in continental and transitional climates. When temperature settings in the snow cover remain cold, such unstable layers can persist for long time spans (several weeks). Depth hoar can also form due to horizontal temperature gradients near rock outcrops (Fig. 9), which warm up more than the surrounding snow, causing them to be likely trigger points for avalanching (McClung and Schaerer, 1993, Weir, 2002).

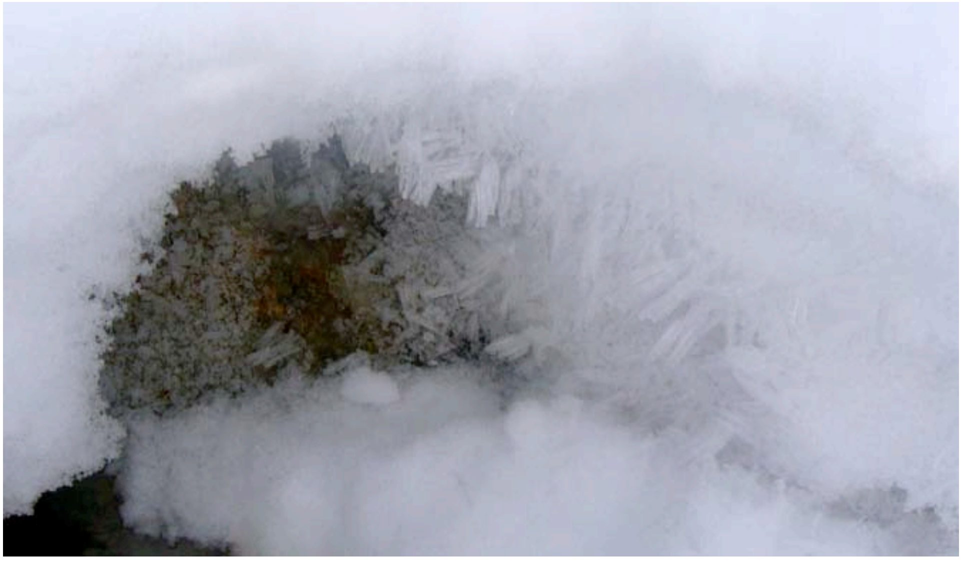

Fig. 9: strongly facetted crystals close to a rock outcrop

3.1.2 Energy Exchange at the Snow Surface

Short and long wave radiation influences can contribute to spatial and temporal variations in a snow pack's stability in several ways. Whether there is a positive or negative energy balance (warming or cooling of the surface) is important for the formation of surface hoar and for the stabilization or destabilization of wet snow. In winter north facing slopes are cooler due to shading from short wave radiation and tend to be more dangerous as facetted crystals and depth hoar are more likely to form. Furthermore instabilities tend to persist longer in cold snow. Under thin fog green house effects can lead to rapid warming of upper regions of the snow cover and may very quickly induce wet snow avalanches. In spring it is the south facing aspects that become dangerous first, because of short wave radiation penetrating into the wet snow, inducing wet snow avalanches. In late spring when air temperatures get warmer wet snow avalanches also occur on north facing slopes. The influences of long wave- and short wave radiation can further cause radiation recrystallization in top layers of a snow pack, as a result of local, strong temperature gradients in the very upper section of the snow cover. This results in the formation of weak layers that consist of strongly facetted crystals. Once they are buried, they form dangerous imperfections within the snow pack.

Incoming short wave radiation from sunlight, incoming long wave radiation from the earth and from water vapor and carbon dioxide in clouds and the long wave radiation leaving the snow determine the energy exchanges at its surface. To a large extent changes in this balance are responsible for rapid temperature changes near the surface of the snow cover. Depending on its moisture content and on its color, which is depending on the extent of the snow cover's contamination, snow reflects a large proportion of solar radiation. On a dry surface about 90 % are reflected, on a wet surface about 80 % (McClung and Schaerer, 1993). The remaining proportion penetrates into the snow pack, while exponentially loosing intensity with depth. Referring to McClung and Schaerer (1993) it is estimated that in dry alpine snow, of a density that is typically found in slab avalanches (about 100kg/m^3), only about 10 % of the originally incoming solar radiation are left 10cm below the surface. In fresh, fine-grained snow this distance is even shorter; in wet coarse-grained snow it would be larger. Wet, dense snow absorbs more radiation from sunlight and once absorbed, the light also can penetrate deeper. Hence, once wet, a snow pack destabilizes quickly under the influence of solar radiation (McClung and Schaerer, 1993). As a porous surface the snow cover is almost perfect absorber with respect to long-wave radiation and approximates a blackbody radiator. About 50 % of the incoming long wave radiation is absorbed after 1 cm (McClung and Schaerer, 1993).

On clear days differences in the amount of incoming radiation can lead to large temperature differences between north facing and south facing slopes. North facing slopes are shaded from direct sunlight and there is no input of long wave radiation, due to the lack of clouds. Therefore outgoing long wave radiation may cause snow surfaces on north facing slopes to be much colder. While south facing slopes warm up, north-facing slopes cool due to outgoing long wave radiation. This often results in large differences in thermal settings between north and south facing slopes, which further lead to different metamorphic processes, snow pack properties and stability conditions. Leaving long wave radiation in open areas during clear nights can cause the snow cover to be 5 to 20 °C colder than the surrounding air. Under a continuous cloud cover or under forest canopies cooling due to outgoing long wave radiation is strongly reduced. Surface hoar may form on cool snow surfaces at night if air temperatures are high enough to cause a significant temperature gradient and when enough moisture is available (McClung and Schaerer, 1993, Weir, 2002).

3.1.3 Snow Metamorphism and Bond Formation

Snow Metamorphism

The initial shape of newly fallen snow is defined by the temperature and humidity in the atmosphere at the time of its formation. Modifications may already start during their descent through the lower atmosphere. They may for example get rimed, which in its most extreme form leads to the development of "graupel". When they reach the ground, crystal forms can be further changed, for example, by the influence of warm temperatures, which cause the rounding of dendrites. During snowfall accompanied by wind, crystals may break into fragments, and then form densely packed, hard layers (Weir, 2002).

Within a snow pack, the snow changes its form due to the influences of temperature and overburden pressure. In seasonal snow packs however, pressure influences on crystal-form-metamorphism are relatively low (McClung and Schaerer, 1993). Temperature settings and temperature gradients though are of great importance. When air temperatures in a snow pack increase from -15 °C to 0 °C, vapor pressure in the pore space with respect to ice, increases by 300 % (McClung and Schaerer, 1993). Temperature differences within a snow pack (temperature gradients) therefore cause vapor pressure gradients, which in turn cause water vapor fluxes that are a major driving mechanism for the snow's metamorphism. Water vapor is forced to move from warmer regions to colder regions, usually from a snow pack's base towards upper parts. It moves through the pore space by leaving one crystal at the top and condensing on some other crystal above. Which forms develop in this recrystallization process depends on the rate of vapor movement through the pore space. As vapor pressure is much harder to measure, temperature gradients are measured instead in avalanche research and for avalanche forecasting. Time scales of metamorphism differ between upper and lower parts of the snow pack as a result of different temperature settings. Dendritic crystal forms, for example, decompose ten times faster in common field conditions, where there is a temperature gradient, than they do under constant temperature conditions in a laboratory (McClung and Schaerer, 1993). Temperature gradients usually are highest in surface regions (McClung and Schaerer, 1993) and also time scales of metamorphism are faster than in lower parts of the snow cover. Whereas at the base, changes happen within weeks or even longer time spans (depending on the depth of a snow pack and the change rate of atmospheric conditions), changes close to the surface may take place within hours (Wiesinger, 1988).

Constructive and Destructive Snow Metamorphic Processes

Two major types of metamorphism of snow crystals, once fallen to the ground, can be distinguished. Depending on the magnitude of prevailing temperature gradients destructive or constructive metamorphosis takes place. Destructive metamorphism indicates rounding of crystals and leads to higher densities; constructive metamorphism causes facetted growth of crystals, destabilizes the snow pack and leads to density losses. Other influencing factors are the moisture content and also the size and geometry of the pore space. The way in which snow crystals develop within the snow pack strongly determines its future stability behavior. The snow cover can stabilize or destabilize depending on prevailing temperature settings. Weak layers or failure layers can disappear as a result of destructive metamorphism, they can develop through extensive constructive metamorphism and usually only do persist in cold conditions. Through recrystallization old snow can be weakened if temperature gradients are high and temperatures are low.

Growth rate and crystal form in seasonal snow packs do also depend on prevailing temperatures in a specific section, and on the local size of the pore space. The major determining factor however remains the temperature gradient, i.e. the vapor pressure gradient. At relatively high snow temperatures rounded crystals tend to develop when the temperature gradient is weak, when the gradient is strong, however, and when pore spaces are large enough, faceted grains or even cup shaped forms (depth hoar) can develop at very high growth rates. The critical temperature gradient is about 10 °C per meter. If the gradient is larger, growth of faceted forms is likely, if it is smaller more rounded forms tend to develop (McClung and Schaerer, 1993).

Prevailing temperature conditions in a specific section of the snow cover mainly define the rate of growth. When temperatures are generally low, growth rates are small and facetted forms, for example, do only form slowly. Often temperatures are only warm enough for cup crystals to form, near the base of the snow cover, close to the ground. This implicates, that in regions where snow accumulates throughout a season, depth hoar usually develops only in the beginning of winter, when snow depths are low and temperature gradients are high, also in the lowest parts of the snow pack. Later in the season surface hoar that forms when relatively moist air become oversaturated, when it moves over a cold snow surface, becomes more important. Further, near-surface facetted crystals can form as a result of radiation recrystalization and faceting adjacent to a wet layer (Birkeland, 1997, in Schweizer et al., 2003). The crystals develop as the result of a flux of water vapor at a high rate, condensing on cold surfaces. Surface hoar and near-surface facets become relevant in terms of avalanche danger when subsequent snowfall events bury it. The formation of facets above crusts and wet layers within the snow pack, when large temperature gradients are present are the only efficient processes to form weak layers within the snow pack (Colbeck and Jamieson, 2001). Together with buried surface- and near-surface hoar, depth hoar and faceted grains they constitute the major weaknesses within a snow pack's layer structure and their development and persistence are highly relevant in terms of avalanche danger.

Wet Snow

As long as snow pack temperatures or the temperatures of single layers in a snow pack are significantly below the freezing point it is generally referred to as dry snow. When temperatures get close to 0 °C their water content becomes important (McClung and Schaerer, 1993). Wet snow differs from dry snow in its metamorphism and in its stability behavior. Wet snow can either be of high or of low water content. In wet snow of low water content (about 3 % to 8 %) grain metamorphism is still controlled by water vapor fluxes. When it has a higher water content (more than 8 %) it is referred to as wet snow with a high water content or as water-saturated snow and particles grow as a result of heat flux through water. As long as the grain size distribution includes particles smaller than 1 mm growth rates of bigger grains on the expense of smaller grains are high. It decreases when average particle sizes increase with time. The most important stability factor in wet snow however not so much the shape of its grains is but is mostly defined by its moisture content. Water within the snow pack can induce avalanching in two ways. Either an increasing water content indicates that bonds between grains had melted, which causes a significant loss of cohesion within the snow pack, or melt water accumulates above confined layers (very dense layers or ice layers) or at the soil snow interface, reduces friction and leads to glide-induced avalanching. The strength of wet snow decreases significantly with increasing water content (McClung and Schaerer, 1993).

Bond Formation

Similar to metamorphism also bond formation between snow grains is driven by temperature- or vapor gradients. It is dependent on prevailing temperatures and pore space geometry. As thermodynamic processes occur faster at warmer temperatures bonds develop at higher rates when general temperatures are higher. Bond formation rates increase significantly with increasing snow temperatures as long as the snow pack is generally dry (temperatures below 0 °C). Cold temperatures support the development and persistence of snow with low cohesion (low bond strength). Bonds form as the result of the movement of water vapor between crystals and of molecular motion on the surfaces when crystals touch. Usually rounded grains do form more bonds than facetted grains. The extent and rate of bond formation strongly contributes to the snow's stabilization. With proceeding snow melt bonds between grains do melt as well and the snow significantly looses cohesion until in saturated snow almost no cohesion remains. This mechanism is responsible for wet loose snow avalanches (McClung and Schaerer, 1993). Techel and Pielmaier (2009) showed that already very small amounts of liquid water in facetted layers could cause avalanching.

Snow Metamorphism and Snow Stability

In terms of stability, rounded forms usually tend to pack closer, form more bonds and are more stable. Broken forms, as established when snow was transported by- or was precipitated during wind at high enough speeds, do even pack closer and form very densely packed layers. On the contrary, faceted grains, surface hoar and depth hoar may form layers of lower density, are more reluctant to bond formation and are relatively weak in shear. They constitute important structural weaknesses within a snow pack. The rate of bond formation immediately after precipitation is important in terms of loose snow avalanches as it determines how quickly cohesion rises within the new snow. Loose snow avalanching occurs if the down slope component of its weight due to new loads increases faster than internal cohesive forces and when, as a result, the snow on a slope reaches its critical angle of repose. The formation of weak layers consisting of faceted crystals or hoar and their persistence within the snowpack is important for the formation of slab avalanches in dry snow. The water content in snow and water accumulations within the snow pack and on the ground contributes to the formation of wet slab avalanches (McClung and Schaerer, 1993).

3.1.4 Temperature Related Snow Mechanical Properties

The mechanical properties of snow are depending on the arrangement and the type of grains, on their size and on the numbers of bonds between them (Schweizer et al, 2003). As described earlier (chapter 3.1.3.) bond formation and grain shapes and sizes are strongly controlled by the snow pack's temperature settings (temperatures and temperature gradients). To a large extent the rate and the magnitude of the responsible stresses determine how deformations and failures within layers develop, but temperatures also significantly influence these processes.

In dry snow (cold snow) slabs release due to the propagation of brittle shear fractures, in wet snow (warm snow) they are initiated through glide-induced tensile fractures when slush can be found in a failure layer. Dry loose-snow-avalanches are most likely to form when major snowfall events go along with cold temperatures, which hinder rapid bond formation and settling, hence prevent the development of strong cohesion within the new snow. Wet loose-snow-avalanches become likely when, at times of warm snow and high air temperatures, local or widespread high water contents within the snow cover develop (McClung and Schaerer, 1993).

Temperatures During Sow Fall

As a porous material, which exists close to its melting point (McClung and Schaerer, 1993, Schweizer et al., 2003), seasonal snow, throughout its entire life span, from precipitation through melting is strongly influenced in its condition by temperatures. The trend and the mean value in air temperatures during a storm are important to avalanche formation, as they determine the temperature of the snow that is deposited. When strong rises in air temperatures happen during a storm, warm snow will be deposited over cold, more instable snow, which is conducive to later slab formation. Long-term observations of avalanche occurrences in Alta, Utah showed that hazard probabilities increased with maximum temperature changes during a storm (McClung and Schaerer, 1993).

Temperature Influences on New Snow's Stability

Freshly fallen snow settles faster under warmer conditions and sintering (bond formation) takes place at a much faster rate. Both processes are important for the development of cohesion in new snow, hence strongly determine its stability and the new snow cover's friction angle. Along with the type of grain size and crystal types of newly fallen snow it strongly depends on the snow's temperature, whether dry loose snow avalanches are likely to develop or not (McClung and Schaerer, 1993, McClung and Schweizer, 1996).

Temperature Influences on a Dry Snow Covers' Mechanical Properties

Dry seasonal snow is influenced by temperatures in two ways, which mainly differ in their time scales and which operate in opposite directions for a given temperature. Temperature gradients influence the type and the rate of snow-metamorphic processes. Temperatures determine how long existing or developing weaknesses (facets or sufaceand depth hoar) can persist and they also control creep rates and accordingly the rate of the snow's densification. These processes contribute to an increase in snow stability during warming but usually do take considerably long times. Especially strength increases within a buried weak layer due to warming of the snow pack may set in with quite some delay (McClung and Schweizer, 1996). As already described (chapter 3.1.3.) warming leads to higher rates of bond formation, it supports creep rates and snow settlement and usually also results in smaller temperature gradients, hence prevents the formation of strongly facetted grains. However, after rapid warming, surface layers may, compared to a subjacent layer, experience increased deformation because of larger creep rates. Instabilities can develop as this can lead to increased strain and strain rates at a weak layer below (McClung and Schaerer, 1993, McClung and Schweizer, 1996, Schweizer et al., 2003).

The mechanical properties of a snow cover; its strength, its failure toughness and especially its stiffness (hardness) are also highly temperature dependent, but react rapidly on temperature changes. Whereas metamorphic processes and creep rates positively affect snow-pack stability with rising temperatures, the mechanical properties do change in an unfavorable direction in terms of strength, when the snow gets warmer. Shear strength decreases with increasing strain-rate and with increasing temperature (Schweizer et al., 2003). The snow gets weaker and significantly looses stiffness. Stiffness, which is a material's initial resistance to deformation, as for example caused by additional loading through a skier, is the mechanical property, which is most sensitive to changes in temperature (McClung and Schweizer, 1996). It increases by a factor of three as the snow temperature decreases from -2 to -15 °C during slow shearing (McClung and Schaerer, 1993) On the long term, however, hardness increases with rising temperatures as warm temperatures promote sintering, settlement and densification (McClung and Schweizer, 1999). Camponovo and Schweizer (2001) found that a snow cover's dynamic shear modulus decreases with rising temperatures, following an Arrhenius relation up to -6 °C to then decrease much faster toward 0 °C. The modulus and its variation is important when determining, for example, travel safety for skiers, as it has a strong influence on the penetration of surface loads deeper into the snow pack. Further, the modulus also has an influence on the probability of fracture propagation (in Schweizer et al., 2003). The strength of weak layers decreases with increasing temperatures. However, at the same time fracture propagation, due to increasing fracture toughness with increasing temperatures, becomes less probable (Schweizer et al., 2003) and requires significantly more energy than in colder snow (McClung and Schaerer, 1993). This is important, for example, when using explosives to trigger controlled avalanching, as it becomes difficult to induce the release of slabs by applying localized, rapid loads when temperatures get too warm (Schweizer et al., 2003). Dry slab avalanches form when stresses exceed the shear strength in a weak layer and cause fast enough deformation to induce fractures in a rather stable slab above, which consequently avalanches. Stresses in a weak layer can either be caused by the down-slope component (weight) of the snow above, by the penetration of additional surface loadings (as for example a skier) or by stresses resulting from deformations of overlying layers, initiated by rapid warming and according larger creep rates (McClung and Schaerer, 1993, Schweizer et al., 2003).

Whether warming leads to stabilization or destabilization of a dry snow pack through changes in its mechanical properties depends on the pack's general layering structure and on its current physical state. Depending on the horizontal configuration (spatial variability and extent of weak layers) and vertical structure (layering characteristics) of the snow cover, as well as its initial (previous) temperature settings, either positive or negative effects may dominate. On the one hand a snow pack gets weaker, and, as its dynamic shear modulus decreases with rising temperatures, stresses caused by surface loadings (as for example skiers) may penetrate deeper into the snow pack, hence it is more likely that a weak layer is affected. On the other hand, colder and harder snow is of a more brittle character and therefore allows easier, and quicker propagation of fractures, which are a major contributing factor to the formation of dry slab avalanches.

Temperature Influences on Wet Snow's Mechanical Properties

Once the snow pack or its upper layers get warmer and temperatures get closer to the melting point, the danger of wet slab-avalanche formation arises at times when air temperatures and incoming short wave radiation are high. Water within the snow pack can either originate from precipitation (rain) or from melting snow, caused by the effect of warm temperatures and short-wave radiation on snow close to 0 °C. Water from precipitation can cause additional loading and melt- and rain water, when penetrating deep enough into the snow cover to reach a weak layer, may change its strength. When water accumulates above a confined layer within the snow pack, as for example a buried surface crust, or in a fine-grained layer above a coarser grained layer, dangerous sliding surfaces develop. All these processes may result in the formation of wet slab-avalanches (McClung and Schaerer, 1993).

Basal snow pack temperatures are of relevance in avalanche research as a temperature of exactly 0 °C is a prerequisite for the existence of free water at the soil snow interface. Free water significantly reduces friction and if existing at the base of a snow pack may induce full-depth slab-avalanches, which are one of the major causes for avalanche hazards in spring. As heat transport in snow is very slow, temperatures at the base of a snow pack do not necessarily have to correspond to air temperatures. It is documented that water at the base of a snow pack has initiated full-depth avalanches during times when air temperatures were below –10 °C (McClung and Schaerer, 1993). Earlier melting periods, warm basal snow pack temperatures as a result of geothermal heat and water from groundwater or surface water could be reasons for such events (McClung and Schaerer, 1993).

It is important to know when a snow pack becomes isothermal. Then, at times of warm air temperatures and, even more, due to incoming short wave radiation, heavy snowmelt can rapidly increase a snow pack's water content, which, apart from reducing its friction on the ground, also reduces its stiffness and allows easier creep over ground roughness features. It is recommended for avalanche forecasters to monitor snow pack temperatures with an increased accuracy once they get close to the melting point. While in general accuracies of +/- 0.5 °C seem to be sufficient, once temperatures are between -1 and 0 °C a measurement accuracy of +/- 0.1 °C is desirable (McClung and Schaerer, 1993).

When snow melt sets in, and when water contents in the snow cover or within its upper layers increase, wet loose-snow avalanches become more probable. Water saturated snow is almost of a cohesionless character, as all bonds between grains are melted. As mentioned above, static friction angles are larger in warmer snow, as it usually forms more bonds and has a higher density and as a result has larger cohesion. However, when water contents increase, as for example due to increasing temperatures and related melting in warm snow, the snow gets wet, bonds melt and friction angles decrease dramatically (McClung and Schaerer, 1993). As a result, water saturated snow is highly unstable and poses a major avalanche danger during snowmelt in spring.

3.2 TEMPORAL AND SPATIAL VARIABILITY OF SNOW PACK PROPERITES

The current state of a snow pack at a certain point in time and at a certain location is defined by metrological and physical processes, which act over different spatial scales and which are variable in time. Therefore an alpine seasonal snow cover is highly inhomogeneous – in time and in space (Schweizer et al., 2008, Schweizer et al. 2003). Snow avalanches are complex phenomena. Small changes in individual components of the snow's condition can result in different activity and different snow strength characteristics (Hägeli, 2004). The formation of avalanches is the result of interactions between terrain, variable snow pack conditions and variable meteorological conditions. These parameters control the snow's mechanical properties as well as their distribution and evolution, which in turn determine whether avalanching occurs at a certain point in time and space, or not.

3.2.1 Characteristic's of a Snow Cover's Variability

Different Rates and Scales

The rate and type of changes of a particular snow property's spatial variability over time is expected to correlate to the magnitude of the scale and the type of forcing (influencing factor) that drives the change (radiation influences, changing air temperatures), and also on its interactions with terrain features. A profound understanding of all these processes and of their interactions and scales would be necessary to identify weaknesses or deficit zones and trigger points on very small scales (Schweizer et al., 2008) and as a result allow detailed danger forecasts, i.e. the prediction of exact locations and timings of avalanche releases. Each slope contains weak and strong spots that cannot be precisely located (McClung and Schaerer, 1993). Local weaknesses can have a destabilizing, so called, knock-down effect on a whole slope's strength (Schweizer et al, 2003). A snow pack can vary in a multimode of parameters including snow depths, snow surface characteristics (distribution of surface hoar or ice layers) and weak layer characteristics and their distribution (www.slf.ch[3]). Depending on the types of the major influencing processes, correlation lengths may vary (Schweizer et al., 2008, Schweizer et al. 2003). In other words, a snow pack's properties can vary in space, in time and can also vary differently over time in different locations. Further, the scales over which properties vary are inhomogeneous and are expected to depend on the scale of the influencing meteorological and physical processes and on their interactions with terrain features (Schweizer et al., 2003, Hägeli, 2004).

External and Internal Causes of a Snow Cover's Properties' Variability on Small Scales

Schweizer et al. (2008) differentiate between external and internal causes for snow cover variability, which either affect the snow during or after deposition. External causes for variability that act during deposition would be precipitation patterns, sublimation and wind effects; radiation, air temperatures and again wind act after deposition (Schweizer et al., 2008). Irregularities within the snow pack develop when the controlling internal and external causes vary in space or in time. As the most prominent internally acting factor Schweizer et al. (2008) name differences in snow metamorphism, which in turn are caused by variations in external factors, mainly through their influences on differences in snow pack temperatures and temperature gradients. Irregular infiltration of melt-water and rainwater and its flow paths may also lead to internal heterogeneities (Schneebeli, 1995 in Schweizer et al., 2008). Mainly though it is the changing of radiation- and wind conditions due to terrain effects, that cause a strong spatial variability in snow properties on a slope scale. Changes in time, in a single spot or in variability characteristics of an entire slope, mostly happen because of temporal changes in the balance between incoming and outgoing radiation and also due to varying ambient air temperatures (Schweizer et al., 2008, www.slf.ch[3]).

Radiation controls the energy balance at the snow surface and strongly influences temperatures in upper layers of the snow cover. For example, the formation and distribution of surface hoar are mainly controlled by radiation influences. Wind controls snow-distribution and redistribution, and accordingly snow depths, layer thicknesses and their positions, and also has an influence on crystal forms, as snow crystals may be broken into densely packing fragments when they are transported by wind of high enough speed.

Wind speeds and directions, as well as the formation of eddies are highly dependent on terrain features and topography. Snow generally gets picked up at locations of acceleration and high wind speeds and is deposited where wind speeds decelerate. As a result, terrain induces variations in snow deposition patterns (McClung, 2002b). The threshold wind speed for snow redistribution depends on the snow’s temperature and humidity (McClung and Schaerer, 1993).

Terrain and vegetation contribute to variations in a snow pack’s characteristics mainly through their influences on wind and radiation but also have an influence on the snow pack itself. Obstacles affect snow drifting and temperatures in their vicinity (McClung and Schaerer, 1993). Rocky outcrops and slightly covered rocks readily absorb incoming short-wave radiation and can cause horizontal temperature gradients, which may lead to the growth of facetted crystals (chapter 3.1.1. and 3.1.3.). Snow interception, in forests and under trees, modifies the snow surface and may prevent weak layer formation and also changes the distribution and accumulation rate of new snow during a storm (Schweizer et al. 2003). Precipitation amounts may vary with elevation due to orographic effects and also as the result of terrain influences. Snowfall amounts can vary by a factor of 10 over less than 1km due to topographic influences (topographic convergence, lifting, subsidence, shadowing) (McClung and Schaerer, 1993, McClung, 2002b). Haegeli and McClung (2004) suggest that it is the terrain effects on snow-cover variability that are the major source of uncertainty in avalanche forecasting.

Temporal Changes In Spatial Variability of Snow Cover Properties

Snow-internal processes, controlled by interactions between radiation and terrain features are the strongest driving forces for the temporally variable character of spatial variations in snow cover properties. For example weak-layer-strengthening can take place at different rates in different locations as the snow is exposed to spatially variable temperature gradients, which are caused by differences in radiation influences or in snow depth (Schweizer et al., 2008). Depending on temporally variable processes, such as weather effects (existence, extent and thickness of cloud cover) and the variation of incoming radiation throughout a season, the energy balance at a snow surface, and also the character of its interactions with terrain features, vary in time. Kozak et al. (2002) calculated amounts of incoming short wave radiation for south- and north-facing slopes. Whereas for both aspects radiation increased from January through March, the magnitude of difference in incoming radiation between the two slopes decreased with the proceeding season. The south-aspect in general received considerably more radiation (Kozak et al., 2002).

On a cloudy day terrain effects that cause shading of a slope, or of certain parts of it, would not lead to significant spatial variability of the snow cover, during clear sky conditions snow properties might vary strongly due to different radiation influences. Shaded spots on a slope would cool off because of energy losses through outgoing long wave radiation, while upper layers in locations exposed to the sun would warm up due to incoming short wave radiation (McClung and Schaerer, 1993). An energy balance for any aspect, slope angle and elevation can be calculated for any time of the year (Durand et al., 1999 in Schweizer et al., 2003) but shading effects, reflections from surrounding slopes and emission from surrounding terrain may lead to irregularities in the snow cover's energy balance and may cause deviations from calculated values in reality (McClung and Schaerer, 1993, Schweizer et al., 2003). As a result of reflection on the side, snow in gullies, for example, receives more heat from incoming radiation than open slopes and it loses heat through outgoing long wave radiation at a slower rate. Therefore snow in gullies destabilizes faster at times of incoming short-wave radiation and regains strength slower through outgoing long-wave radiation during nights. Differences in snow conditions between gullies and open slopes are much stronger on clear days in spring, when rates of incoming short-wave radiation are high, than they would be, for example, in mid-winter or on a cloudy day (McClung and Schaerer, 1993). So far these influences are only known in a qualitative sense (Schweizer et al., 2008, www.slf.ch[3]).

3.2.2 Relevance of a Snow Cover's Variability to Avalanche Forecasting

The variability of a snow pack's layering structure is relevant to avalanche forecasting in two ways. It determines to which extent extrapolations from measurement locations are valid and it influences fracture propagation. As the goal is to identify possible locations of locally concentrated trigger spots within an area, detailed point-to-point extrapolations and interpretation of individual observations are necessary (Hägeli, 2004). The similarity of locations determines whether extrapolation is possible. To assess different locations' similarity, in turn, requires detailed knowledge about the influencing parameters' variability and also about typical correlation lengths of measured snow pack properties. Therefore basic knowledge about scale characteristics of snow pack stability or of its influencing parameters is fundamental for further development of appropriate monitoring networks and useful forecasting models (Hägeli, 2004). Currently there is still a lack of knowledge about the conditions under which snow pack properties can be extrapolated and over which distances extrapolations can be considered to be reliable (Hägeli, 2004).

The variability within the snow and its layering structure also influences fracture propagation and consequently controls slab avalanche formation (Schweizer et al., 2008). It also depends on the character of the snow's variability-pattern whether fractures, once they were initiated in a single point, can propagate far across the slope or whether they get stopped in areas of changed snow- and layer characteristics. According to Hendrikx et al. (2009) conditions for fracture propagation are highly variable on the slope scale, but the exact amount of variability and its changes in time have been a subject of debate.

Knowledge about spatial variations and according correlation lengths is important when choosing representative sample spots in slope-stability observations. And the combination of temporal and spatial variability – the temporal changes in spatial variation – are important for avalanche practitioners who issue warnings, as it informs them to which extent observed patterns tend to persist over time (Hendrikx et al., 2009).

For given slopes the degree of spatial variability is currently not known, neither is known how it changes over time, or how it changes in relation to environmental factors. No reliable guidance exists for avalanche practitioners and observers to identify typical correlation lengths when conducting their measurements (Hendrikx, et al., 2009, Schweizer et al., 2008).

3.2.3 Studying Snow Cover Variability – A Brief Literature Review

In forecasting on the micro scale (individual slopes), which is the most relevant for temporary protection of traffic lines, villages, skiing resorts and especially for backcountry travelers, decisions are supported by information on a regional scale issued by avalanche warning services. Members of local avalanche committees, and also sometimes backcountry travelers, may also carry out their own local stability observations. Then, to assess avalanche risks, these observations and information need to be extrapolated, with respect to a careful analysis of the terrain and of current weather data (McClung and Schaerer, 1993). Due to the snow pack's high variability the extrapolation of results from single point measurements found at an earlier point in time may involve large uncertainties. Stability tests, as for example the Rutschblock test or the extended column test, which directly reveal information about a snow pack's strength, are limited to small areas and to a low temporal resolution. As they are time intensive, it is barely feasible to perform these tests at a high spatial distribution and on a frequent regular basis in practice, i.e. several times each day in regular avalanche forecasting. Therefore, when employing direct methods to measure stability, it is difficult to resolve diurnal variations in a slope's stability distribution or to track the snow stability's reaction on (quick) weather changes in various locations at the same time.

In recent years numerous field studies were conducted in avalanche research to gain better understanding of spatial and temporal variability of snow stability, or of particular contributing factors (e.g. Deems, 2002, Kozak et al. 2003, Landry et al., 2004, www.slf.ch[3]). Further, though to a much lesser extent, research was conducted in order to investigate the changes in the snow pack's variability over time (Birkeland and Landry, 2002, Hendrikx et al., 2009). Mainly the data from field observations was used for geo-statistical analyses in order to test possible autocorrelations and, if such existed, to derive typical correlation lengths (Hendrikx et al., 2009). Recent studies revealed mixed results; some slopes showed autocorrelations while others did not. When an autocorrelation was found, typical correlation length scales were in the order of several meters, from smaller than 0.5 meters to more than 10 meters (Hendrikx et al., 2009). Schweizer et al. (2008) provide a review of research on spatial variability of snow pack properties and its importance for avalanche formation. Most studies that were based on a slope scale, directly investigated the variability of the snow's strength and stability, employing shear strength- or shear frame measurements, Rutschblock-, Stuffblock- or drop hammer tests or measured the penetration resistance in various locations (Schweizer et al., 2008). Teufelsbauer (2009) and Deems (2002) studied temperature variations in the snow cover. Deems (2002) tried to assess topographic effects on the spatial and temporal patterns of snow temperature gradients. Teufelsbauer (2009) simulated temperature distributions on a two-dimensional slope section.

Birkeland and Landry (2002) were the first to suggest that spatial variability of fallen snow might increase through time, but as their work was based on limited data, they could not form strong conclusions (Hendrikx et al., 2009). Logan et al. (2007) studied the temporal changes in spatial variability of shear strength of buried surface hoar layers at the slope scale. Hendrikx et al. (2009) assessed the temporal changes in the spatial variability of the snow pack fracture propagation propensity over time and were the first to statistically demonstrate temporal changes in snow pack spatial variability at the slope scale (Hendrikx et al., 2009). The goal of their work was to identify beneficial spacing to minimize false stability results and to help develop guidance for observers to well chose their observation points (Hendrikx et al., 2009). They showed that the spatial distribution of fracture propagation propensity within a slope changed in time from a random pattern to a spatially more organized pattern. They had measured on two separate days in two different sample spots. Extended column tests, conducted in a 10-

meter raster across the sampling-slope, were employed to measure fracture propagation propensity. The results revealed that data from the second sample day in both spots showed a spatially organized pattern, while data from the first sample days did not (Hendrikx et al., 2009). They concluded that the extent of the correlation of snow properties and the variability of the snow's stability behavior across a single slope does vary in time. Further conclusions were limited as there was not enough data available to, for example, gain insight in diurnal fluctuations or to derive more precise statements about correlation lengths and their variation in time. Also they mention that measurements on the first sample days might have had an impact on observed results on the second sample days as tests were taken on the same slopes. It is difficult to gather data from extended column tests at a high frequency in time, as they are labor intensive and time consuming. Also the number of tests that can be conducted on a single slope is limited, as those measurements disturb the snow pack and therefore should not be carried out again in exactly the same spot (Hendrikx et al., 2009).

Another problem with many direct stability tests is that in many cases they only provide qualitative data that is strongly depending on the observer's perception and therefore does not yield good input data for numerical models (McClung and Schaerer, 1993). Meteorological data - air temperatures, incoming and outgoing radiation and also wind speeds and directions, can automatically be measured and provide numerical data at high temporal resolutions, however, most of it measured outside of the snow pack. Findings about their correlations to snow- pack or layer properties could allow the reproduction of diurnal fluctuations and rapid changes in snow properties through snow-cover modeling.

Kozak et al. (2002) examined which meteorological variables influenced temporal changes in new and old snow layer hardness (initial resistance to deformation) on a north facing and on a south facing slope. They studied the influence of a temperature index, which was created to represent delayed effects temperatures have on snow hardness. Increasing temperatures cause increasing settlement, densification and sintering when they slowly warm the snow pack. The index was found to be a significant predictor for old snow layer hardness. It included the maximum ambient air temperature of each day of measuring and also took into account for how long (how many days) warm temperatures persisted, as it was suspected that warm or cold temperatures over a multiple day-period are also having a cumulative effect on changes in snow layer hardness. Using ram penetrometers a new snow layer's hardness was measured between 2 and 8 days after deposition and was tracked until it was buried by new snowfall or until it could not be differentiated from older snow beneath it any more. Old snow layers were monitored over the course of the three-month study period (Kozak et al, 2002). Three weather stations recorded weather data including air temperature, wind speed and direction. Also thermometers recorded maximum and minimum air temperatures directly at the study plots. Daily incoming short wave radiation was measured with a pyranometer at one weather station; an index to derive the percentage of maximum incoming short wave radiation that reached the study plots on south- and north-facing slopes was employed, as measurements were not available (Kozak et al., 2002). They found that some old layers showed similar behavior on north and south slopes, while others did differ in their evolution. They attributed this complex behavior of different stability developments in different locations to vertically strongly variable temperature gradients within the snow pack and to differences in these patterns between different locations.

Teufelsbauer (2009) simulated the temperature distribution at a slope-section with varying inclination and snow depths using a two-dimensional snow cover model, which is able to simulate temperatures and densities in two-dimensional cross sections on any chosen slope. Modeled snow temperatures within the snow pack varied by 5 to 10 °C between two sections of the same exposition and of a similar incline. Teufelsbauer (2009) suggested that these differences were mainly the result of differences in snow depth. He found that, while temperature variations at the surface seemed to strongly correlate to changes in slope-incline, changes deeper in the snow pack seemed to be more related to snow depths (Teufelsbauer, 2009). Validations of Teufelsbauer's suggestions through distributed temperature measurements have yet to be conducted.

Deems (2002) observed temperature gradients (profile temperatures) in 30 sample points on each of nine sampling days, and attempted to explain their spatial variation through the use of topographic variables. He designed a 2,3 meters long profile probe of polycarbonate plastic with an aluminum cutting cup for snow pack penetration, which allowed quick temperature measurements along the snow profile and was easily portable between single sampling spots. Terrain variables included the rate of change in slope, the rate of change in aspect, elevation, canopy density and solar radiation input. He found that diurnal fluctuations in air temperatures affected temperatures in the upmost parts of the snow pack. As only one profile probe was available it was not possible to measure at the same time in all sampling spots. Therefore the upper 30cm of the snow pack were excluded from the analysis. Deems calculated a temperature gradient for every 10cm in the snow pack and derived an average temperature gradient and a maximum temperature gradient for each profile and every measuring day. He found that terrain influences correlated to temperature settings in the snow but did not explain the full range of average- and maximum temperature gradient data. Deems concluded that static terrain features alone cannot account for the overall variability in spatial patterns of temperature gradients. He claims that more dynamic processes, such as weather influences are probably responsible for the variability that remained unexplained in his analysis. Further, he showed that temperature gradient's correlation to terrain features varied in time. For some days topographic variables were strongly related to the observed spatial pattern, on other days gradients seemed to be rather independent from terrain influences. In a qualitative analysis of these dynamic weather influences he found that fluctuations in air temperatures and in short wave radiation seemed particularly relevant. Differences between cloudy days and clear periods could be identified. In regression models for measured temperatures following clear periods, solar and canopy variables were included; during cloudy periods these variables did not show significant influence on spatial patterns of gradients. For a complete description of his analysis see Deems (2002). In his outlook for further research Deems calls for analyses of dynamic, potentially non-linear interactions with atmospheric conditions as models that only include static parameters might fall short of explaining and predicting the true level of spatial variability in the snow cover. In order to provide reliable results much larger data sets and sampling in more data points would have been necessary. He suggests the application of several profile probes and of more people to collect data in the field (Deems, 2002).

3.3 MEASURING AND MODELLING SNOW PACK TEMPERATURES

As variable temperature settings are a major contributing factor to the snow stability's spatial and temporal distribution, better prediction of temporal and spatial variability of the temperatures within a snow cover could help improve micro-scale avalanche forecasts. A better understanding of spatial scales, temporal changes and of how temporal and spatial variations correspond to terrain features, vegetation and variable snow-depths on the scale of a slope could help reduce uncertainties when extrapolating measured or modeled snow pack-temperatures from single observation points to avalanche relevant terrain. Knowledge about how snow temperature settings and their variability patterns react on changes in influencing meteorological parameters is important to determine over which time spans forecasts can be trusted.

3.3.1 Standard Methods for In-situ Temperature Measurements in Snow

All in-situ measurements can be disturbed by solar radiation and heat transport from the surface. Also they can be irritated by air or water influences. Some probes, and especially loggers, are sensitive to wetness, and air influences can cause poor thermal contact between the measured medium and a device. The design of sensors should provide a good contact with the surrounding snow, they should have a high albedo i.e. influences from solar radiation should be kept at a minimum (Gerland et al., 2001).

Snow Pits

The conventional method of measuring the temperature settings within a seasonal snow cover is to manually measure temperatures versus depth in vertical snow pits. A snow pit is a trench exposing a flat, vertical snow face from the ground to the snow surface. Pits are routinely used to assess a snow pack's layering structure and also to measure layer properties, snow density, temperatures and water content (http://www.nasa.gov/pdf/186123main_SnowPitProcedures.pdf). The face of a snow pit should always be protected from direct sunlight, and when measuring temperatures additional protections against solar radiation, for example plastic sheets on the snow surface, can be useful (Gerland et al., 2001). Measurements should be started at the upper end of a profile, as influences of ambient air temperatures eventually change the exposed snow's properties, especially within surface layers. The temperatures are usually measured by pushing a thermistor or a thermometer parallel to the slope in the vertical face (McClung and Schaerer, 1993, Gerland et al. 2001). Usually measurements are taken every 5, 10 or 20cm, depending on the total depth of the snow pack and on the scope of the observations. Thermometers or thermistors with accuracies of 0.5 °C are standard, for both air- and snow temperature measurements during snow cover observations (McClung and Schaerer, 1993). When temperatures are between 0 and -1° C, exact temperatures become more important as they are an indicator for the snow's water content and an accuracy of 0.1 °C is desired (McClung and Schaerer, 1993). Thermistor probes provide a higher temporal resolution than thermometers, however, they are very expensive. Frequent calibration of the probes and thermometers in ice-slush baths are necessary in order to achieve reliable results (McClung and Schaerer, 1993).

An advantage of manual measurements is that vertical spatial resolution can be adjusted spontaneously and can be as high as desired. Also, as pits reveal more information about a snow pack than only snow temperatures, they allow other observations of physical and structural properties of the snow, which can be useful for the interpretation of the measured temperature settings. The greatest disadvantage of snow-pit measurements is the low temporal resolution of observations. Diurnal fluctuations and rapid changes cannot be captured with this method. Even though the snow pack's original structure changes on a pit wall shortly after it was freed, when measuring immediately after excavation, the layer structure should be found undisturbed. However, it is not possible to measure snow temperatures several times in the exact same spot when pristine snow is wanted for all observations as pits irreversibly destroy the snow's original layer properties in a sampling spot. They are time consuming and labor intensive, sometimes hard to conduct during bad weather conditions (Gerland et al., 2001) and sometimes accessing a measurement site could be dangerous.

Thermistor Strings

Automatic measurements can be taken with thermistor strings, which are connected to a data logger. The thermistors can, for example, be installed permanently on stakes before the first snowfall sets in or they can be deployed individually within the snow pack during the course of a season, which allows monitoring temperature evolutions in individual layers. It is recommended to protect them against harmful water influences and disturbances from solar radiation, for example, through covering the snow on the top of a pit with a plastic plane, or by cladding thermistors with materials that are waterproof and have a high albedo. Thermistors typically provide an accuracy of about +/- 0.4 °C (Gerland et al., 2001). Advantages of automatic in-situ measurements include the fact that they can be conducted in exactly the same spot throughout the entire course of a season, at a high temporal resolution, allowing observing diurnal fluctuations and fast temperature changes. They can show how far fluctuations and changes reach in depth at a specific point in time. However, automatic measurements are much more cost intensive, hence for financial reasons often can only be conducted on a very limited amount of points in space. Spatially distributed measurements of vertical snow pack temperatures through permanently installed thermistor strings would require the installation of a large number of thermistor probes and data loggers in the snow and permanently installed set-ups (stakes) for automatic measurements can affect the snow's natural layering and deposition pattern during and after precipitation (Gerland et al., 2001).

Both, the snapshot character of manual measurements, not allowing to analyze diurnal and weather-dependent temperature changes and the limited opportunities to conduct areal measurements with automatic string set-ups often set limits to monitoring studies

(Gerland et al., 2001). In order to overcome these shortcomings attempts have been made to model snow-pack properties (Durand et al., 1999, Lehning et al., 1999) and devices that allow a quicker manual assessment (Wiesinger, 1988, Mayr, 2006, Deems, 2002) or enable cheaper automatic measurements (Lundquist, 2008, Lundquist and Rochford, 2007) of snow-pack temperature settings have been developed and tested.

3.3.2 Snow Cover Models

One-Dimensional Models

Various numerical physical and empirical models have been developed, for both, hydrologic applications and for avalanche research and forecasting, to model snow pack properties, including temperatures. The Swiss SNOW PACK (Bartelt et al., 2002, Lehning et al., 2002a, Lehning et al. 2002b), the French CROCUS (Brun et al., 1989, Brun et al., 1992, Durand et al., 1999) and SNTHERM, developed in the United States (Jordan, 1991), are one-dimensional models, which employ numerical solutions to derive snow pack properties in a vertical direction at single points of the snow cover. The primary outputs of these models are attempts to predict profiles of snow temperature, snow density, grain size or snow type (CROCUS) and liquid water content (http://imgi.uibk.ac.at/iceclim/snowmodelling) of individual layers. SNTHERM further provides results for surface fluxes of sensible heat and evaporation and temperature profiles for the soil below as well as frost depths (http://imgi.uibk.ac.at/iceclim/snowmodelling). The models use meteorological input data to calculate the physical state of the snow cover. Temperatures within the snow pack are calculated in order to derive the snow pack's microstructure, which in turn is determining its mechanical behavior. Further the onset of isothermal properties within the snow cover is important to model snowmelt and to predict dangers of wet snow avalanches. Input data usually consists of meteorological factors that can be automatically measured at weather stations. Temperature settings within the snow cover are calculated, with respect to surface and ground temperatures and a snow cover's current physical state (especially density), which determines its effective thermal conductivity. When measured temperatures within the snow pack are available, they are used for model validation rather than in form of input data (Bartelt et al., 2002).

These models are mainly used to fill observation gaps and to allow estimates of snowmelt amounts and of avalanche dangers. They provide high temporal resolution of temperature data, but again, limited by the number of available weather stations, spatial distributions remain too low to help reduce uncertainties in micro-scale avalanche forecasting. Spatial snow cover variability can only be reproduced on a regional scale as a result of regional differences in meteorological conditions. A significant advantage, compared to manual measurements, however, is the fact the weather stations can be positioned at mountaintops close to avalanche starting zones and in areas that cannot be accessed during winter and therefore can provide input data from remote locations.

Distributed Models

In avalanche research attempts have been made to extend model simulations to derive spatial and temporal variability of snow cover properties on smaller scales. The WSL/SLF in Switzerland developed ALPINE 3D, which combines three-dimensional meteorological input data that is computed with respect to terrain effects, with modeled snowdrift and a network of one-dimensional SNOW PACK simulations. The goal is to derive information about variations in snow cover properties (http://www.wsl.ch/forschung/forschungsprojekte/Alpine/index_EN?redir=1&). However, this model has mainly been used so far to estimate expected runoff from snow covers in alpine terrain.

Supported by the Austrian Torrent and Avalanche Control Service, a two - dimensional physical model, which should allow capturing small variations in snow temperatures and its stability behavior on the slope scale, was developed at the Institute of Mountain Risk Engineering in Vienna (Teufelsbauer, 2009). It uses three dimensional laser scanning data to solve the problem of generating realistic and physically relevant model domains (Prokop, 2008, Prokop et al., 2008). Temperature distributions, densities and snow settlements and stresses can be predicted for two-dimensional cross sections of slopes with complicated snow depth distributions. The model is based on partial differential equations that are solved using an FEM method with triangular elements. Automatic weather stations and LIDAR-data are needed to provide the required input information. Cross – section geometries can be adapted to new snow distributions caused by snow drifting or freshly fallen snow and the governing model equations can be solved on time-variable geometries. Small-scaled temperature differences on any slope of known snow cover geometry, which establish due to differences in exposition, inclination or snow depth, can be located. Vegetation effects and shading from terrain features are not considered. So far the model was only validated through quasi-one-dimensional simulations, as only point measurements were available as reference data (Teufelsbauer, 2009).

3.3.3 Special Temperature Devices

Profile Probes

Wiesinger (1988), Deems (2002) and Mayr (2006) employed temperature profile probes that allow quick manual measurements of temperature profiles without freeing a pit wall. Depending on the number of probes and people available, spatially distributed observations are to a certain extent possible. Usually the probes consist of a stake that is equipped with some form of cutting cup to support its penetration into the snow. Sensors that are installed on the stake measure temperatures in predetermined snow depths of any desired resolution. Again, in the upper 30cm of the snow pack results are not reliable due to irritating effects from solar radiation (Deems, 2002, Mayr, 2006). This data can either be excluded form analyses (Deems, 2002), corrected through additional measurements (Wiesinger, 1988) or it can be tried to protect the upper layers of the snow pack from radiation influences (Mayr, 2006). Regular calibrations before measuring in the field and good thermal contact during observations are important to gain solid data sets and it is necessary to assess the sensor's equilibration time, which is needed until it has adapted to the snow's temperature (Deems, 2002, Wiesinger, 1988). Probes can either be designed in a portable manner so that one portable probe can be used to measure in various spots (Deems, 2002, Mayr, 2006), or a larger number of probes can be piled into the snow in several locations to remain there for a longer time (Wiesinger, 1988). Permanently installed probes, if equipped with a data logger usually provide better temporal resolutions. For financial reasons, however, spatial resolutions then often are limited. Wiesinger (1988) also mentions that, if the sensors are installed in avalanche starting zones or in alpine locations exposed to extreme weather conditions, there is a significant risk that they get damaged or destroyed. Data loggers, if available, usually need to be carefully protected from direct contact with water.

An important disadvantage shared by all manual measurement techniques is that bad weather conditions and avalanche dangers might prevent researchers from accessing their sampling sites. Therefore manual measurements are limited to certain areas and meteorological conditions (Bartelt and Lehning, 2002).

Low-Cost Self-Recording Sensors

Lundquist (2008) and Lundquist and Rochford (2007) used low-cost self-recording temperature devices to measure temperatures at high spatial and temporal distributions. Their observations however focused on hydrologic applications. Sensors were buried slightly below the soil surface to monitor snowmelt patterns in spring (Lundquist, 2008) and were used to study correlations of spatial patterns in air temperatures to terrain-, vegetation- and radiation influences and of temporal temperature patterns to weather influences in mountainous terrain (Lundquist and Rochford, 2007). Examples for commercial products of low-cost self-recording temperature sensors are Onset HOBOs, Tidbits and Pendants (www.onsetcomp.com) and Maxim iButtonsons (www.maxim-ic.comp). Costs for such sensors range between 30$ and 100$. They provide accuracies of better than +/- 0.5 °C and can record hourly data for more than a year. Waterproof examples are available (Onset Tidbits). The applicability of low-cost self-storage temperature sensors to measure temperature settings for entire snow profiles, as needed in avalanche research, has not been tested so far. Measuring temperature profiles at a high spatial distribution might require a very large number of temperature devices, which might then again lead to high costs. Also errors between large numbers of sensors could be larger than actual temperature differences that should be monitored (Selker et al, 2006). More information about low cost temperature sensors can be found in Hubbart et al. (2005) and Whiteman et al. (2000).

PART B: THE METHOD – Raman Spectra Fiber Optic Distributed Temperature Sensing

4. RAMAN SPECTRA FIBER OPTIC DISTRIBUTED TEMPERATURE SENSING

Distributed Fiber Optic Temperature Sensing Systems (DTS systems), when they were developed in the 1980s, were originally used for pipeline- and fire monitoring, for example in tunnels. Later, in the 1990s, they were also installed in geothermal wells (Tyler et al., 2009). Around 2000 DTS systems also established in other industrial and engineering applications such as civil structural monitoring/structural health monitoring (Inaudi, 2000, Inaudi and Glisic 2006), monitoring of electric power lines (Peck and Seebacher, 2000, Yilmaz and Karlik, 2005), for leakage detection in dams and levees (http://www.lios-tech.com/DE) and in sanitary engineering, to locate illicit connections in storm water sewers (Hoes et al., 2009). Today they are used in the construction industry, the oil- and gas- and the aerospace industry and in the mining industry (http://www.fos-s.be). As instruments became cheaper, starting in 2006, they also established in environmental-, mainly in hydrologic applications (Selker et al., 2006). For example, DTS systems were employed to investigate the spatial variability of groundwater discharge (Lowry et al., 2007), to reconstruct a ground surface temperature history in a subpermafrost borehole (Freifeld et al., 2008), to study aquifer-estuary interactions (Henderson et al., 2009), to gain insight in the influences of tidal waters and groundwater on channels in a saltmarsh (Moffett, et al., 2008) and to calibrate a temperature model for a stream (Westhoff et al., 2007). Selker et al. (2006) were the first to use fiber optic temperature sensing methods in a snow environment. They measured temperature profiles at a glacier. In 2008 Tyler et al. (2008) for the first time installed DTS systems to measure temperatures in seasonal mountain snow environments.

4.1 THEORETICAL BACKGROUND

4.1.1 Basic Principles of the Method

When measuring temperatures with Raman Spectra Distributed Fiber Optic Temperature Sensing systems, a laser is pulsed through standard telecommunication fiber-optic cables, which allows using them as a thermometer. Temperatures can be measured automatically and continuously along the cables, which can be permanently installed or can be newly deployed for each use. Spatial and temporal distributions of temperatures in the observed environment can be covered at the same time. It is not possible to measure temperatures in distinct points. The derived values are average values along a certain length of the fiber-optic cable, typically of about 1 to 3 m length (Tyler et al., 2009). An instrument box that pulses the laser and which also includes a recording unit is connected to the cable end(s) during times of measuring. Depending on the type of instrument box that is attached, temperatures can be measured along cables of up to 30 km length. Manufacturers state that temperature accuracies of +/- 0.01 °C are possible under optimum conditions (http://www.sensornet.co.uk/technology/distributed-temperature-sensing/sentinel-dts-range). Along the cable line no additional devices and installations are necessary. It is recommended however, to place a few reference devices to allow for controlling of data quality during measuring or data post-processing.

The pulsed laser light travels along the cable and when it collides with the fiber's lattice structure and atoms it causes them to emit small bursts of light at slightly shifted frequencies. Small bursts at three different wavelengths travel back towards the beginning of the fiber, where they are recorded in the instrument box (Smolen and van der Spek, 2003) (Fig. 10).

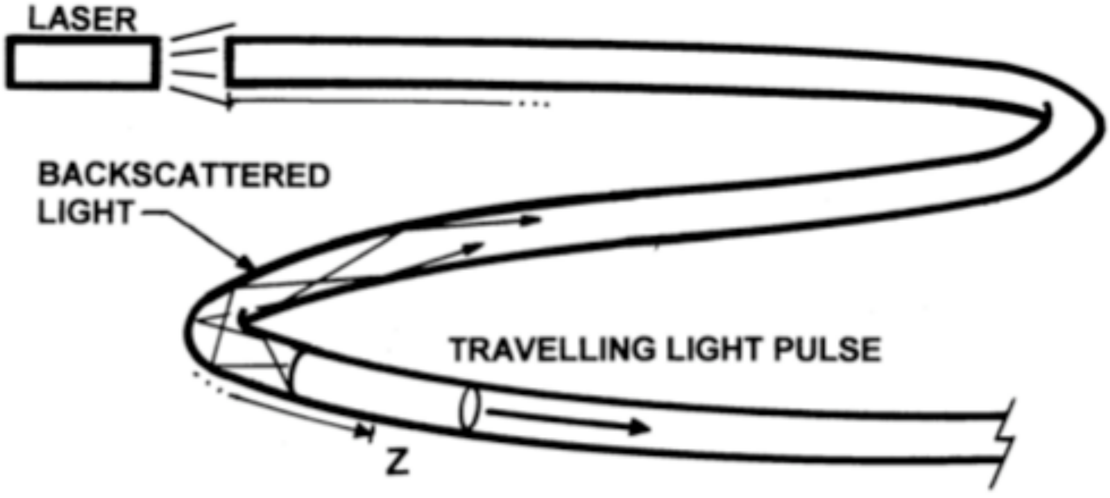

Fig. 10: travelling laser light pulse emitted from instrument box and backscattered light (Smolen and van der Spek, 2003)

The Backscatter Spectrum

Together the small bursts of light form the so-called backscatter spectrum (Fig. 11). Backscatter at three different wavelengths form the Rayleigh, the Brillouin and the Raman bands. The Rayleigh band is the strongest returning signal. It has the same wavelength as the originally pulsed laser light. The Brillouin bands result from the lattice vibrations and their wavelength are very close to the Rayleigh band. The two Raman bands result from atomic and molecular vibrations and are weakest component of the backscatter. The two components of the Raman band are referred to as Stokes and Anti-Stokes. They differ in wavelengths and in their reaction on temperatures. Whereas the intensity of Stokes is mostly indifferent to temperatures, the energy of the Anti-Stokes shows a clear reaction on thermal changes (Smolen and van der Spek, 2003).

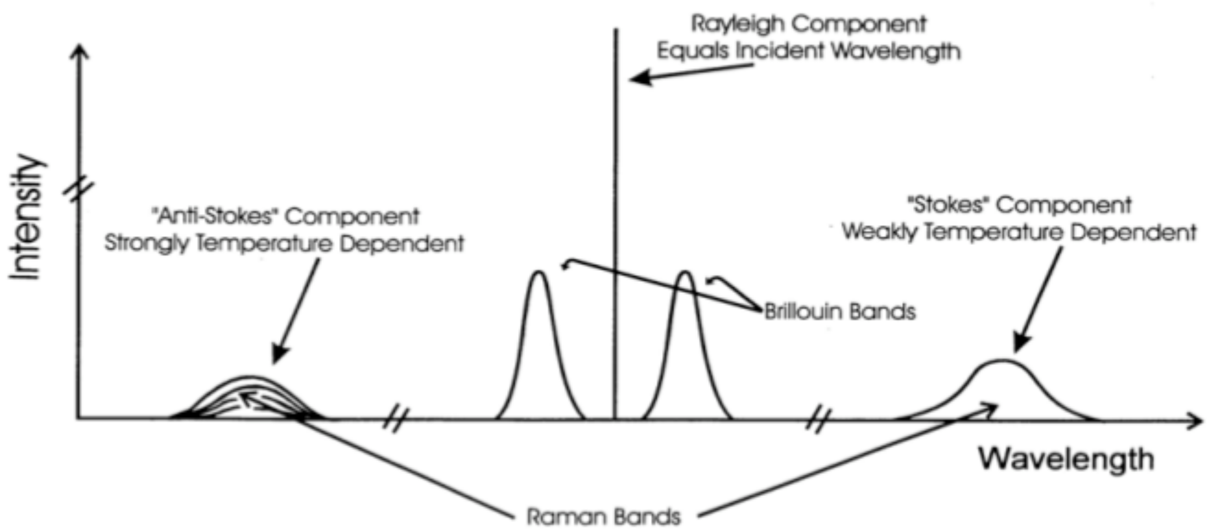

Fig. 11: Backscatter spectrum with Raleigh, Brillouin and Raman bands (Smolen and van der Spek, 2003)

The two Brillioun bands also differ in their reaction on temperature changes, and are used for temperature sensing as well. However, the difference in wavelength between the Raman bands and the other two backscatter components is larger than between the Rayleigh and the Brillouin spectra. For a commonly used laser having a wavelength of 1064 nm the Raman bands' wavelengths are shifted from the main Rayleigh peak by about +/- 40 nm to 1104 nm and 1024 nm. Therefore they are easier to separate from the Rayleigh and Brillouin bands and, despite the fact that their signal is the weakest, they are usually preferred in fiber-optic temperature sensing (Smolen and van der Spek, 2003). Figure 12 shows a flow chart of the measuring process from laser initiation to the processing of backscattered light.

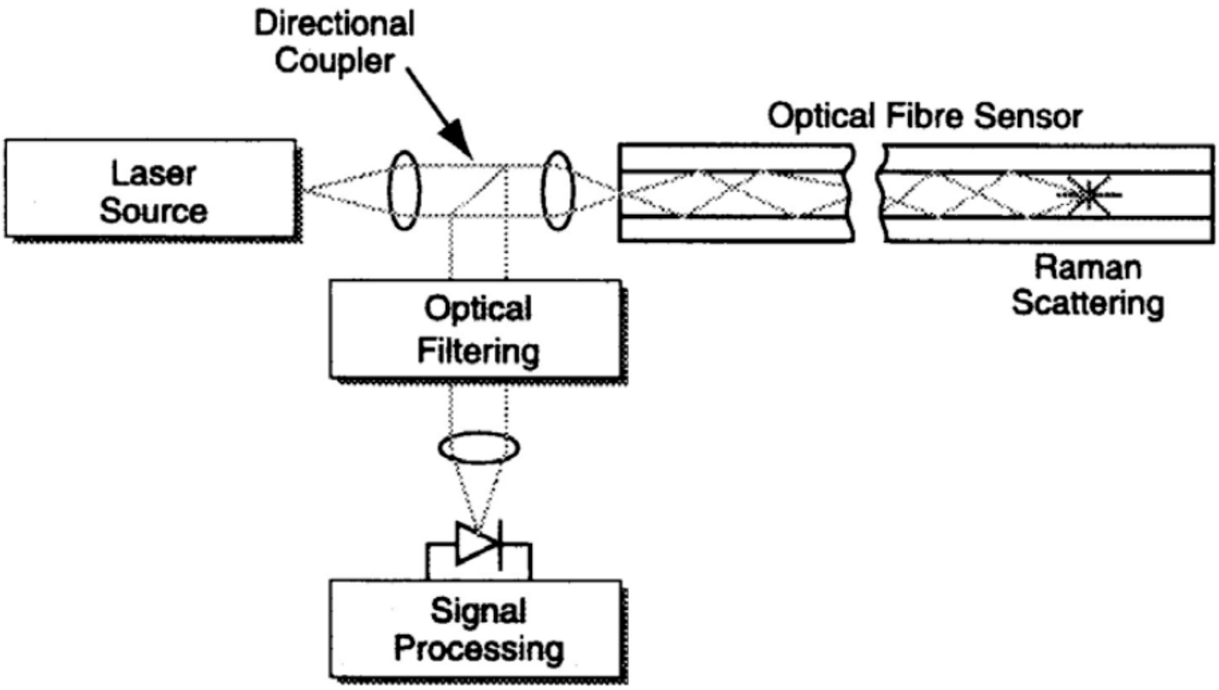

Fig. 12: Laser initiation and processing of backscattered light (Smolen and van der Spek, 2003)

Temperature Calculations Based on the Stokes- and Anti-Stokes Ratio

The Anti-Stokes band of the Raman spectra is at a lower wavelength than the Stokes band. Higher energy within the Anti-Stokes band indicates higher temperatures and vice versa. The measured energy within the Anti-Stokes signal compared to the fairly stable and temperature insensitive Stokes band renders the temperature of the fiber-optic cable at a given spot. Differences in Stokes and Anti-Stokes signals can be related to fiber temperatures by the following equation:

$$\mathbf{T(z) = Tref\ (1 + \Delta\alpha z / ln(C+/C-) + ln(I+/I-)/ln(C+/C-))}$$

Fig. 12: Equation to derive temperatures from Stokes- and Anti-Stokes signals (simplified version) (Smolen and van der Spek, 2003)

T(z) is the temperature at a given spot (z) along the fiber line in °K.

Tref is a reference temperature in °K.

$\Delta\alpha$ stands for the differential attenuation between the Stokes- and Anti-Stokes backscatter per m ($\Delta\alpha > 0$).

I+ represents the intensity of the Stokes band and is a function of (z).

I- represents the intensity of the Anti-Stokes band and is also a function of (z).

I+/I- stands for the ratio between the Stokes and the Anti-Stokes signals.

C+ and C- are constants that relate to the sensitivity of I+/I- to the actual temperatures.

For the complete equation see Smolen and van der Spek (2003).

Attenuation and Differential Attenuation

Attenuation (α) is the loss of signal per unit length of fiber. Its magnitude depends on the fiber construction and on the wavelength of the signal. For standard telecommunication cables of the kind that is typically used with DTS systems, and for standard telecommunication frequencies, attenuation can be expected to be in the range of 0.3 dB/km. An increase in attenuation/losses can be observed at connections and splices or can be caused by external factors, such as tensile stresses on the cable or sharp bends. These locally intensified losses can be either of a permanent or of a transient character. Care should be taken in cable positioning in order to avoid possible sources of strain and sharp bends (Tyler et al., 2009). A possible reason for transient local losses would be variable tensile stresses in a slope where the cable is deployed. With measurements in a so-called double-ended mode (see below, Single- and Double-ended Measurements) instruments provide routines to correct automatically for local losses. When measuring in a single-ended mode, additional corrections for step losses are necessary. Special care has to be taken with adjustments for transient step losses. In both cases, with double-ended and with single-ended measurements, it has to be kept in mind that the larger the attenuation or the higher the number of local losses, the noisier is the signal, as less light returns to the detector (Tyler et al., 2009).

Attenuation rates are wavelength dependent. Therefore this process differently affects the Stokes- and Anti-Stokes signals of the Raman band and corrections for this differential attenuation $\Delta\alpha$ are necessary in order to achieve correct temperature measurements (see Fig. 12, equation). Depending on the type of experimental set-up (single-ended- vs. double-ended mode) there are different ways to control for the differential attenuation (Tyler et al, 2009).

Calibrations and Corrections

A function describing the temperature dependency of ln (I+/I-) has to be derived. Figure 13 shows the calibration of the so called backscatter power (ln (I+/I-) against temperatures.

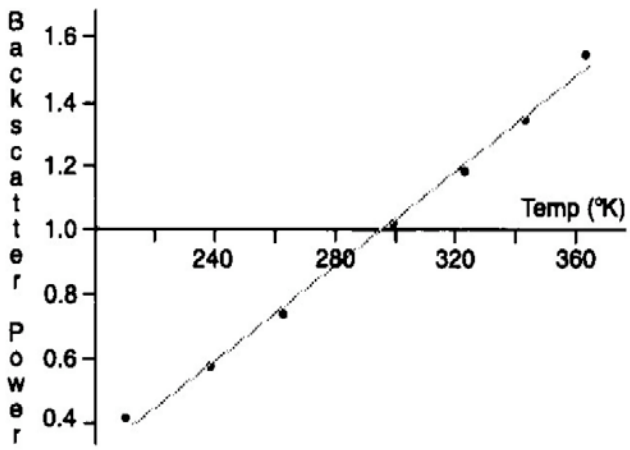

Fig. 13: calibration of backscatter power vs. temperature (Smolen and van der Spek, 2003)

If the sensitivity (C+/C-) of the ratio between Stokes- and Anti-Stokes signals (I+/I-) to actual temperatures is known, the raw temperature data provided by DTS system is the sum of three components: of the actual measured temperature, of the offset (Tref) and of the drift due to differential attenuation (Smolen and van der Spek, 2003). Figure 14 shows a log of uncalibrated DTS results for a 1000 m section at a constant temperature.

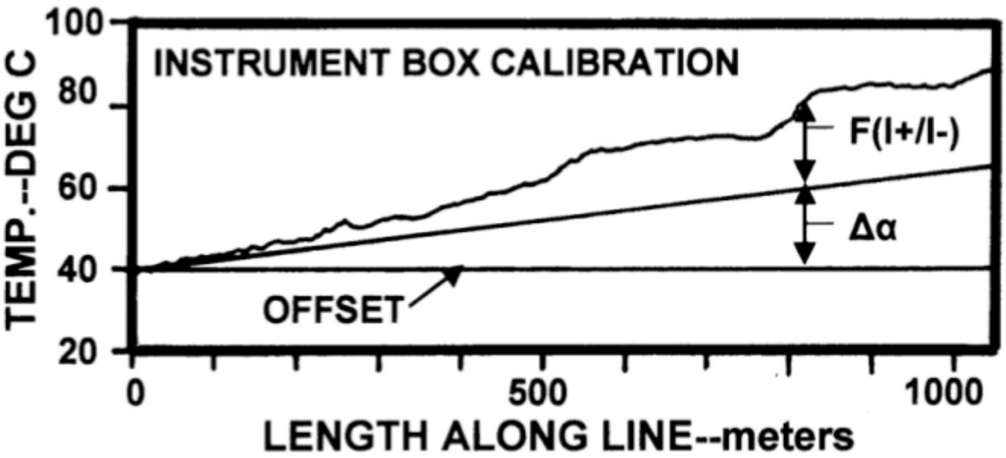

Fig. 14: linear differential attenuation and constant offset (Smolen and van der Spek, 2003)

In order to calculate temperatures the function of how the backscatter power ln (I+/I-) relates to temperatures, the sensitivity of this ratio to temperatures, the differential loss and the offset have to be known. Usually instrument boxes are calibrated for the backscatter power and they supply user interfaces to assist in calibrations for offsets and differential attenuation. DTS instruments usually render corrected temperature data as well as the raw Stokes- and Anti-Stokes bands, which leaves it open to the user to conduct his own calibrations and calculate temperatures himself.

All measurement set-ups with Distributed Temperature Sensing require an offset calibration each time the DTS system is installed at a new site. The instrument is provided with the information that it needs to calculate the reference temperature Tref (see Fig. 12, equation). A reference bath (or oven) near the instrument of a known temperature T (0) at a distance z (0) is defined as Tref plus ln (I+/I-) at z (0) (Smolen and van der Spek, 2003).

When instruments are set to measure in single-ended mode a particular experimental geometry is required to allow internal DTS algorithms to calibrate for linear differential attenuation. With measurements in double-ended mode multiple laser sources and DTS internal algorithms automatically correct for this effect (Tyler et al., 2009). As in case of local losses (step losses) attenuation can locally reach higher values, (see above, Attenuation and Differential Attenuation) additional corrections in data post-processing become necessary for single-ended measurements. With measurements in the double-ended mode also increased local attenuation can be corrected automatically.

Single-ended and Double-ended Measurements

With single-ended measurements temperatures are calculated from light transmissions in only one direction in the fiber. Single-ended measurements are most precise near the instrument and accuracy is degrading with distance. Single-ended measurements should be chosen when a high precision is needed close to the instrument or when it is problematic to install a fiber return, which would be necessary to conduct measurements in a double-ended mode. Fiber returns require a little box for protection, which in some applications can pose a problem (Tyler et al., 2009).

Fig. 15: Turnaround box used in experimental set-ups for double-ended measurements

For double-ended measurements a fiber loop, which is connected to the instrument box at both ends, is needed. It requires twice the sensor length capacity, two input channels at the instrument box and a doubling of the minimum measurement rate (measurement intervals in time). The fiber loop can run inside a single cable cladding and turns within a turnaround box as shown in Figure 15. Two convolving single-ended measurements are made from each end of the loop. The instrument renders two Stokes- and Anti-Stokes traces, called the forward- and the reverse trace. In each point it incorporates data from traces in both directions to calculate temperature values. With this information differential attenuation can be computed continuously and the instrument can locate and correct local losses (step losses) automatically. However, experience on Mammoth Mountain showed that these automatic step loss corrections have their limits.

In a data set that included two local step losses within a short distance they could not be corrected sufficiently and the calculated temperatures were incorrect (chapter 4.2.3, Step Losses). With double ended measurements the greatest data noise is found closest to the instrument, the smallest at the midpoint of the cable (turnaround). In general, they always have greater data noise than single-ended measurements. Double ended measurements are recommended for applications in long term monitoring (several days or more), when the fiber might be subjected to stresses or to other possible sources of locally increased attenuation (step losses) or when there is the danger of time dependent attenuation (transient step losses) (Tyler et al., 2009).

A third option is to install a fiber loop the same way as used for double-ended measurements but to use it in the single-ended mode. One single-ended measurement is sent through the cable and provides extra redundancy as the fiber loops back within one single cladding. Thus the measurement retrieves temperatures twice from each location. Calibration for differential attenuation can be achieved by matching sections that are known to have the same temperature i.e. by matching temperatures from positions along the fiber loop that are located in the same spot in the field. Given a loop of 1000 m length, with the turnaround at meter 500, meter 20 to 40 and meter 460 to 480 would constitute such a matching section. A coiled up section of cable that includes two fiber loops, kept in a well-mixed temperature bath would constitute a reliable section to match temperatures.

Single Mode- and Multimode Fibers

Usually, if a glass fiber has a higher refractive index than its surroundings and when the angle of incidence between the light ray and the interface of the fiber does not exceed a critical value, the light is trapped within the cable and is forced to propagate through it. Snell's law of total inner reflection describes this effect (Gowar, 1993). It defines a certain critical angle above which light is not internally reflected but dissipates to the surroundings. The maximum angle at which light is still internally reflected can also be referred to as the cone of acceptance. Depending on the way in which light travels though them, fiber-optic cables can be classified as single mode- or multimode fibers (Smolen and van der Spek, 2003).

Single mode fibers have a very thin glass core (about 5 µm). A glass cladding with a smaller refractive index surrounds the core to a diameter of 125 µm. The light can only travel in the main mode, following the axis of the fiber, within the core. Due to the core's small diameter the cone of acceptance is small and is very difficult to put light into it. The backscattered signal is weak. It would require a large number of samples to retrieve statistically significant temperature information. Therefore most DTS applications use multi mode fibers (Smolen and van der Spek, 2003).

Multimode fibers consist of a much larger glass core than single mode fibers (about 50 µm) that is also surrounded by a glass cladding to a diameter of 125 µm. The core's refractive index is by 5 % larger than the one of the glass cladding. Multimode fibers allow the light to travel in three different ways (Fig. 16). It can either follow the fiber axis in the main mode, or, when entering the core at some angle, can travel within the core in a zigzag- or spiral path. However, when the angle at which the light travels relative to the fiber axis in the core, exceeds the cone of acceptance the signal is lost as it dissipates to the surrounding (Smolen and van der Spek, 2003). Thus bend radii of less than 2.5 cm should be avoided in fiber-optic cable installations used for Distributed Temperature Sensing (Tyler et al., 2009).

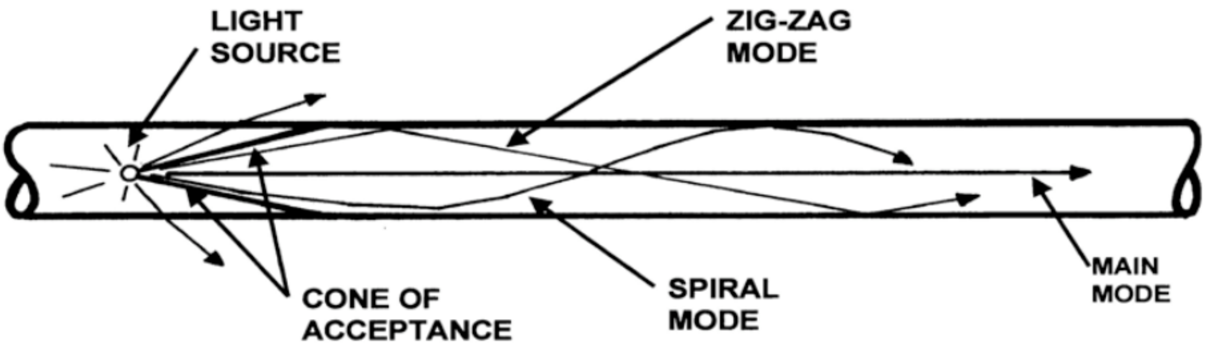

Fig. 16: possible light travel paths in a multimode fiber (Smolen and van der Spek, 2003)

The optical paths in the zigzag mode and in the spiral mode are longer than in the main mode. Therefore the differently travelling parts of signals along a normal multi mode fiber arrive shifted in time. To solve this problem graded index fibers with a refractive index that gradually decreases towards the boundary of the core were developed. As a result they allow slightly higher travel speeds of light in the zigzag- and spiral mode, which compensates for the longer travel paths. Modern communication lines mainly use graded multimode fiber-optic cables (Smolen and van der Spek, 2003).

Instrument Internal Factors Determining Data Resolution and Accuracy

Launched laser light pulses typically have duration of 10 ns or less. Their wavelength ranges between 800 and 1600 nm, which lie in the near infrared spectrum. Travel times within the fiber-optic cables are defined by the velocity of light in a vacuum (c) and by the refractive index of the glass in the given fiber (n) (Smolen and van der Spek, 2003).

$$v = c/n = (3 \times 10^{+8})/1.5 = 2 \times 10^{+8}\ \mathrm{m/s}$$

Fig.17: travel velocity of laser light in a fiber-optic cable

Most glass has a refractive index of 1.5 to 1.7. Given a speed of light in vacuum of $3*10^{+8}$ m/s and a refractive index of 1.5, the laser light travels in the fiber with a velocity of $2*10^{+8}$ m/s. The light is launched at the instrument box and when the returning signal is expected a window is opened to capture the backscatter. The window size determines the spatial resolution of captured backscatter signals. The total travel time t of the laser light to a distinct location z on the cable, and of the backscatter back to the instrument box is calculated as $t = 2z/v$ (Smolen and van der Spek, 2003).

The length of the launched light pulses in the fiber and the size of the time windows that are opened at a time at the instrument box to collect the returning backscatter are important for the spatial resolution of measurements (Smolen and van der Spek, 2003).

The length of a light pulse in the fiber depends on the duration of the light pulse and on the travel velocity of the laser light in the cable. For a pulse duration of 10 ns and a travel velocity of $2*10^{+8}$ m/s the length of the pulse can be calculated as:

$2*10^{+8}$ m/s * $10*10^{-9}$ = 2 m (Smolen and van der Spek, 2003)

The size of the time window Δt during which backscatter signals are collected at the instrument box corresponds to a section along the cable of a length Δz along which return signals are captured. To get sections Δz of 1 m the required window size Δt can be calculated as follows:

$\Delta t = 2\Delta z/v = 2x1/(2x10^{+8}) = 10^{-8} = 10$ ns (Smolen and van der Spek, 2003)

If the pulse length is 2 m the backscatter returning of the instrument at any time t is representative for a section of 2 m length at a distance along the cable, which is depending on the travel time. If the window size is 1m, this means the 2 m long pulse travels 1 m while signals are collected at the instrument box. Together the pulse length and the window size determine the spatial resolution that can be achieved with an instrument (Smolen and van der Spek, 2003).

There can never be two light pulses within the cable at the same time. Backscattered signals would get mixed and it would become impossible to derive reliable temperature data. One pulse must reach the end of the fiber and the backscatter must return to the instrument box before the next can be launched. For a 3000 m long cable with a refractive index of 1.5 about 33,000 launches per second would be possible. Usually launch rates range between 4000 and 10,000 pulses per second, which also allows for data processing after the backscatter of one pulse arrived at the instrument and before the next one is launched (Smolen and van der Spek, 2003).

Raman signals are weak and provide a relatively poor signal to noise ratio. A large number of launches, in the range of 1,200,000, is necessary to retrieve statistically significant information. Therefore a typical DTS log is recorded over one or several minutes. A DTS system's resolution should always be stated in terms of cable length and sampling time, as this determines the number of launches that were collected in each log. At a given fiber length the system's resolution is proportional to the sampling time by $\sqrt{n}$, where n is the number of samples (launches). To improve a given resolution by a factor of two requires a four times longer sampling time (Smolen and van der Spek, 2003).

4.1.2 Setting up a DTS System at a Site

Components of a DTS System

A DTS system consists of an instrument box of a given make (different manufacturers are available); of one or more connected cable(s); of calibration baths (ice-slush baths or water baths), or other constant-temperature calibration sections, with reference temperature devices; and of connectors, which link the cable to the box. Figure 18 shows an example of a DTS system set-up for measurements in a so-called double-ended mode (chapter 4.1.1, Single- and Double-ended Measurements), similar to the one installed in 2008/2009 on Mammoth Mountain. At the beginning of the cable two ends of a fiber loop that runs through a single cable coating are attached to the instrument box through connectors. A monitor and a keyboard are necessary during calibration and configuration when starting measurements, but usually can be removed afterwards. They are needed again when data stored in the box has to be downloaded to an external drive. 20 to 40 m of cable are coiled up and are put in a well-mixed water bath for calibration. The bath is equipped with a pre-calibrated reference temperature device. Parts of the cable are still coiled up and stored for later deployment. Several reference devices positioned along the cable track provide data for control and corrections during post-processing. A turnaround box ensures space and protection for a safe turn of the fiber string at the end of the cable cladding.

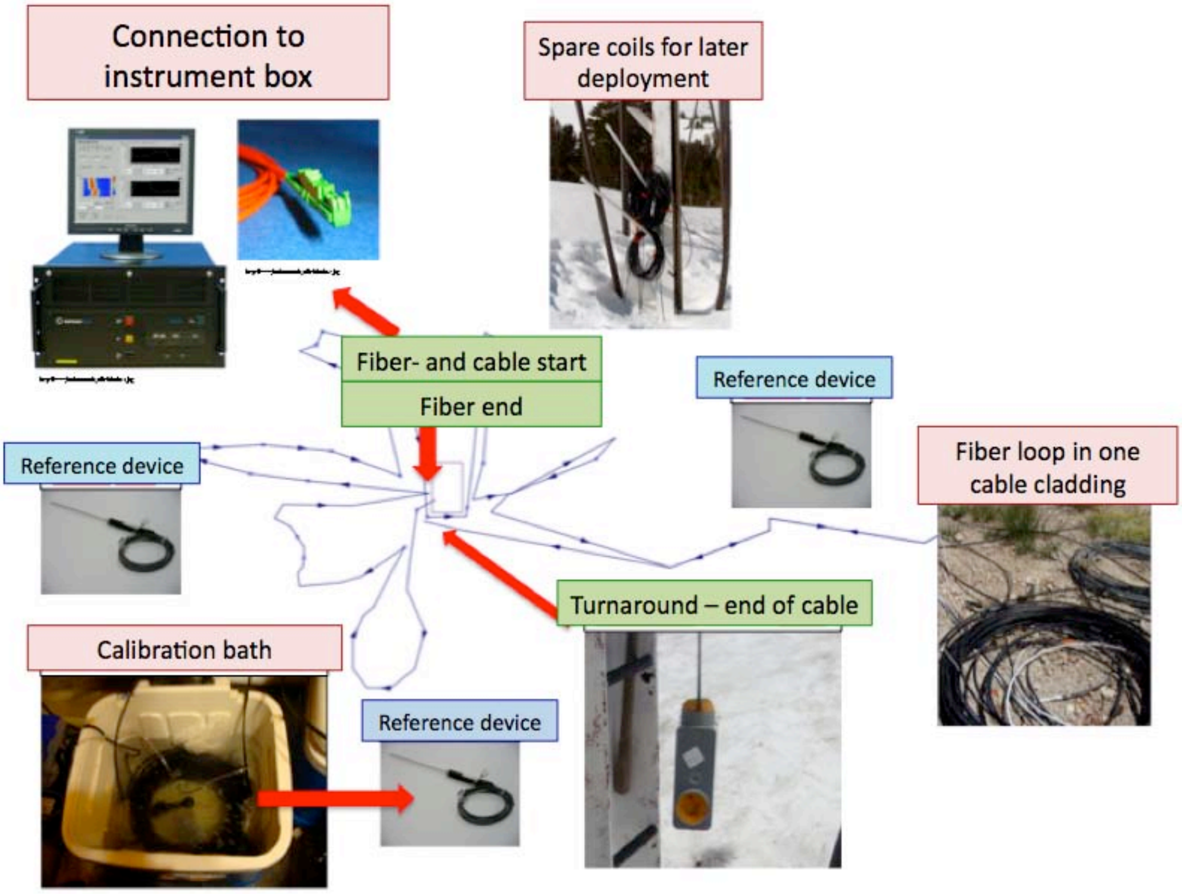

Fig. 18: Sketch of a DTS system for double-ended measurements

DTS Instrument boxes

Different instrument types for DTS measurements are available from various manufacturers. Instruments differ in their size and weight, in maximum length of cable along which they can measure, in possible spatial sampling resolution and in temperature accuracies that can be achieved as a function of chosen measurement time intervals. They provide different numbers of channels for cable connections and have different environmental needs and different power needs for storage and operation.

http-//www.lios-tech.com/Menu/Technology/Distributed+Temperature+Sensing

Fig. 19: fiber-optic cables connected to an instrument box

Figure 19 displays channels for cable connections at a DTS instrument box. This specific instrument offers eight channels, three of which are currently connected to fiber-optic cable ends.

Which instrument type is the most appropriate depends on the character of the field application (Tyler et al., 2009). See Appendix C for examples of manufacturers' instrument data sheets. Table 1 compares selected attributes of four different instrument types; the Sensornet Sentinel, which can measure over the longest distances and with a better temperature resolution, but is larger and heavier than the others; the Sensornet Halo and the Sensornet Oryx, which can operate with low power supply and at lower temperatures and the FOS&S 012 system, which can measure at colder temperatures than the Halo but provides lower accuracies than the instruments from Sensornet Ltd (www.sensornet.co.uk[1], www.fos-s.be[1], Tab. 1).

	Sensornet Sentinel	Sensornet Halo	FOS&S 012	Sensornet Oryx
Dimensions [cm]	18*43.5*48	8.7*43.5*44.5	8.8*44.8*36.4	-
Weight [kg]	21 kg	9 kg	9kg	-
Range [km]	Medium range: 8 km Maximum range: 30 km	0 – 4 km	0 – 12 km	0 – 5 km
Temperature Resolution (4 km cable, 5 min and 1 m – 2 m intervals)	0.01 °C	0.1 °C	0.16 °C (10 min interval)	0.1 °C
Operating temperature of instrument [°C]	5 °C – 40 °C	0 °C – 40 °C	-10 °C – 60 °C	-40 °C – 65 °C
Power needs [W]	100 W	40 – 50 W	15 W (at 0°C) 28 W (at 60°C)	18 W
Number of channels for cable connection	4	Available with 2 or 4	1 - 4	Available with 2 or 4

Tab. 1: comparison of selected properties of different DTS instrument boxes (www.sensornet.co.uk[1])

Note that the temperature resolution that can be achieved with a specific instrument is also depending on the length of the fiber-optic cable along which measurements are taken. Accuracies of measurements depend on the length of the installed fiber-optic cable, on the chosen measurement intervals in time and in space and on continuous and local attenuation along the fiber-optic cable (chapter 4.1.3). Figure 20 displays temperature resolutions that can be achieved with a Sentinel Halo instrument box, as was used on Mammoth Mountain, CA.

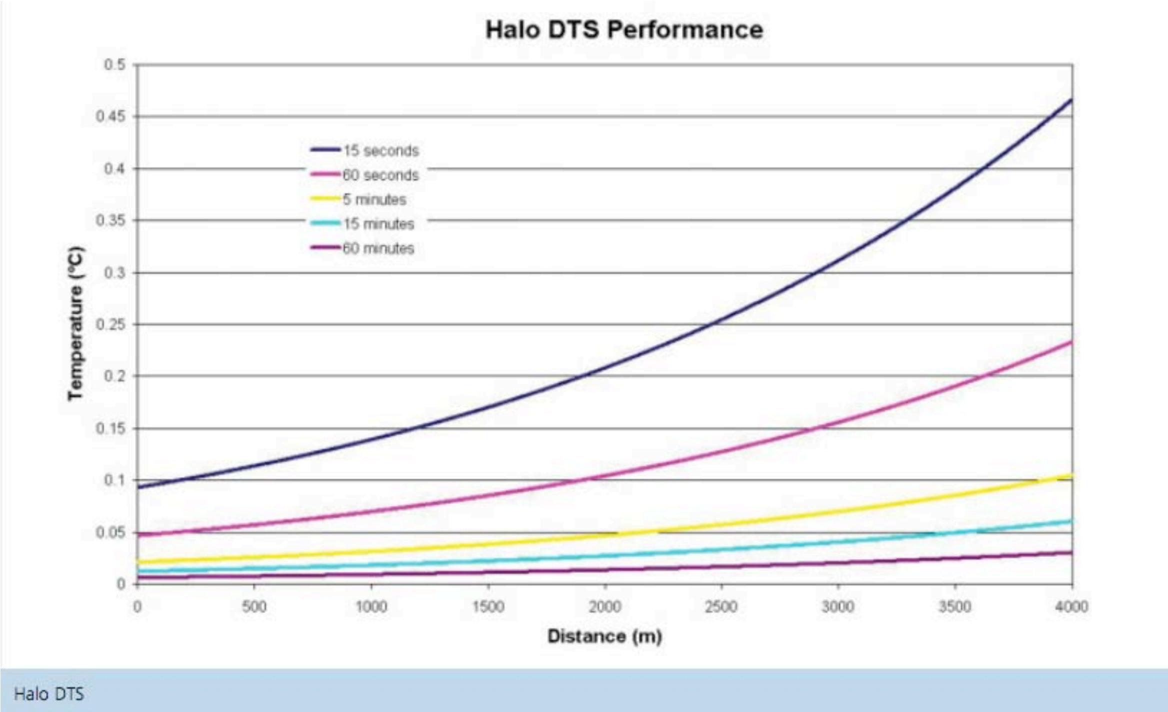

(www.sensornet.co.uk[1])

Fig. 20: Temperature resolution that can be achieved with a Sentinel Halo instrument box as a function of cable length and the length of intervals along which measurements are taken.

The Sentinel, the Halo and the FOS&S 012 are sensitive to humidity and, as most DTS instrument boxes, have to be set-up in non-condensing environments. Whereas the Halo and the Oryx can handle interruptions, a continuous power supply is crucial for the Sentinel. All these instruments operate with user interfaces that assist in calibration and configuration (www.sensornet.co.uk[1]). The Oryx offers several data transfer options. Data can be communicated via satellite, wireless modems or GSM modems, through radio links or through direct links to PCs and laptops. All instruments allow data transfer with a serial RS-232 or through Ethernet. Large amounts of data can be stored on board of DTS instrument boxes. It is possible to keep them running over long time periods (several months or more) before transferring data. For an easy transfer data can always be copied to an external USB- or hard drive (www.sensornet.co.uk[1]). Two more examples for companies providing DTS instrument boxes are Lios Technology GmbH (www.lios-tech.com) and Sensortran Inc. (www.sensortran.com). All companies provide contacts for instrument purchase and usually also offer a certain extent of education about the handling of DTS systems when a product is bought (www.fos-s.be[1], www.lios-tech.com, www.sensornet.co.uk[1], www.sensortran.com). Figure 21 shows a Halo DTS together with a monitor and a keyboard. Figure 22 displays the graphical interface (configuration wizard) that assists the user during calibration and configuration.

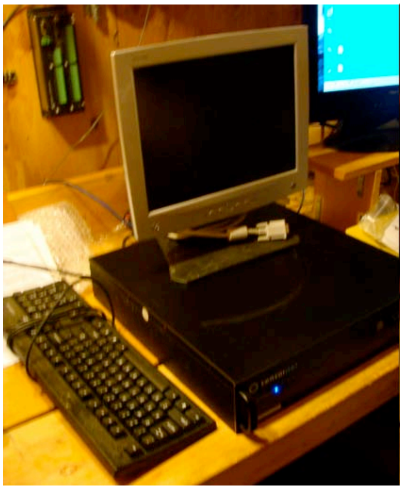

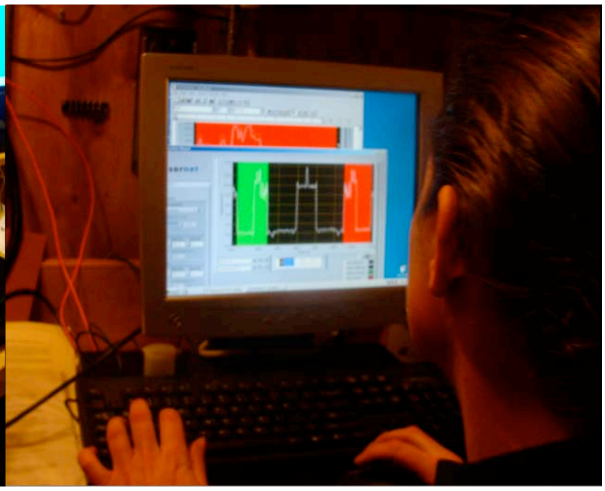

Fig. 21: Halo-DTS with monitor and keyboard

Fig. 22: using a graphical interface for calibration and configuration

Fiber-Optic Cables

Various cable types with different attributes are available for distributed fiber optic temperature sensing. They typically are multimode fibers consisting of a 50 μm glass core with a 37 μm cladding (Tyler et al., 2009, Smolen and van der Spek, 2003). Fibers are available in coats of different colors (black, white, etc.) and of different thicknesses and fabrics (plastic, steel). Impacts of solar radiation on measured temperatures can be minimized, however not extinguished, when refractive coatings hose the fibers. Various materials can be used to protect them against water influences and mechanical impingements. With stainless steel covers cables can be protected against impacts from vehicle passages or high water pressures. "Overstuffed" cables prevent strains to an elongation of 1 % (Tyler et al., 2009). The choice of the cable depends on the application and on according protection demands, for example, against animals, debris, pressure influences or loads from vehicles. Highly protected (armed) cables should only be chosen if they are unconditionally necessary as they are heavy and more expensive. Cost for a standard, plastic coated, unarmed cable is in the range of 0.5 $/m. Armed cables can reach costs of more than 10 $/m. They can reach a weight of more than 30kg/km, which has to be considered for transport. Furthermore, heavier cables are more difficult to handle and do only allow large bend radii; and they have a greater thermal inertia resulting in delayed responses to temperature changes (Tyler et al., 2009). The diameter of the cables, the heat capacities of their coatings and of possibly included strength elements influence how quick a DTS system responds to temperature changes in time. Such delays usually are in a range of a few seconds to a minute (Tyler et al., 2009). In many applications fiber-optic cables with distance markings printed on their coatings prove to be very useful as these marks provide a good reference for georeferencing. Fiber-optic cables can be used several times, they can be left in the field and be reconnected to the instrument or can be taken down and deployed in a new location. However, the cables can age, which results in rising step losses and accordingly leads to a lower temporal repeatability (accuracy, see chapter 4.1.3) (Tyler et al., 2009). Also care has to be taken with older cables as meter marks can fade out and be no longer available for georeferencing of measurement positions (Tyler et al., 2009). Figure 23 displays the handling of an unarmed fiber-optic cable on Mammoth Mountain after a series of measurements; the cable is coiled up on large spools for transport and storage.

Fig. 23: taking down a fiber-optic cable after a series of measurements

Figure 24 shows meter marks on a fiber optic-cable. In Figure 25 a loop of fiber-optic cable, deployed on Mammoth Mountain in 2008, is shown. The red bag marks the location of a meter mark on the cable that was used as a reference for GPS measurements.

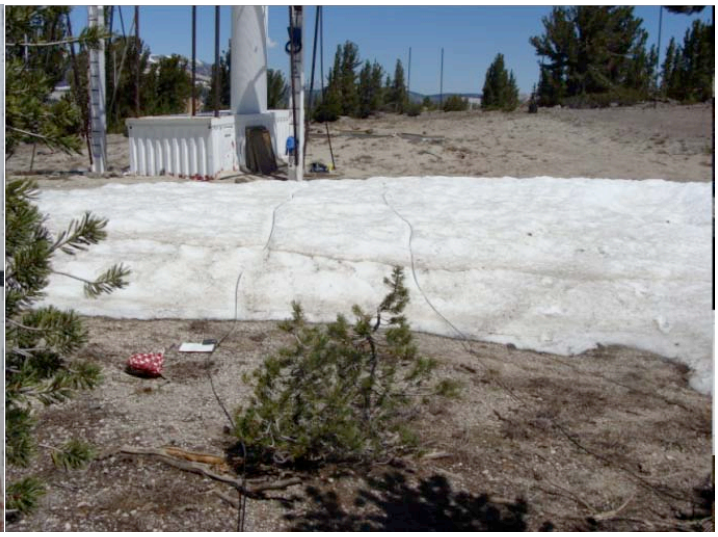

Fig. 24: meter marks on a fiber-optic cable

Fig. 25: locating of cable position with GPS, the small book marks the position or referenced cable meter mark in the picture

The fiber-optic cables that are used are relatively cheap and allow many different ways of field installations. However, instrument boxes, which pulse the laser and collect and analyze the returning backscatter, are related to high acquisition costs (Tyler et al., 2009). See Appendix C for the product information on a fiber optic cable that was used to study snow temperatures on Mammoth Mountain.

Connectors

Special angle polished fabrics of E2000 connectors should be used with DTS systems as they reduce backscatter of the injected light that establishes directly at connectors. For multimode fibers as used with DTS systems they are not standard in industry and therefore have to be specially ordered (Tyler et al., 2009). Tyler et al. (2009) mention further, that care should be taken as such connectors are of a variable quality. Increased losses at the connectors can result from scratches or dust on connecting faces, from air gaps and from poor alignment (Tyler et al., 2009). To keep losses at connectors low they should be cleaned each time they are used (Fig. 26), they should not be too old and they should be well protected during transport and storage (Tyler et al., 2009). Losses at the connectors cause local temperature anomalies in the reported DTS data and also increase data noise along the entire trace (Tyler et al., 2009). When they are used at some place along the cable, connectors can also be referred to as mechanical splices,. The alternative to mechanical splices would be fusion splices, which require specific instrumentation and can, for example, be used to repair broken fiber-optic cables (Tyler et al., 2009).


Fig. 26: cleaning supplies for fiber-optic cable connectors

Calibration set - ups

Measurements with DTS systems require careful experimental design (Tyler et al., 2009) and personal experience in instrument- and data handling in order to achieve reliable results. 20 to 40 m cable sections (or sections of a minimum length of 10 times the length of the spatial sampling interval) kept at a constant temperature in space and, if possible, also in time, form the basis for DTS calibrations. Well-mixed and insulated water baths or ice-slush baths but also well-mixed portions of stream channels, equipped with precision-calibrated thermometers as references, have established for calibrations in environmental DTS applications (Tyler et al., 2009). When using water baths it is important to control for thermal stratification in the bath as this might limit the comparability between temperatures along the, usually coiled up, cable sections and the reference measurements from a single point in the bath (Tyler et al., 2009) (see also chapter 4.2.1). Special care should be taken to ensure a close thermal contact between the reference device and the calibration cable section (Tyler et al., 2009). Figures 27 to 29 display an insulated, mixed water bath, a coiled 40 m cable section and different types of reference devices - a VWR thermometer, a pt 100-temperature device and thermistor strings that can be connected to a data logger.

Fig 27 to 29: calibration set-up: bubble bath (Fig. 27), cable coil (Fig. 28) and reference devices - pt-100 (Fig. 29, http://www.allproducts.com/ee/tecpel/Product-2008613181757), thermistor strings and VWR thermometer (Fig. 29)

Double-ended measurements only have to be calibrated for an offset, which requires **one** bath, or some other isothermal environment, to provide a long enough section of known cable temperature. The temperature offset accounts for the instrument specific sensor- and laser performance and drives the absolute accuracy of DTS measured temperatures (Tyler et al., 2009). Single-ended measurements further have to be calibrated for differential attenuation, -gains and -losses. Two constant-temperature environments, one at the beginning and one at the end of the cable are needed (Tyler et al., 2009); for example, to derive matching sections as described above (chapter 4.1.1). As described below (chapter 4.2.3.3), experiences on Mammoth Mountain showed that also with double-ended measurements at least two sections, one at the beginning and one at the end of the cable, should continuously be monitored with reference devices. This provides redundancy and allows for data control and possibly necessary corrections during post-processing.

Instrument boxes may allow choosing between fixed and dynamic calibrations. For fixed offset calibrations the 20 - 40 m segment of the fiber-optic-cable, kept at a constant temperature in space, is assigned a fixed temperature value during instrument set-up. A fixed temperature offset is calculated as the difference between the assigned temperature and averaged DTS temperatures measured along the cable segment at this time. Throughout the entire measurement period this initially calculated and fixed offset value is added to DTS measured temperatures at every time step. Fixed calibration only requires real-time temperature readings in the calibration bath or environment during instrument set-up. However, continuous monitoring of temperatures along the 20 - 40 meter long cable transects allows identifying and correcting of potential measurement- and drift errors. Instrument drift errors have to be expected in DTS long-term applications (measurements of several days) and when the instrument is exposed to strongly varying or extremely low temperatures (Tyler et al., 2009). Dynamic calibrations can help reduce instrument drift. In this case offset values are newly calculated for each time step, as the difference between known temperatures along the calibration transects and the actual DTS measured temperature. Calculations are either based on a known temperature environment that is constant in space and also in time, or they refer to a constantly measuring, independent, temperature sensor that provides continuous reference temperatures and that is directly connected to the DTS instrument box. Not all makes of instrument boxes allow the direct attachment of such additional independent temperature sensors.

Other Considerations

Environmental conditions (dust, humidity, ambient temperatures) have to be considered at remote sites and have to be related to specific instrument requirements in order to assess possible needs for protection (Tyler et al., 2009). Power supply, if no electrical connection is available, depending on the instrument’s power needs, can be provided through solar panels, batteries, generators, or they can operate on wind power (Tyler et al., 2009). Some instruments require continuous power supply; some are able to restart measurements after interruptions (see above – DTS instruments) (Tyler et al., 2009, www.sensornet.co.uk). Figure 30 shows a DTS system being set-up in February 2009 at a remote site in Great Basin National Park to run on a fuel-operated generator.

Figure 31 displays a transport box used to transport a Sentinel Halo to Mammoth Mountain. Such boxes can also be used for protecting the instrument boxes against environmental disturbances at a field site.

Fig. 30: fuel operated generator for power supply

Fig. 31: transport box for DTS instrument

Some instruments allow near real time data transmission. If they are connected to a monitor, according near real time data displays can help to control site management and they can provide quick insights in instrument performance (Tyler et al., 2009). To a certain extent this also allows data interpretations and conclusions that cannot be drawn any more once a DTS system was taken down at the end of measurements. Detected anomalies, for example, can be immediately investigated at a site (Tyler et al., 2009). At least when measurements are carried out only once at a site and when first analyses are planned after the cable was already removed, near real time displays of the DTS data at the site can be very helpful for the understanding of measured temperatures and for data quality control (Tyler et al., 2009).

Data Handling

Different instrument types provide different on-board storage capacities and storage modes (Tyler et al., 2009). The Halo-DTS used at a site on Mammoth Mountain could easily store measurements from several months that were taken at a time interval of five minutes. Also file structures vary between instruments from different manufacturers. The Halo stored each temporal trace (data from a single time step) in a distinct file (ddf-files). Further, it produced configuration-files, which included information about the configurations during instrument set-up. The measured data can either be transported through various communication options as listed above, or can simply be downloaded on an external drive (USB), PC or laptop (Tyler et al., 2009). Configuration files include information about chosen averaging intervals in time and in space, about the calibrations, about the instrument that was used, etc. For an example of a configuration files see Appendix B. For further use in data analysis the single ".ddf – files" usually have to be parsed together, which can for example be done in MatLab (www.mathworks.com). Appendix A shows two MatLab routines written at the University of Reno, Nevada, to automatically import ddf – files with DTS measured information into MatLab and parse them together in time-by-space matrices of the Stokes – signal, the Anti-Stokes – signal and of accordingly calculated temperatures. Further outputs are vectors of measurement time steps and of measurement distances.

4.1.3 Assessing Instrument- and System Performance

The absolute accuracy of a DTS system at a distinct point can be referenced to an arbitrary standard measurement method (Tyler et al., 2009). Tyler et al. (2009) mention that absolute accuracies up to +/- 0.1 °C can be achieved. In general, the precision of the measured ratio between Stokes- and Anti-Stokes- backscatter and of according temperatures is proportional to the number of photons that are collected at the detector in the instrument box. Consistent with the central limit theorem this number is proportional to the square root of the measurement time, which implies that, given that all other influencing factors remain equal, a longer time averaging period will lead to more precise temperature measurements (Tyler et al., 2009). The length of measurement time intervals can be chosen during instrument configuration but can also be extended through calculations during data post-processing. The DTS instrument boxes collect data throughout each measurement interval. The provided output values of one interval are the average of all signals that were collected during this time. Local losses at connectors, sharp cable bends or where the cable is subjected to strain stresses result in lower signal strengths returning to the instrument box and can also negatively affect a DTS system's precision (Tyler et al., 2009).

The performance of a DTS system i.e. its relative accuracy and resolution can be described by four factors: its spatial- and its temporal repeatability, which together determine its absolute accuracy; and its spatial- and temporal resolution, which indicate how fast and along which distances temperature changes can be fully detected (Tyler et al., 2009).

Spatial Repeatability

The spatial repeatability of a DTS system is described through the standard deviation in space, of DTS-measured temperatures along a section that is known to be at a constant temperature. It determines the method's ability to correctly interpret a sequence of temperatures in space i.e. how reliably it can detect spatial patterns (Tyler et al., 2009). In an experimental set-up at Lake Tahoe, CA, U.S.A., Tyler et al. (2009) investigated the spatial repeatability that could be achieved with three different instrument types. For the three different instruments they observed spatial standard deviations (repeatability) of 0.02 °C, 0.04 °C and 0.08 °C (Tyler et al., 2009).

Temporal Repeatability

The temporal repeatability can be evaluated by monitoring a section of fiber that is held at a constant temperature. It is the DTS-temperature's standard deviation in time, measured in a temporally isothermal environment (Tyler et al., 2009). Tyler et al., (2009) suggest subjecting the instrument box to environmental stresses, as for example varying instrument temperature to identify and quantify possible instrument drift errors and their effects on the measurement's temporal resolution. If instrument drift errors are noted, either through a test or during data control in post-processing, they usually can be corrected according to information from a precision calibrated reference device (chapter 4.2.3.1). The temporal variability of a DTS system determines how reliably it can interpret temperature changes in time (Tyler et al., 2009). Over a time duration of two hours, for a DTS system installed at Lake Tahoe, Tyler at al. (2009) noted temporal standard deviations (repeatability) of 0.08 °C, 0.13 °C and 0.31 °C for three different instrument types. They observed instrument drifts in the range of +/- 1 to 2 °C during multiday experiments, especially when instrument boxes were exposed to significant internal temperature changes (Tyler et al., 2009).

Spatial Resolution

The spatial resolution is the spatial integration scale over which a unique value of temperature is reported (Tyler et al., 2009). If the manufacturer provides a value of 1 m or 2 m for an instrument, this implies that temperature values are provided for each meter or for each two meters. The reported value is the average temperature according to the Stokes- and Anti-Stokes- range observed along this meter/these two meters at a given time step (Tyler et al., 2009). Usually the distances reported by manufacturers pose minimum spatial resolutions, which can be adjusted upwards for environments where measurements at a coarser scale seem appropriate (Tyler et al., 2009).

Tyler et al. (2009) further define a DTS system's spatial resolution as the distance it takes to detect 90 % of a known, abrupt temperature change, which is not the same distance as the manufacturer stated sampling interval. A similar definition can also be found in Smolen and van der Spek (2003) where the spatial resolution of a DTS system is defined as the distance between the 10 % point and the 90 % point of a measured temperature trace of a step change in temperature in reality (see Figure 32). Tyler et al. (2009) suggest that the spatial resolution of every DTS system should be tested before its application in the field. Figure 33 shows how a small abrupt temperature anomaly is detected with DTS measurements. Temperatures are averaged along a distance that is equal to the spatial integration scale. If a temperature anomaly is smaller than this spatial integration scale it cannot be fully detected (Smolen and van der Spek, 2003).

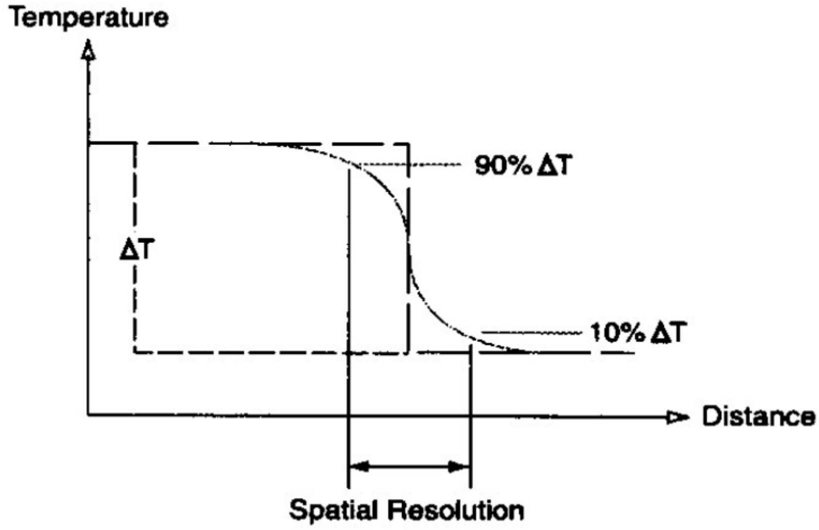

Fig. 32: spatial resolution of a DTS system (Smolen and van der Spek, 2003)

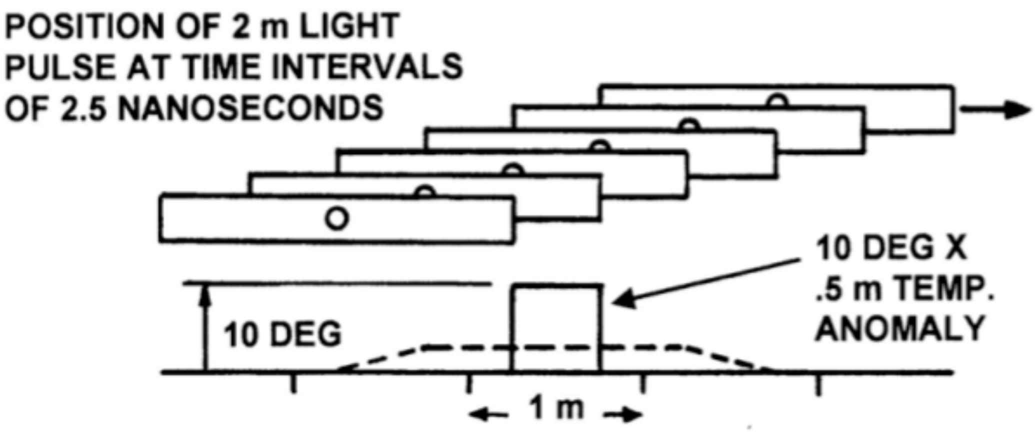

Fig. 33: Temperature anomaly measured with a DTS system (Smolen and van der Spek, 2003).

Temporal Resolution

The temporal resolution is equivalent to the time intervals of DTS measurements. Most instruments allow intervals as small as 10 seconds. However, as described above, the length of time intervals strongly affects data accuracy. Therefore, and also for reasons of efficient use of memory capacity, measurement intervals should be set only as small as necessary for a given application (Tyler et al., 2009). It is also possible, however, to achieve the same statistical reduction of variance (and accordingly standard deviation) and increase of accuracy through averaging of short sampling intervals during data post-processing (Tyler et al., 2009). Care has to be taken when armed fiber-optics are used, as, due to their large diameter and possible high heat capacity of their coatings and of included strength elements, responses to temperature changes might be delayed (Tyler et al., 2009).

For detailed descriptions of experiences with Raman Spectra Distributed Temperature Sensing systems in environmental applications see also Selker et al. (2006) and Tyler et al. (2009).

4.2 CASE STUDY ON MAMMOTH MOUNTAIN, CA

4.2.1 Study Site and Experimental Set-up

Location

The Cooperative Snow Study Site at Mammoth Mountain, CA, U.S.A., is located on a northeast-facing slope in the Mammoth Mountain Ski Area on the eastern side of California's Sierra Nevada (37 deg. 37 min. N, 119 deg. 2 min. W, 2940m above sea level) (Fig. 34 and 35).

(http://maps.google.com/maps?hl=de&tab=wl)

Fig. 34: Location of Mammoth Mountain, California, U.S.A Fig. 35: location of the Cooperative Snow Study Site on Mammoth Mountain

Snow and energy budget conditions have been monitored at the Mammoth site since the 1970ies. The skiing resort's infrastructure provides easy all-year-round access for researchers. The site itself is strictly closed to any skiing traffic in order to guarantee that the snow pack remains undisturbed from accumulation through melting. Today's permanent holdings at the site include radiometers, measuring incoming and outgoing radiation, sensors to measure air temperatures, relative humidity, wind speed and direction and temperature sensors placed at various depths in the soil and in the snow pack. A steel cargo container (Fig. 36), partly buried in the soil and completely buried in the snow by February or March during most winters, serves as a small laboratory, which is connected to power supply and which provides shelter for various instruments and computers.

Fig. 36: steel cargo container at the snow study site on Mammoth Mountain

A Campbell CR7 data logger records environmental measurements from the instruments on the site. On an hourly basis they are downloaded and quality-checked by the University of California, Santa Barbara and then are stored at the MMSA data base, a Microsoft Access relational data base management system (RDBMS). The data are available on an SQL Server 7 RDBMS and can be accessed via the Internet (http://neige.bren.ucsb.edu/mmsa/description.html).

Climate

The Sierra Nevada is the highest mountain range of the lower 48 states of the United States of America. The Eastern Sierra region constitutes a part of it, which lies mostly in eastern California and partly in western Nevada (Smith, 2000). Temperatures are relatively moderate, and winters are warm and summers are dry. The mountain range is within about 300 km of the Pacific Ocean and is located in a Mediterranean climate zone. 75 % of the precipitation fall between November and April, with its highest concentration between December and March. Winter in the eastern Sierra Nevada comes in a series of steps, during which air temperatures drop rapidly and snow levels increase with successive storms until snow packs reach their maximum depth around mid-March (Powell and Klieforth, 2000, Whitney, 1979). The first snowfall in autumn usually melts on the warm ground (Whitney, 1979); snow covers can persist until June, July or longer. The Sierra Nevada is one of the snowiest places in Northern America (Whitney, 1979). Snowfall totals near the crests of the Sierra Nevada typically reach between 7 m to 11 m; in wet years they can be as high as 15 m (Powell and Klieforth, 2000). Storms from the Pacific Ocean are the major source of precipitation in the region. Therefore snowfall amounts are lower on the east side of the Sierra range, as it lies in the rain shadow. However, the area around Mammoth Mountain constitutes an exception as storms from the Pacific move through a gap in the crest, bringing an annual snowfall that can approach 12.7 m (Whitney, 1979). In terms of avalanche climate zones, which are defined by the temperatures, amounts of snowfall, typical densities of the snow covers and magnitude of snow temperature gradients in an area, the Sierra Nevada can be allocated in the Coastal Zone (Mock and Birkeland, 2000). Coastal avalanche climates are characterized by mild temperatures, abundant heavy snowfall and high-density snow covers with a relatively small temperature gradient. On the opposite, the Continental zone stands for cold temperatures, less abundant snowfall, lower density snow covers and steeper temperature gradients. The Intermountain zone lies in between these two extremes (Mock and Birkeland, 2000). Mock and Birkeland (2000) studied snow avalanche climates also on a smaller scale. They analyzed data from various locations within the mountain ranges of the western United States and separately assessed their snow avalanche climate characteristics for each particular winter season. In a total of eighteen analyzed winter seasons the Mammoth Mountain region was twelve times classified as a Coastal- and six times as an Intermountain avalanche climate (Mock and Birkeland, 2000).

Measurement Set-up and Calibration

General Set-up

A multimode AFL flat drop fiber-optic cable (see Appendix C) was deployed in November 2008 prior to the first snowfall. A single cable cladding of 1000 m length contained a 2000 m **loop** of multimode fiber. The fiber loop started at the research container, crossed the site in several loops and turned around in a turnaround box, again close to the container, at 1000 m. It returned along the same path, in the same cable cladding, and arrived back at the start with a total fiber length of 2000 m. Figure 37 provides an overview of the fiber-optic cable deployment at the research site, close to the middle station of Mammoth Mountain's skiing resort.

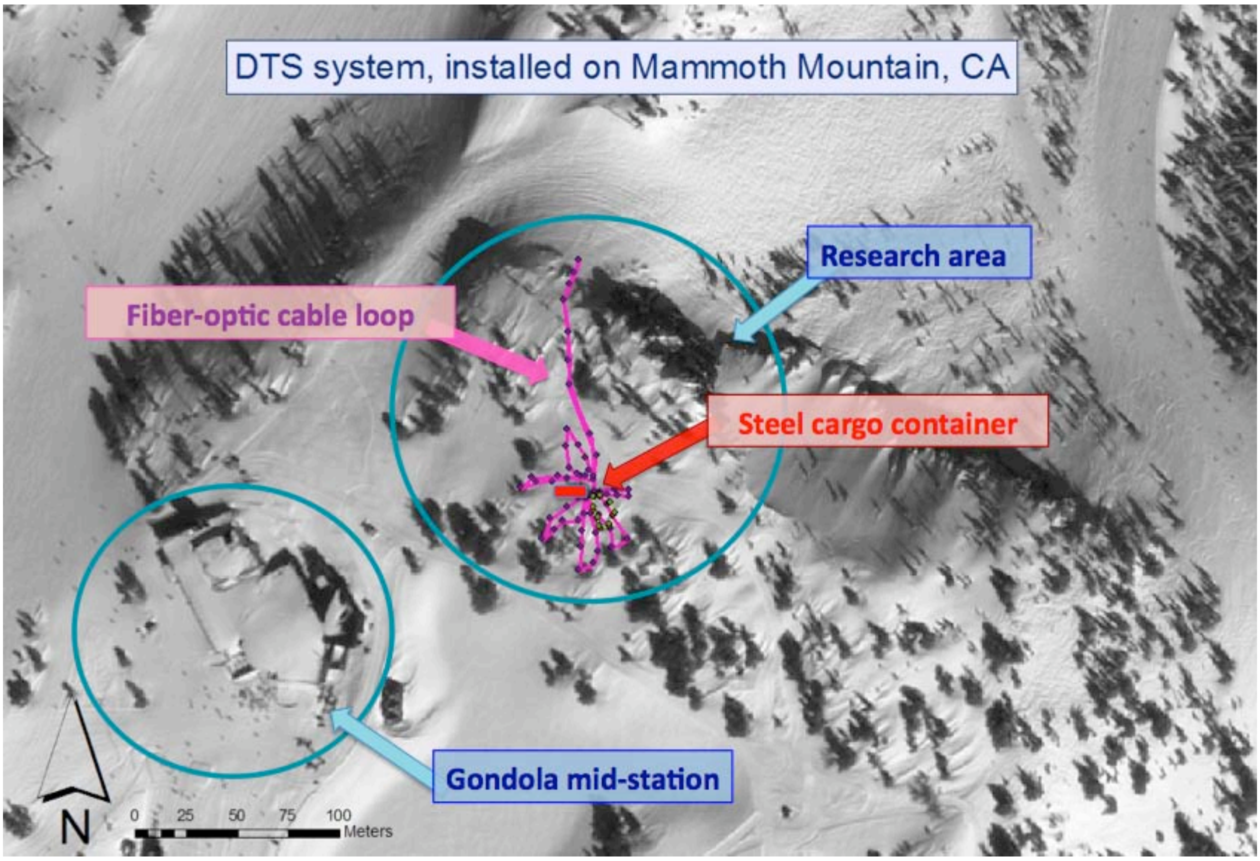

Fig. 37: Overview DTS installation on Mammoth Mountain, CA

Both ends of the multimode fiber were accessible in the container where they could be connected to a DTS instrument box, allowing double-ended measurements. 660 m of cable were deployed on the ground in seven loops around it, which lead over varying soil conditions and different vegetative covers. Another 100 meters were kept in reserve to be laid out on about 1 m and 1.9 m of snow later in the season, right above the southeast loop of the ground deployment. The remaining cable meters consisted of coils of 40 to 60 m length, some of which were placed on the ground, two of them were slightly buried in the soil and some were used in calibration and configuration set-ups during measurement sessions. Thermistor strings that were connected to the Campbell CR7 data logger and self-recording pt-100 temperature loggers were placed in several spots along the cable to provide data for control and potentially required corrections. The cable ends were connected to a Sensornet Halo DTS instrument box. The box was installed in the container, which offered protection against the harsh winter environment. Power supply was provided through an electrical connection in the container. The Halo can measure temperatures along a fiber-optic cable of up to 4km length, with a manufacturer stated spatial resolution of 2 meters. Temperatures were measured during four distinct measurement sessions of one to three weeks in December/January 2008/2009, February 2009, March 2009 and April/May 2009.

Calibration

As temperatures at the site on Mammoth Mountain would drop below the freezing point, maintaining a constant temperature ice-slush bath or a well-mixed water bath for calibration was not possible. Alternatively to an ice-slush- or water bath a portion of the snow-pack was chosen as calibration environment. 30 m of coiled cable were buried in the snow, together with a reference device. In December/January and in February a pt-100 thermologger was buried together with a 30 m calibration coil under about 30 to 50 cm of snow. Before they were buried, coil and logger were put in a snow filled river bag, which had been used to transport the instrument box to the site, (Fig. 38) to prevent warming of the black cable through solar radiation.

Fig. 38: river bag for instrument transport and protection of the calibration coil against solar radiation

As the logger data was not available while the device was buried, additional measurements were necessary to retrieve real-time temperatures for calibration. VWR-thermometers were used to measure these calibration temperatures. After bag, calibration coil and thermologger had been excavated at the end of February measurements, the 30 m coil was buried again immediately, together with a thermistor, which was part of the Cooperative Snow Study site's permanent holdings. The thermistor was connected to the Campbell CR7 data logger, which allowed for online queries and real time readings at the site (http://dub-snow.icess.ucsb.edu/mmsa/) during measurement periods. Additional VWR thermometer measurements for calibration were not necessary in March and April/May. The calibration coil and the reference thermistor remained buried in the snow and the whole calibration section was sufficiently covered to protect it against influence from solar radiation. Another 60 m coiled section of the cable had been deployed at the soil snow interface, next to another thermistor of the Cooperative Snow Study site that was also connected to the data acquisition system. Figure 39 displays the layout of the DTS system on Mammoth Mountain. The start and end of the fiber loop were located in the container; the turnaround box, at the end of the cable cladding, was kept in a coil outside of the snow and close to the container.

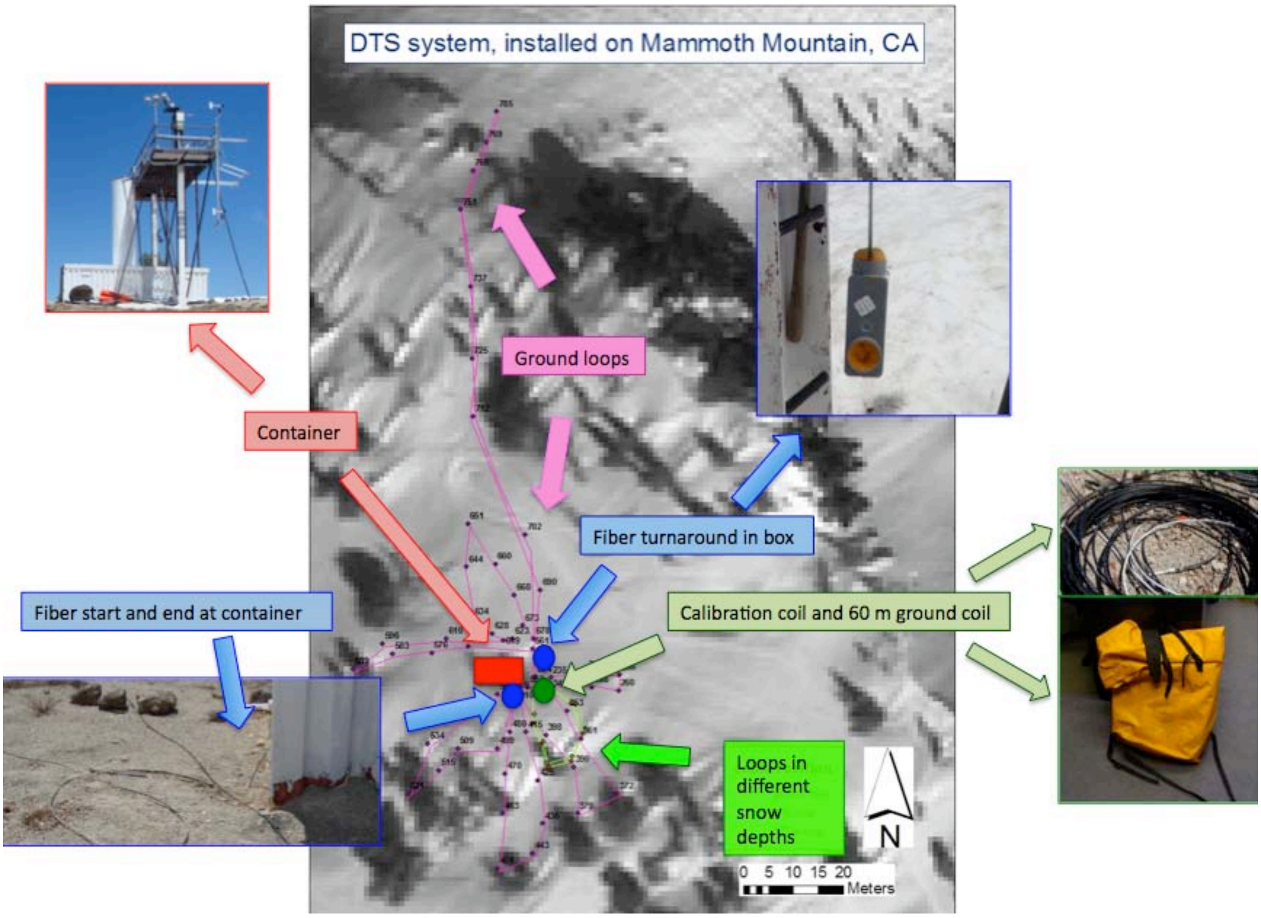

Fig. 39: components of a DTS system installed on Mammoth Mountain, CA

Depending on the type of cable a coiled 20 to 40 m section covers an area of about 0.3 to 0.5 m^2 width and of 0.1 to 0.3 m height. Standard temperature measurement devices that can be used as a reference typically provide point measurements. Therefore, as the two devices cover different areas, thermal stratification within calibration environments needs to be controlled. Close thermal contact between DTS-cable and reference devices is crucial (Tyler at al., 2009). On Mammoth Mountain where maintaining ice-slush baths or well-mixed water baths was not possible and where a part of the snow pack was chosen as a calibration section, inevitably temperature gradients established within these environments. When calibration sections were buried by less than 1 m of snow in December and at the beginning of February measurements, prevalent temperature gradients in the calibration section varied strongly and variations correlated to changes in ambient air temperatures. These effects lead to a low absolute accuracy of measured temperatures.

Despite the fact that it was to a certain extent sheltered in the container, the instrument box was still exposed to strong instrument internal temperature variations and because measurement sessions were planned over the course of several days to a couple of weeks, instrument drift errors had to be expected. However, as it was not possible to maintain a constant temperature bath and, as the Halo instrument box did not provide an independent internal temperature sensor (chapter 4.1.2 - DTS Instruments), only a fixed offset calibration was possible and fixed calibration temperatures were assigned during instrument configuration. Data from the additional external reference devices placed with calibration coil and with the 66 m coil on the ground were used to correct for instrument drift during data post-processing.

4.2.2 Data Collection

Measurements were taken during four distinct measurement sessions: from December 29th 2008 to January 09th 2009; from February 4th to February 16th 2009; from March 7th to March 11th 2009 and from April 21st to May 9th 2009. The Halo instrument box was set to take consecutive measurements over five minutes, which, according to the manufacturer, corresponds to a temperature resolution of better than +/- 0.05 °C (chapter 4.1.2, Fig. 20, www.sensornet.co.uk). The spatial resolution was set at the smallest possible value, which was 2.09 m. The instrument box was transported to the site in a river bag (Fig. 38) and remained in the container only throughout measurement sessions. The data was stored on board of the instrument box and was downloaded to a computer for processing and analysis at the end of each measurement session.

PART C: RESULTS

5. DATA POST PROCESSING – QUALITY CONTROL AND CORRECTIONS

Errors caused by instrument noise could be corrected successfully. Also an erroneous offset in the February trace that was introduced during calibration was removed during post-processing. A step loss was encountered in all traces, which might have caused additional data noise but did not lead to erroneous temperature measurements as it was corrected successfully by the instrument, with the exception of the April- and May trace, where automatic corrections failed. A lack of two comparable temperature environments at the beginning and at the end of the cable prevented corrections for this step loss error during post-processing. Data from December through March were included in further analyses of temperatures measured along the entire length of the deployed cable; from April and May only data measured before the encountered step loss was used, which still allowed analyses of temperatures in different snow depths.

5.1 INSTRUMENT DRIFT

To assess instrument-drift, DTS-measured temperatures averaged along a section of cable were compared to temperatures measured by an external device. Differences were identified as artificially introduced. To ensure that reference-device temperatures were representative for the cable transect, a cable section located in a temperature environment constant in space and close to the device was chosen. For easier identification of instrument drift errors temperature environments also constant in time should be preferred (Tyler et. al, 2009). Temperatures measured by a reference device close to the 60 m cable section that was coiled up on the ground showed close to constant behavior during distinct measurement sessions, also in time. Only during December/January small changes were observed (variance of 0.0072 °C, Fig. 40).

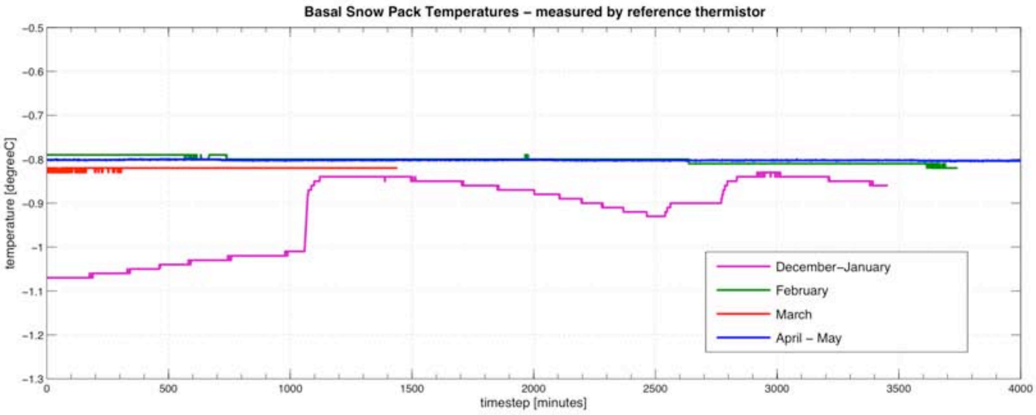

Fig. 40: evolutions of temperatures at the base of the snow pack, absolute values are colder than in reality

Figure 40 shows evolutions of temperatures at the base of the snow pack, measured by the Cooperative Snow Study site's thermistor. Changes in temperatures were only observed during December and January when the snow pack was still relatively shallow (155 to 130 cm) and when ambient air temperatures were varying strongly (+10 to -10 °C). Absolute temperature values shown in this graph are by about 0.6 °C colder than those measured with the DTS system.

DTS temperatures were averaged along a 55 m section within the 60 m ground coil, and were compared to temperatures measured by the close by thermistor (ground thermistor). Differences in their pattern could be identified as instrument drift over time. Absolute thermistor-temperatures shown above were colder than those measured with the DTS system (by about 0.6 °C). The thermistor measured temperatures below were corrected for this offset, as it was decided that the DTS temperatures, even though they were of a limited absolute accuracy seemed more reasonable. As no reliable calibration was available, neither for the thermistors nor for the DTS system, absolute temperatures remained unknown. For each time step a difference between offset corrected thermistor temperatures and averaged DTS measured temperatures was calculated. Also DTS temperatures, averaged along the 30 m calibration section, were compared with associated reference thermistor temperatures (calibration thermistor). As drift errors showed similar behavior along both cable transects, it could be assumed that they were constant in space i.e. affecting the entire length of the cable. Differences derived from the 55 m ground section were subtracted from uncorrected DTS measured temperatures along the entire length of the cable. Each drift corrected trace showed good agreement with according reference device's traces in both sections, at the 55 m ground coil and at the 30 m calibration coil. Figures 41 to 48 display the steps of instrument drift corrections during data post-processing:

December/January

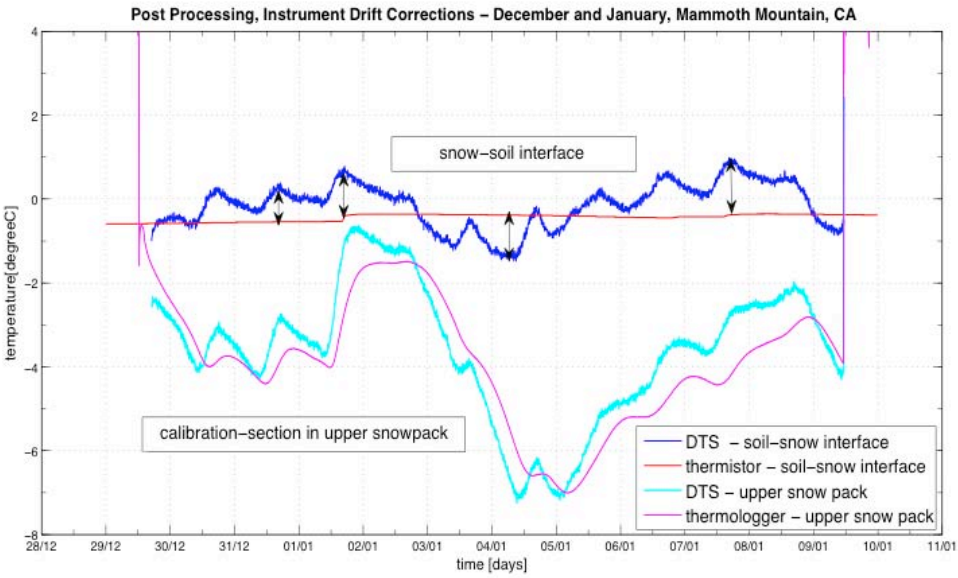

Fig.41: uncorrected DTS data and reference temperatures, December/January 2008/2009

Figure 41 shows uncorrected DTS temperatures and thermologger temperatures at the soil snow interface and in the calibration section, which was located about 30 cm below the snow surface. Deviations between DTS temperatures and thermologger temperatures are the result of instrument drift over time. Differences for each time step were calculated and were used for data corrections during post-processing.

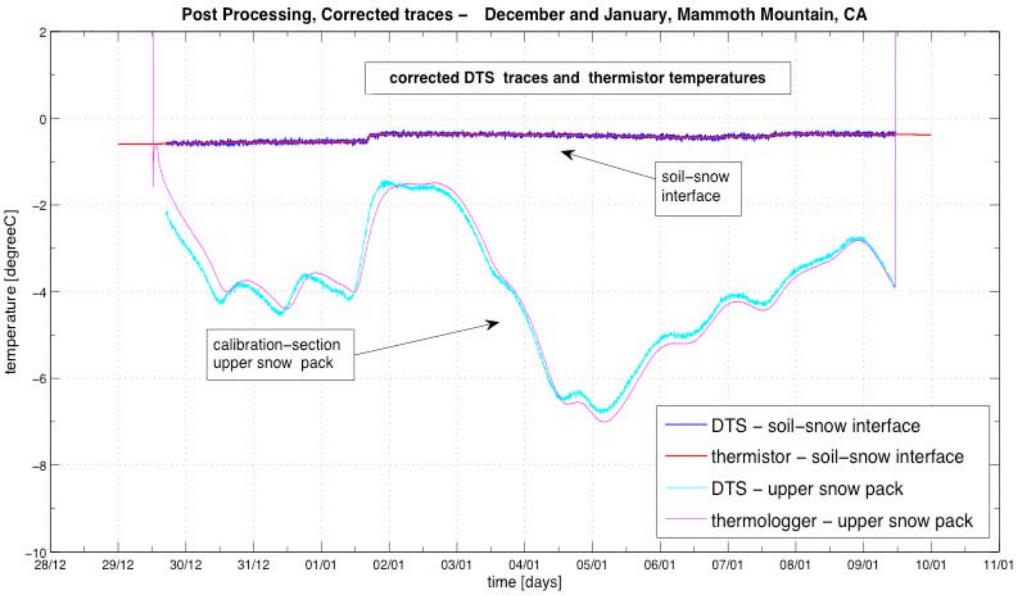

Fig.42: corrected DTS data and reference temperatures, December/January 2008/2009

Figure 42 shows corrected DTS temperatures and thermologger temperatures at the soil snow interface and in the calibration section. Small deviations between absolute values and pattern of DTS temperatures and themologger temperatures are the result of a strong, variable temperature gradient in the calibration section at accordant times.

February

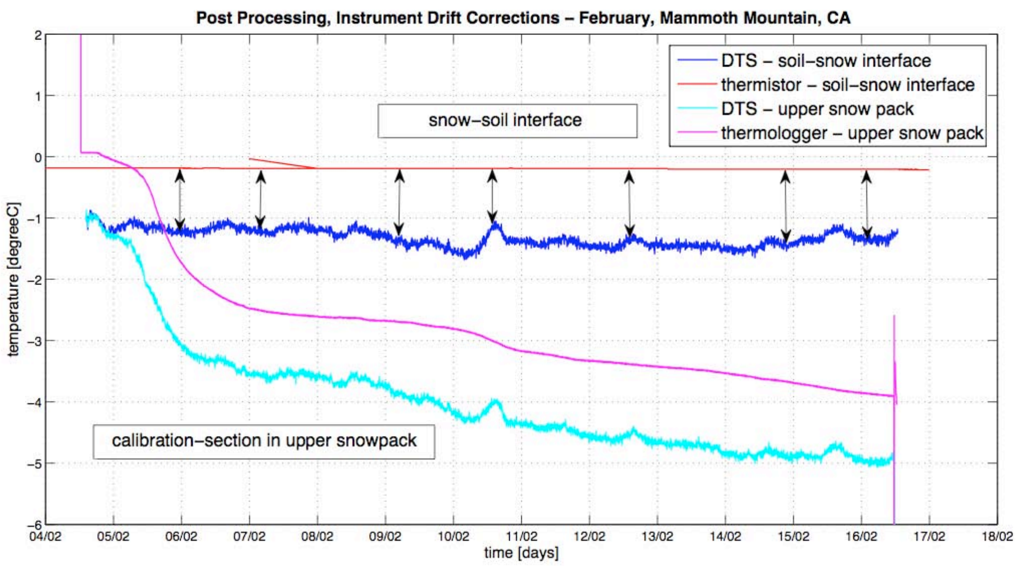

Fig. 43: uncorrected DTS data and reference temperatures, February 2009

Figure 43 shows uncorrected DTS temperatures and thermologger temperatures at the soil snow interface and in the calibration section, which was located about 60 cm below the snow surface. Deviations between DTS temperatures and thermologger temperatures are the result of instrument drift over time. Differences for each time step were calculated and were used for data corrections during post-processing. Deviations from the reference device's traces shown in the February data are not only resulting from instrument drift over time, but also include a temperature offset caused by inaccurate calibration (see below, chapter 4.2.3.2, for further explanations).

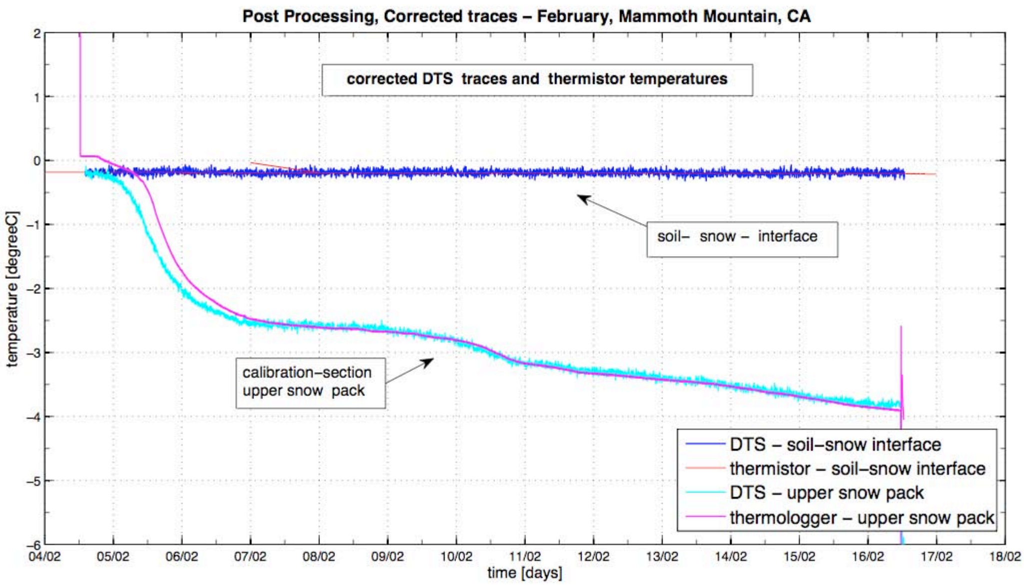

Fig. 44: corrected DTS data and reference temperatures, February 2009

Figure 44 shows corrected DTS temperatures and thermologger temperatures at the soil snow interface and in the calibration section, located in the upper part of the snow pack. The February data was also corrected for an offset error (see below, 4.2.3.2). Deviations in absolute values and pattern of DTS temperatures from themologger temperatures at the beginning of the February trace are the result of a strong temperature gradient in the calibration section at this time.

March

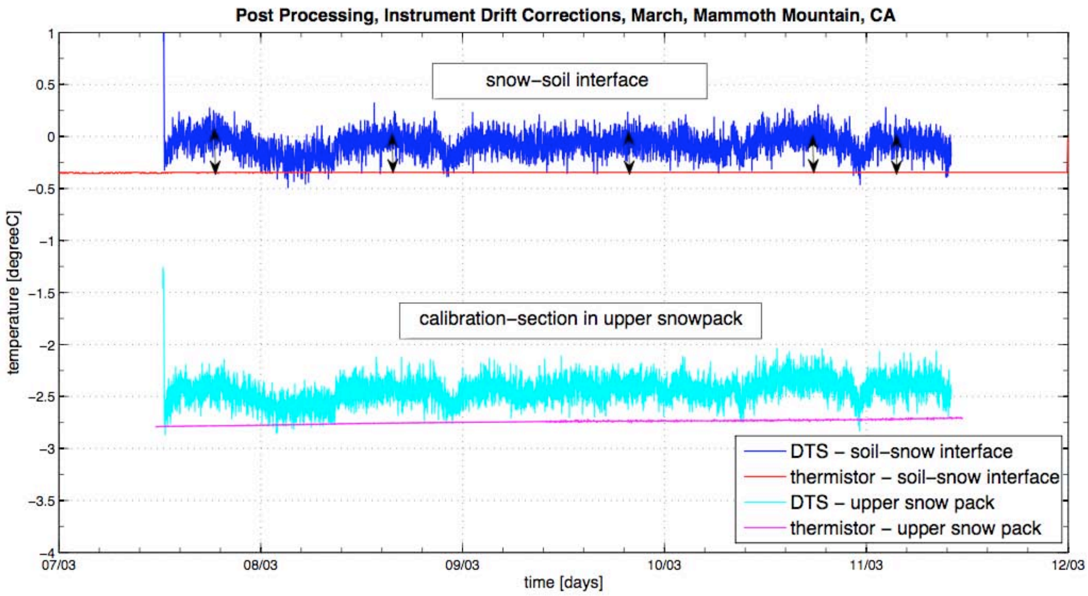

Fig. 45: uncorrected DTS data and reference temperatures, March 2009

Figure 45 shows uncorrected DTS temperatures and thermologger temperatures at the soil snow interface and in the calibration section, which was located within the snow pack, about 1.5 m to 1 m below the snow surface. Deviations between DTS temperatures and thermologger temperatures are the result of instrument drift over time. Differences for each time step were calculated and were used for data corrections during post-processing.

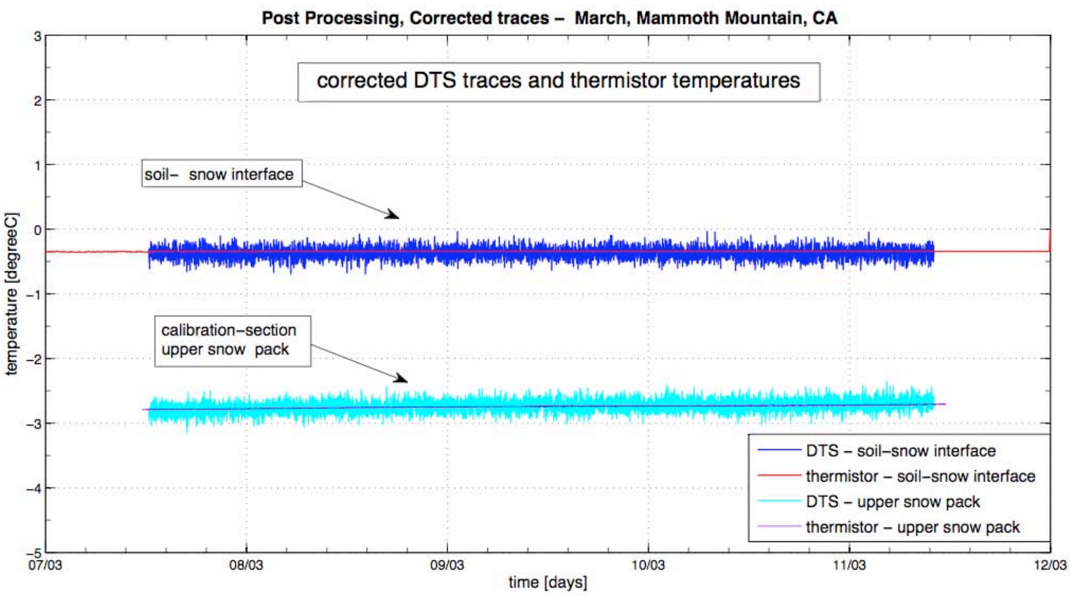

Fig. 46: corrected DTS data and reference temperatures, March 2009

Figure 46 shows corrected DTS temperatures and thermologger temperatures at the soil snow interface and in the calibration section, located in the snow pack.

April/May

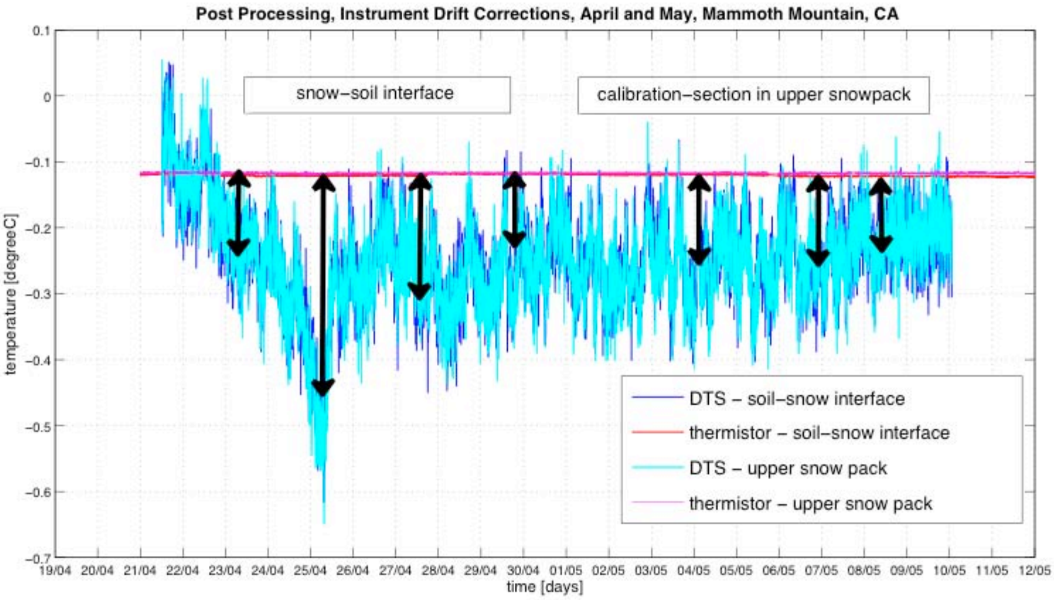

Fig. 47: uncorrected DTS data and reference temperatures, April/May 2009

Figure 47 shows uncorrected DTS temperatures and thermologger temperatures at the soil snow interface and in the calibration section, which was located within the snow pack, about 1 to 0.5 m below the snow surface. Deviations between DTS temperatures and thermologger temperatures are the result of instrument drift over time. Differences for each time step were calculated and were used for data corrections during post-processing.

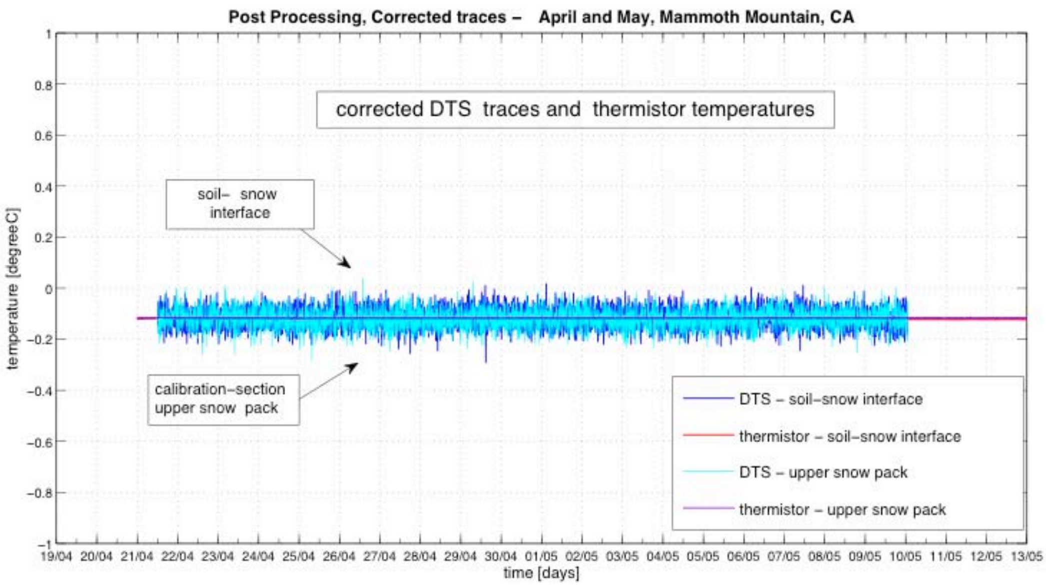

Fig. 48**:** corrected DTS data and reference temperatures, April/May 2009

Figure 48 shows corrected DTS temperatures and thermologger temperatures at the soil snow interface and in the calibration section, located in the snow pack.

Instrument drift errors correlated to changes in ambient air temperatures. In December and January, when the steel cargo container that sheltered the Halo instrument box was buried by less snow than during the following months and when air temperatures outside the container varied by 20 °C within few days, the observed instrument drift was larger than during the following months. In May, when the container was still covered by a deep snow pack and when air temperatures showed less variation, instrument drift decreased to a minimum. Figure 49 displays the ranges of necessary instrument drift corrections for all measurement sessions conducted on Mammoth Mountain and the means and variances of measured ambient air temperatures in the steel cargo container at according times. Note that the corrections that are displayed for February include an offset error, which is not the result of instrument drift but was introduced through an erroneous offset calibration.

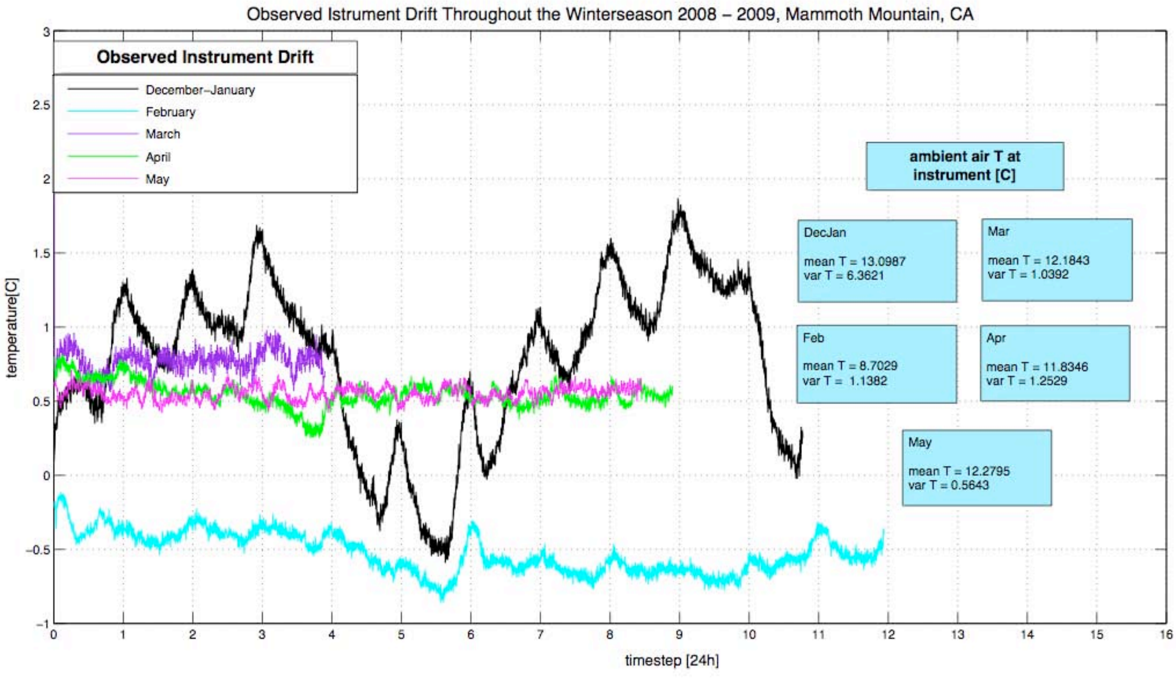

Fig. 49: Instrument drift related to ambient air temperatures and their variability

5.2 TEMPERATURE OFFSETS

Compared to reference devices, raw (uncorrected) DTS temperatures from Mammoth Mountain showed two kinds of offset errors: Traces in December/January 2008/2009 and at the beginning of February 2009 showed temperature offsets, which were inconsistent in time and in space. These inconsistent offset errors affected the calibration sections only (Fig. 50, Fig. 51). Raw February temperatures also included an offset error that was consistent in time, and that was present along the entire length of the fiber-optic cable (Fig. 52). Inconsistent offset errors in the calibration sections correlated to changes in ambient air temperatures.

Inconsistent Offsets

During December- and January measurements no major snowfall events occurred on Mammoth Mountain. Throughout the entire measurement period the calibration section remained shallowly buried (by about 30 cm of snow). At the same time ambient air temperatures varied within a range of -10 to +10 °C, indicating a strong, variable temperature gradient within the calibration section during this time. Differences in DTS measured temperatures and temperature data from the thermologger resulted from different snow **areas** that were covered by the instruments (areal measurement vs. point measurement, chapter 4.2.1 - Calibration). Similarly, at the beginning of the February session, differences in snow areas covered by the instruments led to differences in their reported temperature traces. Air temperatures dropped quickly by about 7 °C on February 5th, when the calibration section was still shallowly buried. At this time the existence of a steep temperature gradient within the calibration section was very likely. This was the only time when temperatures, measured by the DTS system in February, deviated from those measured by the reference device. Figure 50 and 51 show the evolution of offsets in December/January and in February related to ambient air temperatures and snow depths:

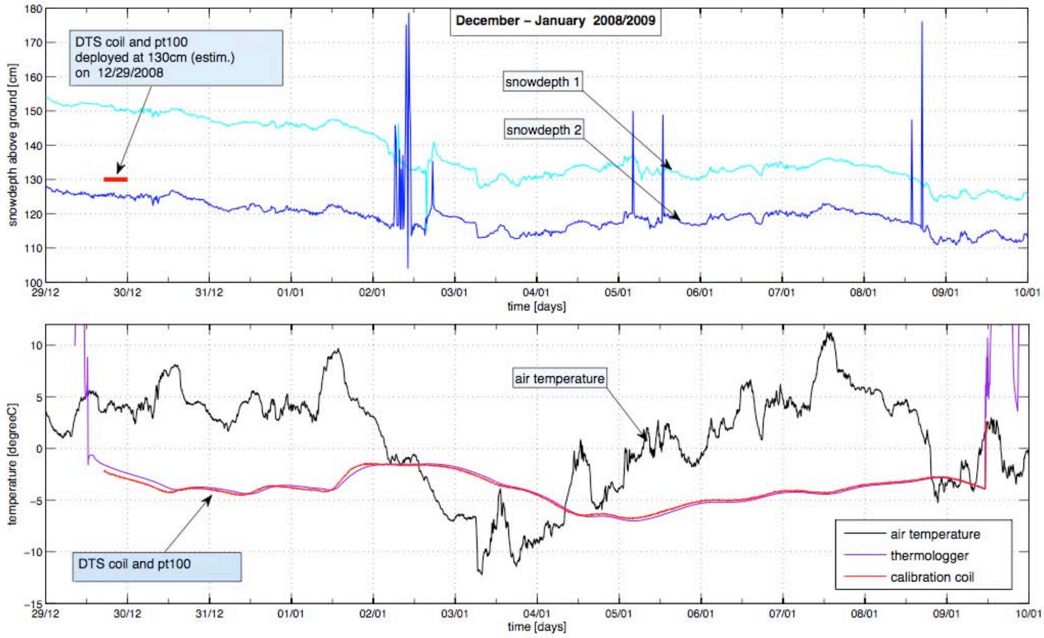

Fig. 50: evolution of snow depth, air temperatures and DTS temperatures within the calibration section, Dec/Jan 2008/2009

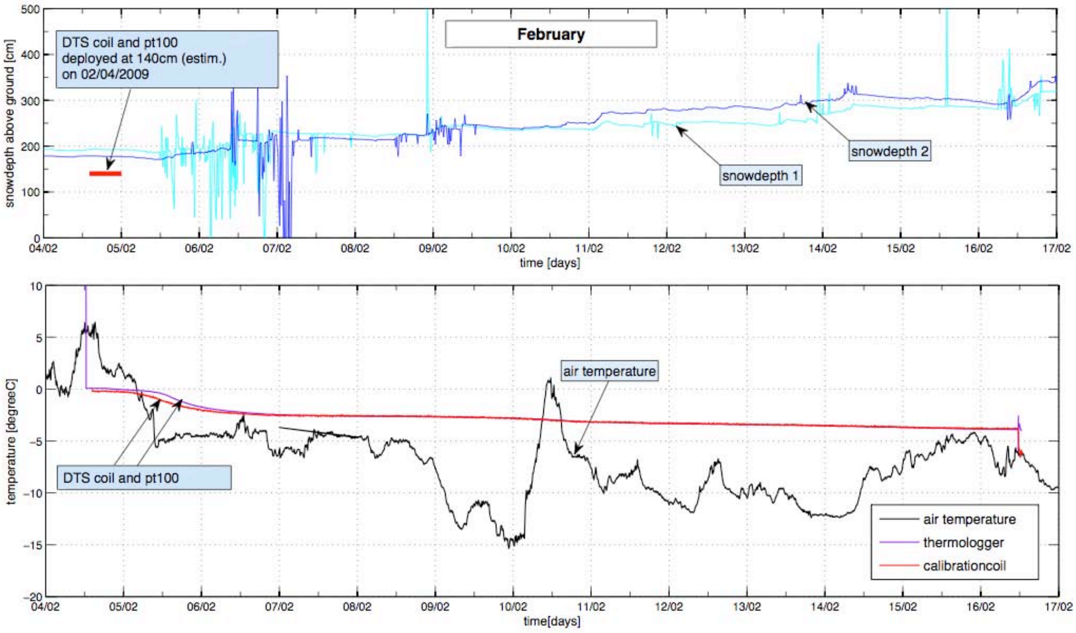

Fig. 51: evolution of snow depth, air temperatures and DTS temperatures within the calibration section, February 2009

Figure 50 and 51 show temperatures in the calibration section related to ambient air temperatures and evolutions of snow depths in December/January 2008/2009 and in February 2009. Snow depth 1 was measured next to the calibration coil and -logger. Snow depth 2 represents a section about 10 meters further west.

Consistent Offset

Poor thermal contact between a VWR thermometer and the calibration coil during calibration caused an additional offset error in the February DTS data. The instrument was told an inaccurate calibration temperature, as the VWR thermometer data was not representative for the calibration coil. An incorrect temperature offset was calculated. During post-processing offsets between drift-corrected (chapter 4.2.3.1) DTS temperatures, averaged along 20 m within the 30 m calibration section, and thermologger temperatures were calculated (Fig. 52).

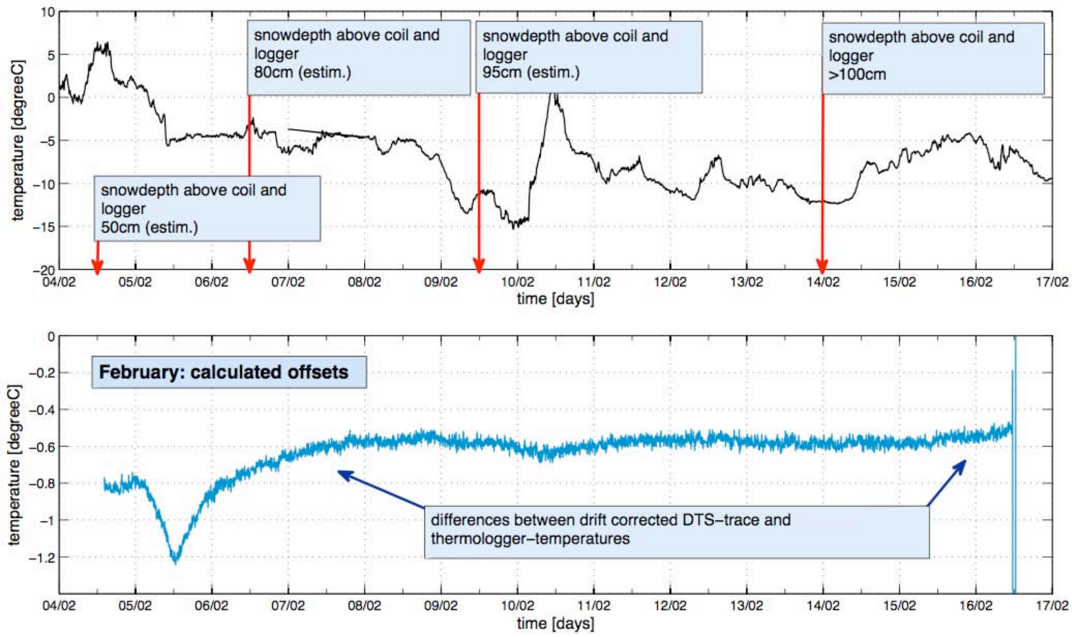

Fig.52: offset errors, air temperatures and snow depths, February 2009

Figure 52 shows evolutions of temperature offsets related to air temperatures and snow depths above the calibration section.

Figure 52 shows calculated offsets between averaged DTS temperatures and thermologger temperatures in the calibration section related to the evolution of snow depths and air temperatures during February 2009. After February 8th offsets stabilized around -0.6 °C. Strongly varying offsets at the beginning of February measurements correlated to a drop in air temperatures during the night from February 4th to February 5th. At this time the calibration section was located in the upmost part of the snow pack; a steep, variable thermal gradient was likely to exist (Fig 52). When snow depths increased above the coil and the logger, influences on offsets by changes in ambient air temperatures decreased. Only around February 10th, when air temperatures varied by 15 °C within half a day, temperature differences between coil and logger showed a reaction. To determine a correction value for the offset error that was introduced during calibration, only temperature deviations between February 12th and February 15th were considered. The offset correction value that was added to the drift corrected DTS temperatures was averaged over this time span in order to avoid an introduction of additional data noise. Data from the entire February measurement session, over time and over space were corrected for this offset (for corrected trace see above, chapter 4.2.3.1, Fig. 44).

5.3 STEP LOSSES

Figure 53 shows the signal attenuation along the fiber-optic cable and local step losses, which were encountered along the Stokes signal's- and AntiStokes signal's traces (temperatures measured along the cable at a single time step) measured on Mammoth Mountain. Expectedly losses can be seen at the beginning of the fiber, where it was connected to the instrument box and at 1000 m where the fiber loop turned around in the turnaround box (chapter 4.1.1 – Attenuation and Differential Attenuation).

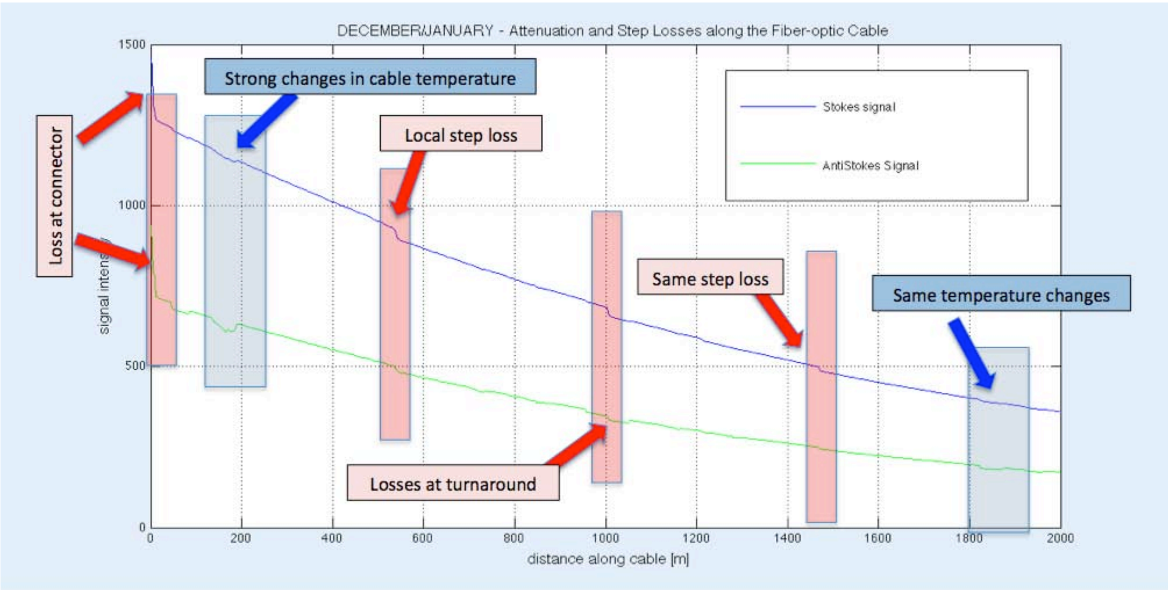

Fig. 53: step losses encountered in the Stokes- and AntiStokes signal, measured on Mammoth Mountain, December/January 2008/2009

An additional, unexpected step loss around 490 m was detected. The traces' pattern after 1000 m was the same, as the fiber looped back within the same cable cladding. The blue areas mark changes in signal strength, which can be mainly seen in the Anti-Stokes signal and which are the result of **real** temperature changes in the cable's environment.

Figure 54 displays the according part of the cable where the unexpected step loss was encountered. No clear indication of a reason for a step loss at this point could be identified. However, around cable meter 490 the cable crosses itself. The red bag in the picture marks cable meter 488 in the picture (Fig. 54). Also, shortly before meter 550 (marked by the GPS device in the picture) the cable went over a small, sharp ground feature right next to the corner of the container. Under the heavy load of a deep snow pack the cable crossing itself and bending over the small sharp ground feature might have caused increased signal losses within the fiber.

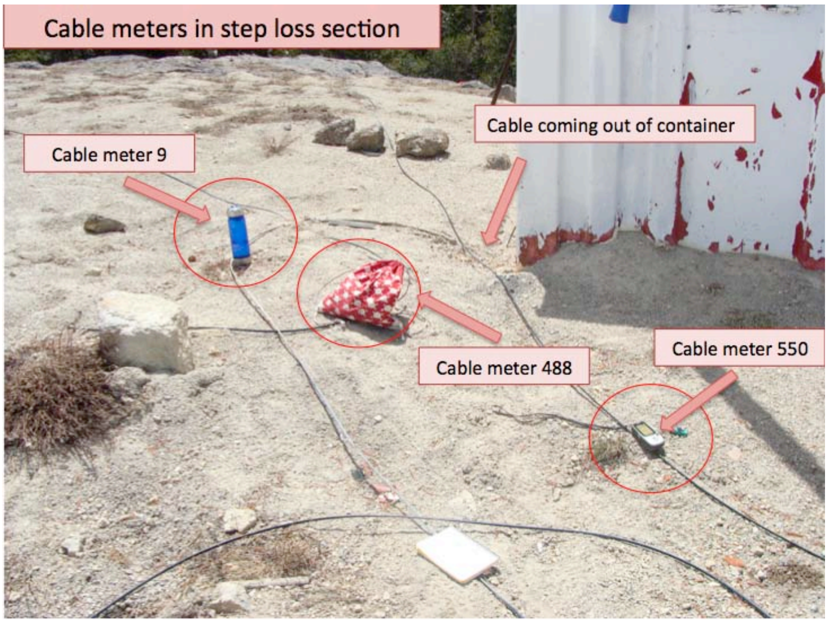

Fig. 54: meter markings at cable section where an unexpected step loss was encountered

The step loss at about 490 m was present throughout all measurement sessions. From December to March its effect increased, in April and May a second loss appeared at cable meter 550 (Fig. 55 and 56).

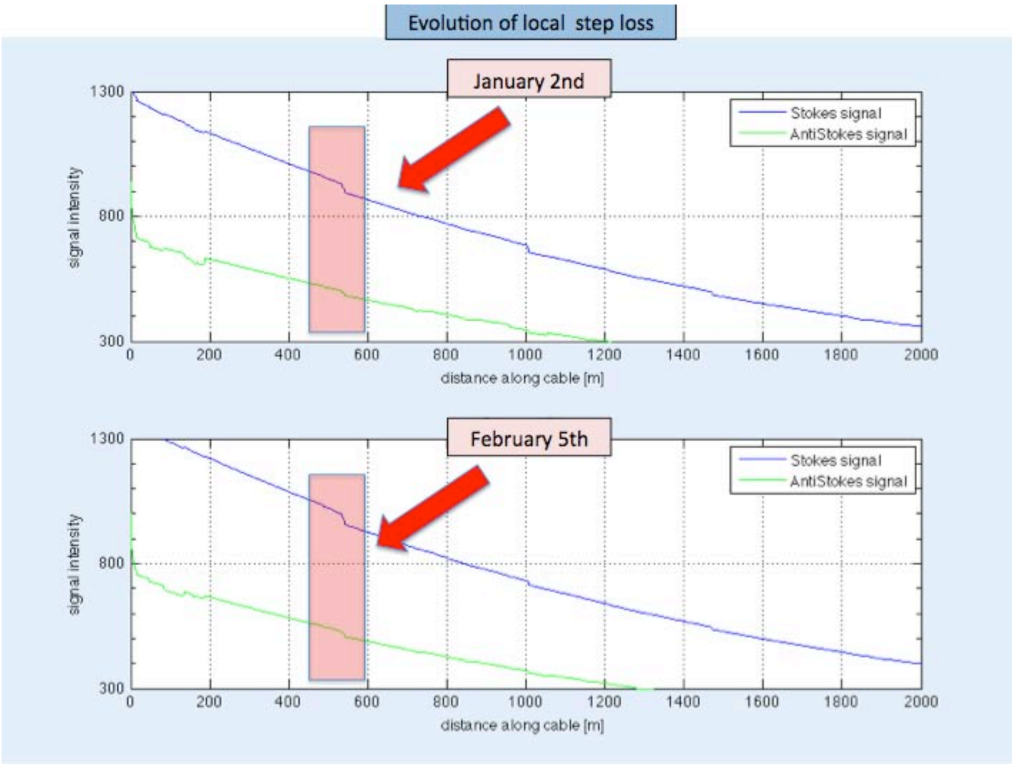

Fig. 55: encountered step losses at about 490 m in January and February

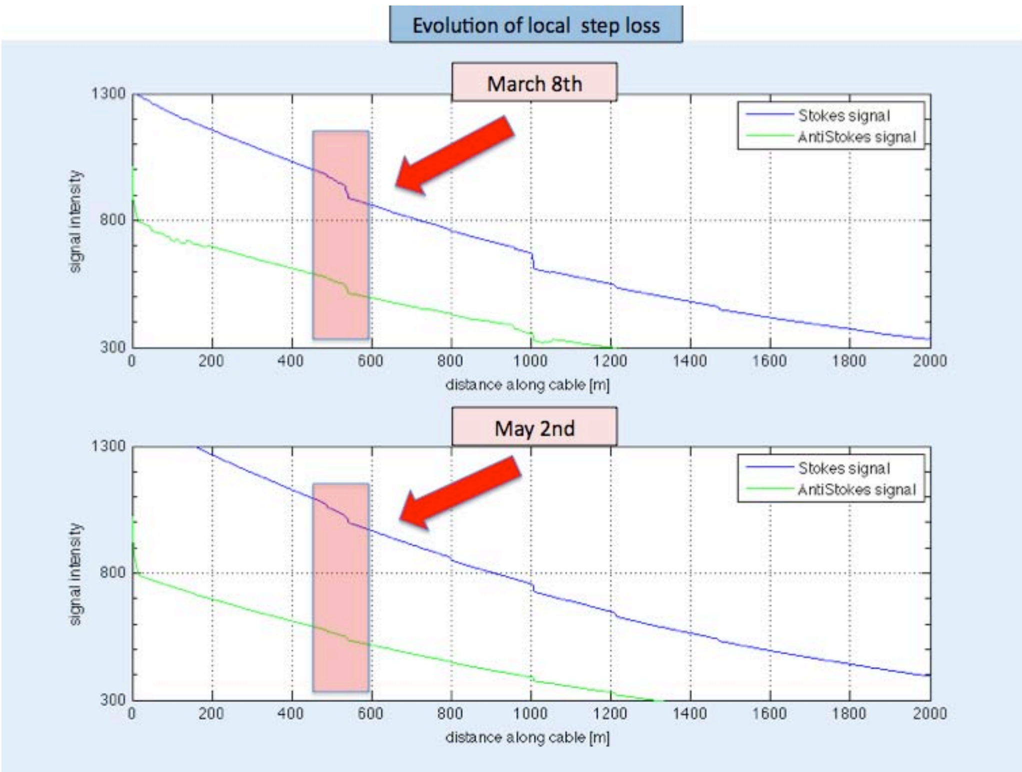

Fig. 56: encountered step losses at about 490 m in March and at about 490 m and 550 m in May

As measurements were taken in the double-ended mode the instrument box was able to automatically correct for the step losses and rendered correct temperature values for the measurements from December through March. In April and May, however, it rendered an erroneous temperature trace (Fig 57). The temperature trace was shifted by an offset of about 0.2 °C after the loss.

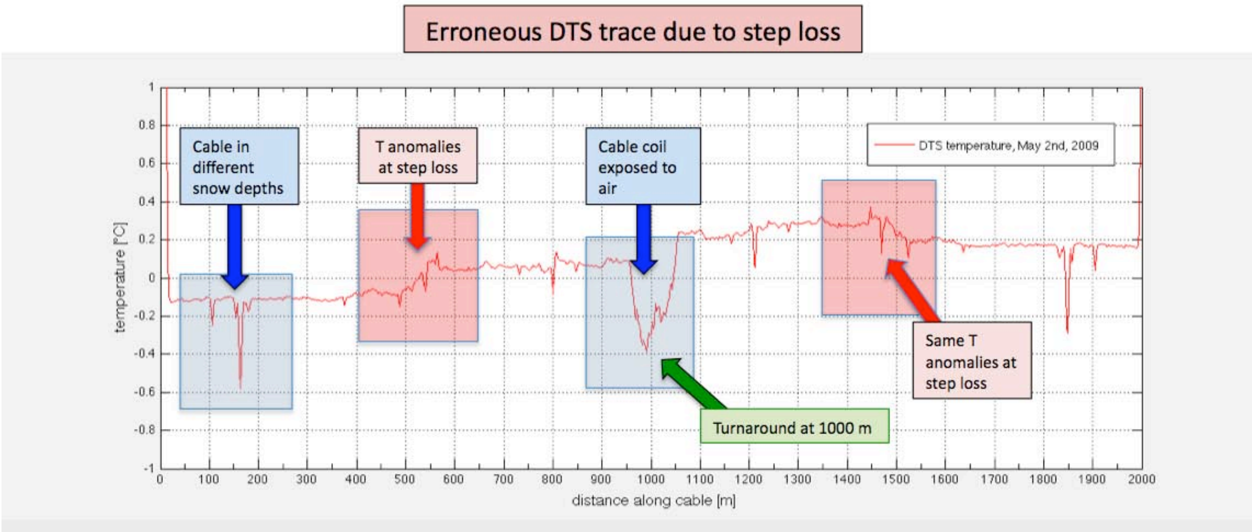

Fig. 57: erroneous temperature trace measured on Mammoth Mountain, May 2009

Two sections of cable, at the same temperature, of a length of at least three times the spatial integration scale, one before and one after the step loss would have been necessary in order to allow corrections for its effects. As such sections were not available the data could not be corrected during post-processing and it was excluded from further analyses of the ground temperature data (chapter 5.2). As temperatures along the loops in snow depths of 1 m (cable meter 132 to 182) and 1.9 m (cable meter 80 to 130) and along the ground loop below them (cable meter 345 to 409) were measured before the step loss and seemed unaffected by the error, they could still be included in later analyses (chapter 5.3).

6. RESULTS AND DISCUSSION

6.1 DATA ACCURACY

Absolute Accuracy

Due to the lack of a well-mixed ice-slush bath, or any other not stratified temperature environment, absolute DTS temperatures' accuracies measured on Mammoth Mountain were of a limited extent. As described above, the section of the snow that was covered by the reference devices differed from the section covered by the DTS calibration coils (point measurements vs. areal measurements, chapter 4.2.1 - calibration).

Relative Accuracy - Spatial and Temporal Repeatability

As no ice-slush bath was available as a reference for data accuracy assessments, a 55 m long section within the 60 m coil that was deployed on the ground, next to the steel container, was chosen. The section was covered by a snow pack, of at least 1.3 m depth at its minimum in December, and therefore was assumed to be located in a close to constant temperature environment, in time and in space. To assess the spatial repeatability (chapter 4.1.3) standard deviations of temperatures measured along this 55 m section were calculated for every time step of a measurement session and for data that was averaged over the course of 24 hours. Table 2 displays the average value of all standard deviations that were observed in space during an entire measurement session; for measurements with a temporal resolution of 5 min (minimum temporal resolution). Further it shows the largest observed spatial standard deviation of each measurement period. Table 3 shows the average of all spatial standard deviations and the largest spatial standard deviations for each measurement session; for temperature data with a temporal resolution of 24 hours. To assess the temporal repeatability (chapter 4.1.3) a single 2 m segment in the middle of the same 60 m section of the fiber-optic cable was used to calculate temperature standard deviations over time; it was calculated for measurements with a spatial resolution of 2 m (minimum spatial resolution) and with a temporal resolution of 5 min and of 24 hours. Table 4 shows the temporal standard deviations over the full length of each measurement session, of measurements taken at a 5 min interval. As small snow temperature variations over time could not be fully excluded in the reference section, especially in December/January when the snow pack was still shallow, also temporal standard deviations over the course of only 24 hours were calculated. It can be assumed that snow temperatures in this part of the snow pack remained fairly constant over the course of 24 hours. The temporal standard deviations over the course of only 24 hours are also shown in Table 4. Table 5 displays the temporal standard deviations over the full length of each measurement session, of data averaged to a temporal resolution of 24 hours.

Spatial Repeatability of Measurements Taken with a 5 min Temporal Resolution

Spatial Repeatability	**Dec/Jan**	**Feb**	**Mar**	**Apr/May**
Largest observed standard deviation [°C]	0.069	0.057	0.061	0.060
Average of all standard deviations [°C]	0.046	0.039	0.042	0.034

Tab. 2: spatial standard deviations over a constant temperature 55 m section along the fiber-optic cable, representative for a temporal resolution of 5 min

The slightly larger spatial variability in December can be explained by smaller snow depths and the according influence of a temperature gradient on the 55 meter of cable that were used for the calculations.

Spatial Repeatability of Data Averaged to a 24 h Temporal Resolution

Spatial Repeatability	Dec/Jan	Feb	Mar	Apr/May
Largest observed standard deviation [°C]	0.03	0.02	0.03	0.01
Average of all standard deviations [°C]	0.03	0.02	0.03	0.01

Tab.3: spatial standard deviations over a constant temperature 55 m section along the fiber-optic cable, representative for a temporal resolution of 24 hours

Temporal Repeatability of Measurements Taken with a 5 min Temporal Resolution

Temporal Repeatability	Dec/Jan	Feb	Mar	Apr/May
Over entire measurement session [°C]	0.085	0.038	0.039	0.038
Over 24 hours [°C]	0.033	0.038	0.038	0.039

Tab.4: temporal standard deviations of a 2 m segment within a constant temperature section along the fiber-optic cable, representative for measurements at a spatial resolution of 2 m and a temporal resolution of 5 min.

Temporal Repeatability of Data Averaged to a 24 h Temporal Resolution

Temporal Repeatability	**Dec/Jan**	**Feb**	**Mar**	**Apr/May**
Over entire measurement session [°C]	0.087	0.006	0.006	0.006

Tab.5: temporal standard deviations of a 2 m segment within a constant temperature section along the fiber-optic cable, representative for measurements at a spatial resolution of 2 m and a temporal resolution of 24 hours.

The larger temporal standard deviation over the entire measurement session in December/January of measurements taken at a 5 min interval and at a 24 hours interval can be explained by additional influences through real temperature variations within this reference section. At that time the section was not as deeply buried under snow as during the following months (1.3 m in December, up to 3.5 m in March and up to 3 m in April) and air temperatures varied within a range of 20 °C. Over the course of only 24 hours the standard deviation in December/January is similar to those calculated for the following months.

Comparability

Whereas the relative spatial and temporal distribution of temperatures measured along the cable can be compared throughout all measurement times, absolute temperature values can only be compared within one distinct session. Calibration set-ups for offset calibrations varied slightly and different reference devices were used during configuration, calibration and for corrections. Therefore care has to be taken with interpretations of absolute temperature values and with their comparison over different measurement sessions.

6.2 GROUND TEMPERATURE VARIABILITY

6.2.1 Spatial Variability of DTS Measured Ground Temperatures

Georeferenced points along the fiber-optic cable were imported into ArcGis (www.esri.com). An areal photo was used as a reference for small adjustments of point locations according to field notes, in order to improve the accuracy of their positioning. Temperature data that was averaged over the course of 24 hours was imported for each point included on the map; and interpolations using the Natural Neighbors tool, which can be found in the Spatial Analyst toolbox, were conducted. The maps below show temperature variations in space that were encountered at the base of the snow pack. For this specific field deployment the calculated temperature distribution was strongly influenced by the course of the deployed cable. Therefore it should be noted that conclusions about the areal distribution of temperatures based on the DTS data are only possible to a limited extent. The according pictures display terrain features of distinct locations of interest and the tables show the according field notes for a given spot. As described above (chapter 5.1.), data with a spatial resolution of 2 m, that was corrected for instrument drift (chapter 4.2.3.1) and averaged to a temporal resolution of 24 hours had a spatial repeatability (instrument caused standard deviation in space over a constant temperature section) of 0.03 °C or less and a temporal repeatability (instrument caused standard deviation in time in a constant temperature environment) of 0.006 °C. The temperature resolution, which can be achieved with a Sentinel Halo for measurements along a 2 km cable, averaged over 24 hours is better than 0.02 °C, which is the resolution corresponding to an averaging interval of 1 hour (chapter 4.1.2, Fig. 20). The absolute values are of a limited accuracy (chapter 5.1.). Absolute temperatures can be compared to each other within a distinct measurement session (January and December, February, March) but should not be compared between different sessions.

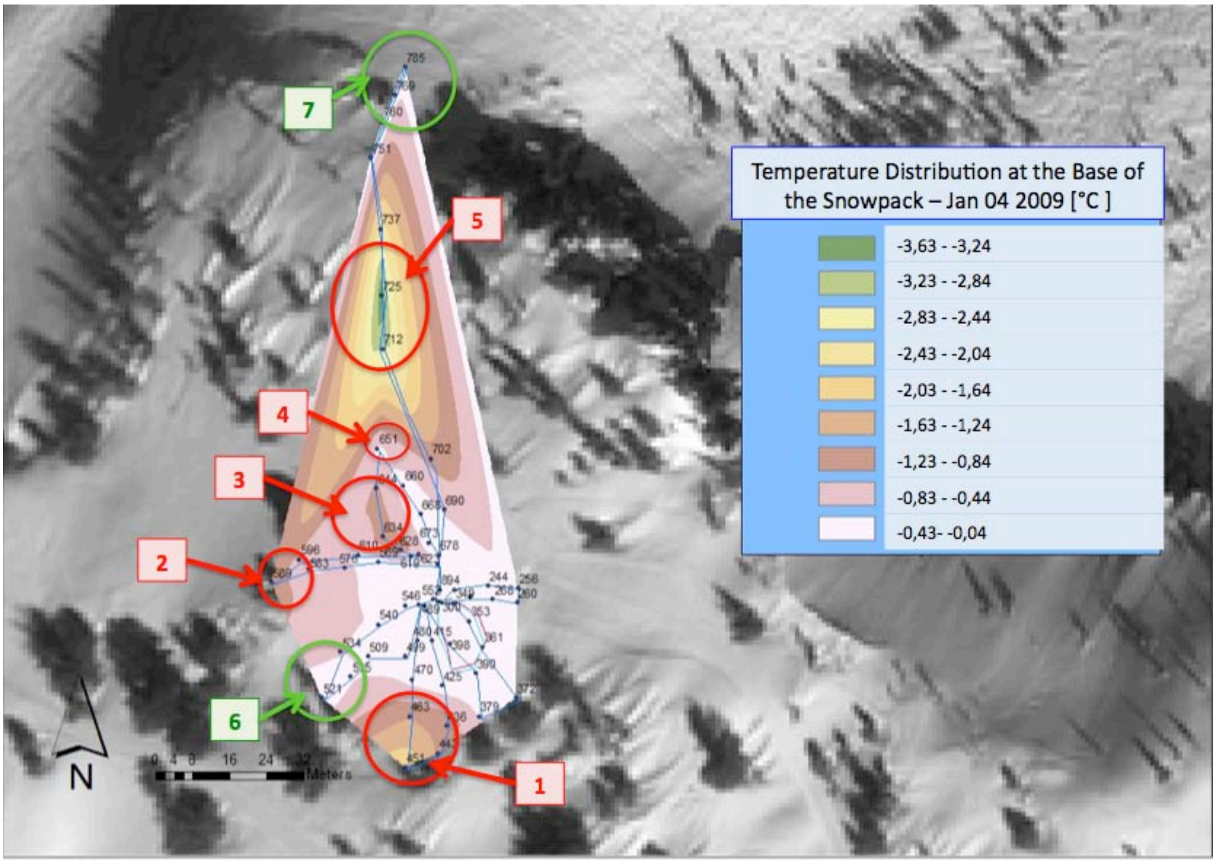

Fig. 58: Distribution of temperatures at the base of the snow pack; values were averaged over the course of 24 hours.

Figure 58 displays the ground temperature distribution measured on January 4th 2009. The snow depth at the container during that time was about 1.3 m. Air temperatures were colder than – 10 °C. One temperature class in the picture represents a temperature range of about 0.4 °C. The numbers 1, 2, 3 and 5 indicate locations where colder ground temperatures than in their surroundings were encountered. Number 4 marks a spot where ground temperatures were warmer. The numbers 6 and 7 mark spots where terrain features changed compared to the prior path of the cable, but where measured ground temperatures did not show a reaction. See below for information about the terrain features at the marked spots.

1 The cable went over terrain at a slightly changed aspect towards a group of trees.

cable Meter	GPS (UTM)			accuracy in m	comments	photo number (s)
410	11s 0320	980	4168 150	2	turns around again here; at 9513 it is close to bunker	1437
412			goes under snow again 06/23/09			
422	11s 0320	984	4168 139	2	comes out of snow again, 06/23/09	
436	11s 0320	985	4168 124	2	slope aspect changes; falls off west? towards lake	1438
443	11s 0320	983	4168 118	2	starts going down the steeper slope	
451	11s 0320	976	4168 115	3	down on loop, still other slope aspect, close to tree, 9473 is South arm turn	1439
463	11s 0320	977	4168 126	3	end other slope aspect, passes tree on way back to bunker aerea	1440
476			cable goes under snow 06/23/09,		checked on 08/04/09 - cable goes straight under snow;	1441

Tab. 5: field notes describing terrain features in location 1 on the maps (cable meter 440 to 461).

Fig 59: cable meter 440 to 461.

Fig. 60: changed aspect and large trees.

2 The cable was deployed on a slightly different aspect and turned at a small tree.

cable Meter	GPS (UTM)			accuracy in m	comments	photo number (s)
561	11s 0320	983	4168 159	3	at next bunker corner (NW), is bag in picture	1451
569	11s 0320	970	4168 160	3	starts going out on next loop	
583	11s 0320	955	4168 158	2	on loop, open field, dry soil (2-10mm diameters); hardly and veget.	1452
585 to 595			slight slope in this loop, gets steeper towards the turn, goes over rocks towards turn, turns at a little tree			
589	11s 0320	947	4168 155	3	turn at a little tree	1453
596	11s 0320	953	4168 160	3	back in EBENE; from here it goes straight back towards bunker until 9304	

Tab.6: field notes describing terrain features in location 2 on the maps (cable meter 589).

Fig. 61: bag indicates cable meter 589; changed aspect, close to small tree.

3 The cable went over a small rock outcrop.

cable Meter	GPS (UTM)				accuracy in m	comments	photo number (s)
619	11s 0320	978	4168	160	3		
623	11s 0320	979	4168	161	2	crosspoint, turns into next loop here	1454, 1455, 1456
628	11s 0320	975	4168	162	3	on soil, passes lysimeters	
632			enters rock surface, straight until 9289				
634	11s 0320	971	4168	165	2	slightly turns, still on rock, coninues straight after that	
640			continuous rock underground ends, from here on soil and rock vary				
651	11s 0320	970	4168	184	2	turns on rock underground, behind a small tree; goes back straight	1457

Tab. 7: field notes describing terrain features in location 3 on the maps (cable meter 625 to 646).

Fig. 62: cable meter 625 to 646; cable went over rocky ground.

4 The cable turned close to a small tree on rocky ground.

	cable Meter	GPS (UTM)		accuracy in m	comments	photo number (s)
	640		continuous rock underground ends, from here on soil and rock vary			
	651	11s 0320 970	4168 184	2	turns on rock underground, behind a small tree; goes back straight	1457
	673	11s 0320 982	4168 162	2	back at profile probe	

Tab. 8: field notes describing terrain features in location 4 on the maps (cable meter 651).

Fig. 63: cable meter 649 to 651; between rocks and close to small tree.

5 The cable went over slightly rising, free terrain (no trees) and led over a small stone ramp.

cable Meter	GPS (UTM)		accuracy in m	comments	photo number (s)
678	11s 0320 980	4168 156	2	turns again, goes in North Loop	1458, 1459
680 to 702	cables led straight, parallel, on dry soil, diameters aboout 10mm to 20cm; picture shows outgoing North Loop				1460
702	11s 0320 983	4168 179	2	outgoing North Loop, 1461 is view back to bunker, 1462 is view out	1461, 1462
725	11s 0320 980	4168 202	3	small cliff, outgoing North Loop	1463
749	11s 0320 982	4168 224	2	turns slightly towards big cliff, outgoing North Loop	1464
749	11s 0320 982	4168 224	2	big cliff drop off	
756	11s 0320 977	4768 231	3	goes under snow at North Cliff, outgoing North Loop	1465, 1466

Tab. 9: field notes describing terrain features in location 5 on the maps (cable meter 712 to 737).

Fig. 64 to Fig. 67: cable went slightly upslope (meter 712 to 740) and went over a stone ramp (meter 725).

6 The cable went over terrain at a different slope angle, passed a group of trees and turned in the open field.

cable Meter	GPS (UTM)				accuracy in m	comments	photo number (s)
485			cable out of snow again 06/23/09				
489	11s 0320	979	4168	155	2	cable turns at bunker; crossover point, see pics 1449, 1448 etc	
499	11s 0320	976	4168	139	4	at PROFILE PROBE PR2; is already on next loop! - South West arm	1442
505			changes slope aspect here; also underground changes - starts going over rocks				
509	11s 0320	968	4168	139	2	changes aspect again, gets even steeper, cable is under small tree	
521	11s 0320	958	4168	130	3	turns around at a point down the slope (towards station), in small trees	1444
534	11s 0320	962	4168	140	2	came up slope, on rock, close to trees, steep part ends here	1445
538			end of part where cable was on rocks, it goes in a MULDE				
543			end of MULDE				

Tab. 10: field notes describing terrain features in location 6 on the maps (cable meter 509 to 537).

Fig. 68: cable meter 509 to 537.

Fig. 69: changed slope aspect.

7 The cable dropped over a north-facing cliff, between rocks.

		cable Meter	GPS (UTM)				accuracy in m	comments
		749	11s 0320	982	4168	224	2	big cliff drop off
		756	11s 0320	977	4768	231	3	goes under snow at North Cliff, outgoing North Loop
		756						slope gets steep
		813						goes straight to next point
		765						end steep slope; cable goes between cliffs until next point
		804						pic 1963
		772						end cliff section, 1964
		797						

Tab. 11: field notes describing terrain features in location 7 on the maps (cable meter 749 to 797).

Fig. 70: cable meter 749 to 797.

Fig. 71: changed slope aspect, steep terrain and cable between rocks.

Figures 73 and 74 display the ground temperature distribution measured on December 30th and on February 14th 2009. The snow depth at the container was about 1.6 m on December 30th and about 2.5 m on February 14th. Air temperatures were about 5 °C on December 30th and about -10 °C on February 14th. One class in the pictures represents a temperature range of about 0.2 °C. Number 8 marks an additional area of temperature variability that was encountered at this resolution. No specific changes in terrain were observed along this section. The cable was deployed in an open field on flat ground. The snow cover and the snow depth distribution in this part, however, were strongly influenced by wind drift (Fig. 72).

8 The terrain did not change but the snow cover was subjected to wind drift.

	cable Meter	GPS (UTM)				accuracy in m	comments	photo number (s)
	345	11s 0320	983	4168	151		cable goes under snow	
outgoing AND! incoming	361	11s 0320	992	4168	140	2	cable comes out of snow	
left side of tree	372	11s 0321000		4168	130	2	turns left of tree; south turn of this loop, South East arm turn 1	1432
	379	11s 0320	992	4168	126	2	turns at a small tree after passing a big tree, South East arm turn 2	1433, 1434
(as opposed to 1m and 2m loop)	390	11s 0320	992	4168	134	2	goes back again to tree where 2m, 1m coil hanging; passes it on other side	1435

Tab. 12: field notes describing terrain features in location 8 on the maps (cable meter 340 to 390).

		cable Meter	GPS (UTM)				accuracy in m	comments
		395			leaving tree; point where bag is in picture			
		398			goes under snow 06/23/09 exactly at 952			checked on 08/04/09 - cable goes straight under snow; straigth between known points; pic 1954
		408			comes out of snow again 06/23/09			
		410	11s 0320	980	4168	150	2	turns around again here; at 9513 it is close to bunker

Tab. 13: field notes describing terrain features in location 8 on the maps (cable meter 395 to 410).

Fig. 72: cable meter 340 to 390 and 395 to 410; snow cover influenced by wind.

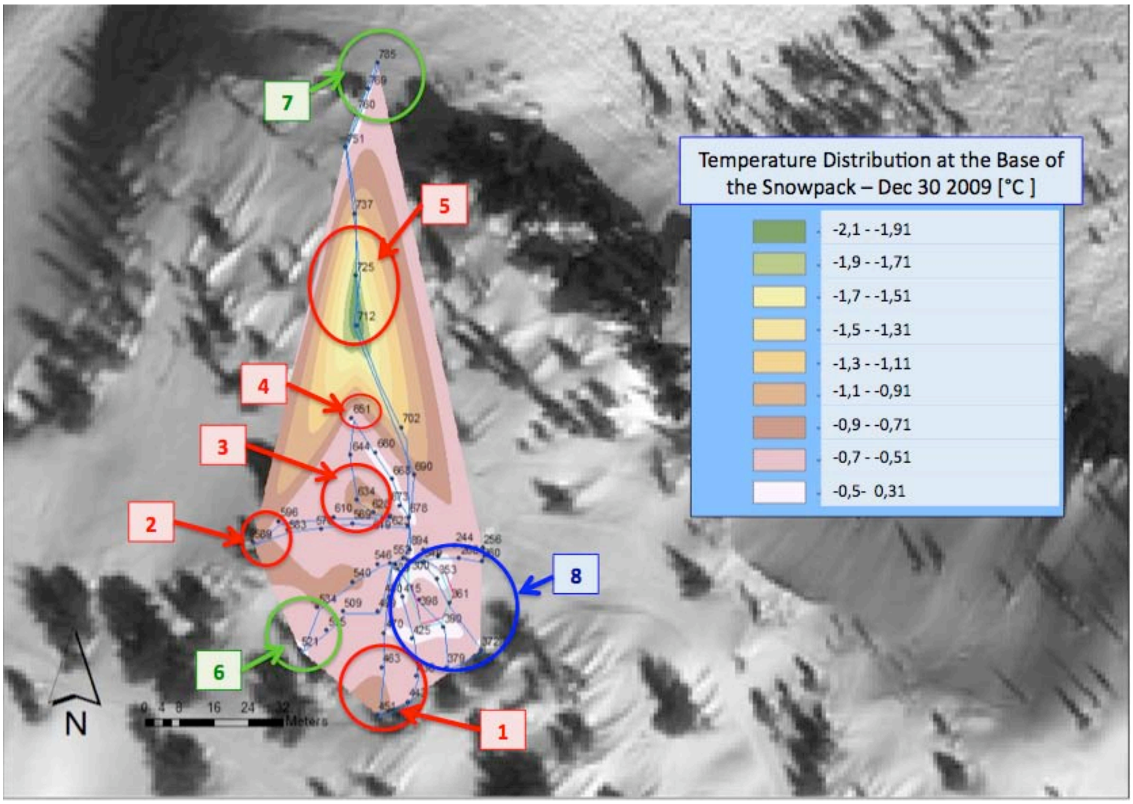

Fig. 73: Distribution of temperatures at the base of the snow pack; values were averaged over the course of 24 hours.

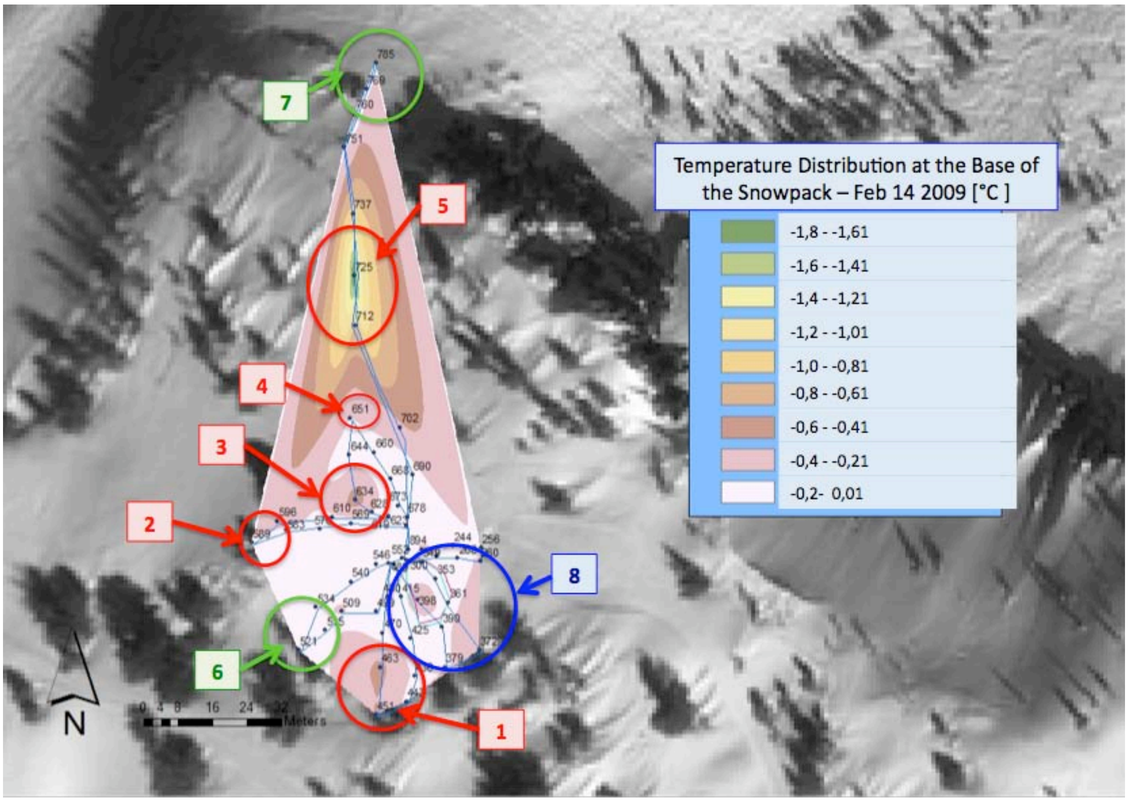

Fig. 74: Distribution of temperatures at the base of the snow pack; values were averaged over the course of 24 hours.

Absolute temperatures should not be compared between the results of the two measurement sessions (December and February). The pictures however show relative changes in the patterns of the temperature distributions, especially in the sections 8, 1 and 2. The picture from January 4th shows differently classified temperatures. This was necessary as the range of temperature variations measured on that day was much larger than on the other two days (about 3.6 °C on January 4th vs. about 1.8 °C on December 30th and on February 14th). Even though temperatures varied more in their absolute values on January 4th the pattern of their distribution was similar to the one observed on December 30th and in the locations 3, 4, 5 and 7 also resembled the distribution measured on February 14th.

6.2.2 Evolution of Spatial Ground Temperature Variability in Time

Figures 75, 77, 79 and 81 display the evolution of air temperatures and of the snow depths measured next to the container during the measurement sessions in December/January, February and March. In February and March also the snow surface temperatures, which are an indicator for the balance between incoming and outgoing radiation, are shown. No measurements of surface temperatures were available for the period of DTS measurements in December and January. The figures display raw (uncorrected) data; extreme values (outliners) are the result of measurement errors. Figures 76, 78, 80 and 82 show DTS measured temperatures at according times, averaged over 5 min in time and over a distance of 4 m within section 3 and section 5 on the ground (Fig. 57), and within section 8 at snow depths of 1 m and 1.9 m above the ground (Fig. 73 and Fig. 74).

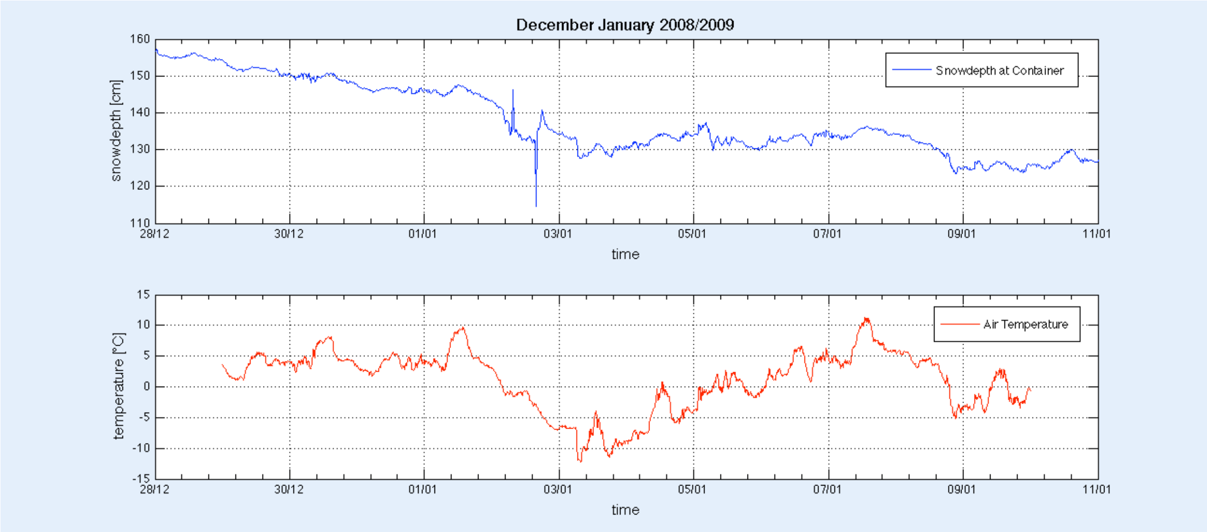

Fig. 75: evolution of snow depths at the container and air temperatures, December and January

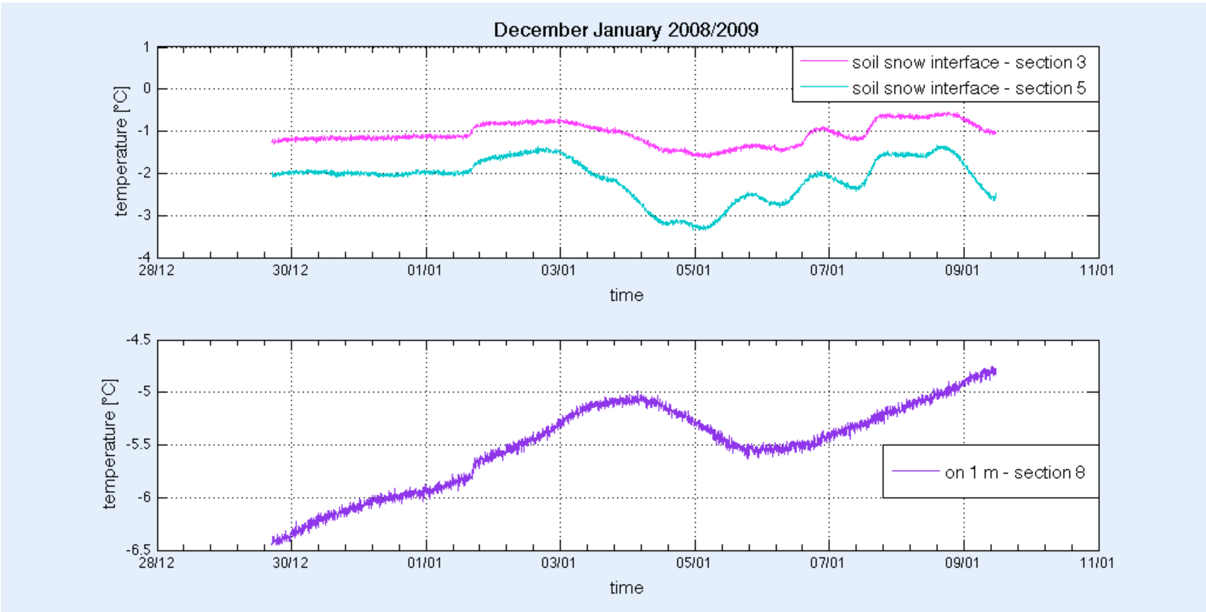

Fig. 76: evolution of DTS temperatures in section 3 and section 5 on the ground and in section 8 at a snow depth of 1 m above the ground, December and January

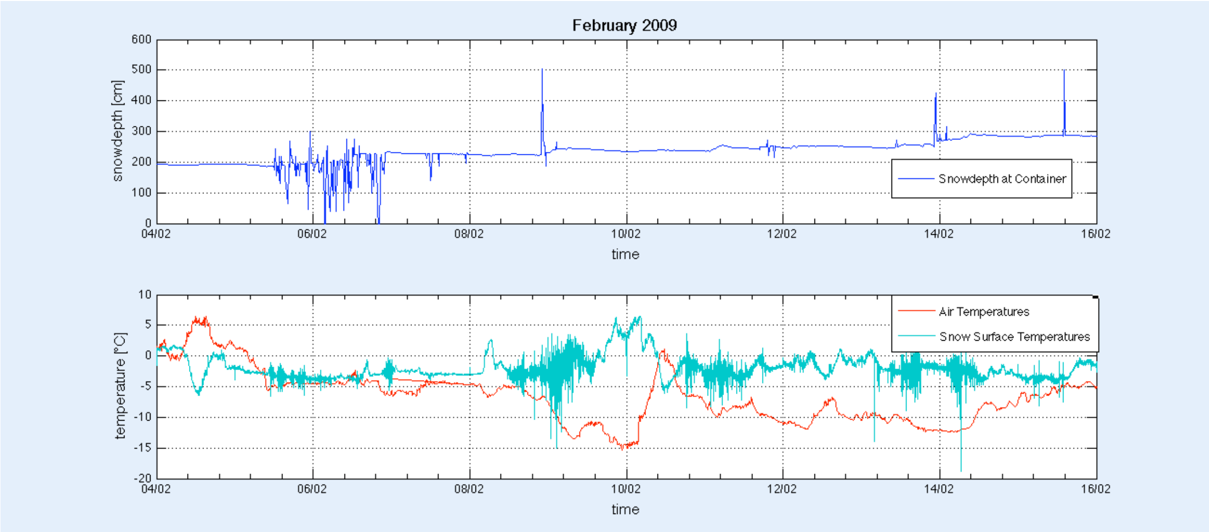

Fig. 77: evolution of snow depths at the container, air- and snow surface temperatures, February

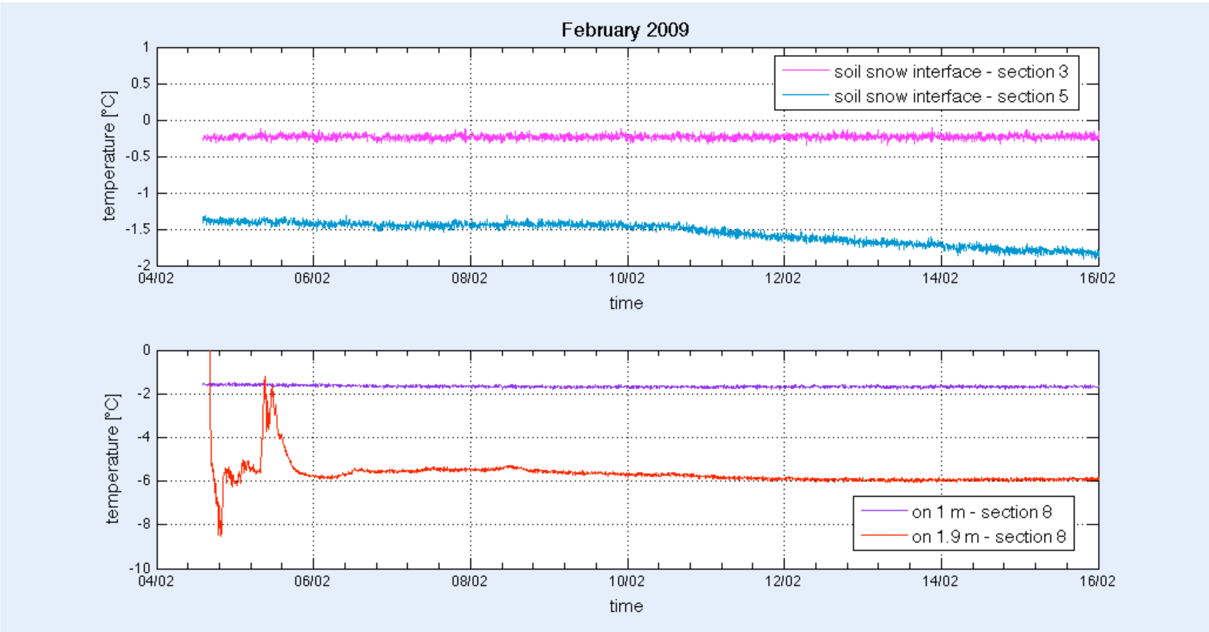

Fig. 78: evolution of DTS temperatures in section 3 and section 5 on the ground and in section 8 at snow depths of 1 m and 1.9 m above the ground, February

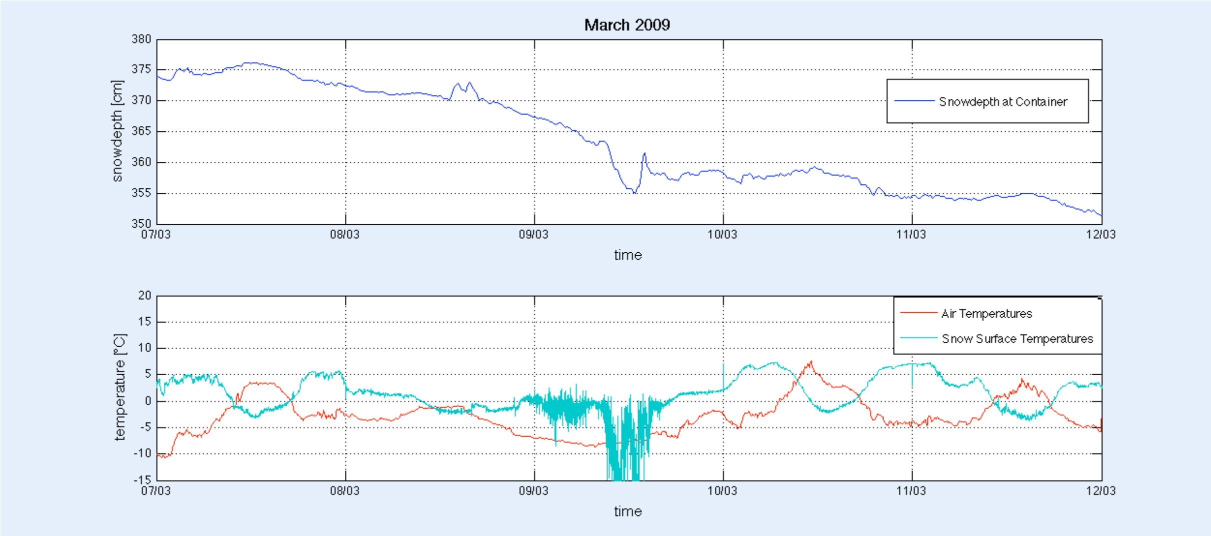

Fig. 79: evolution of snow depths at the container, air- and snow surface temperatures, March

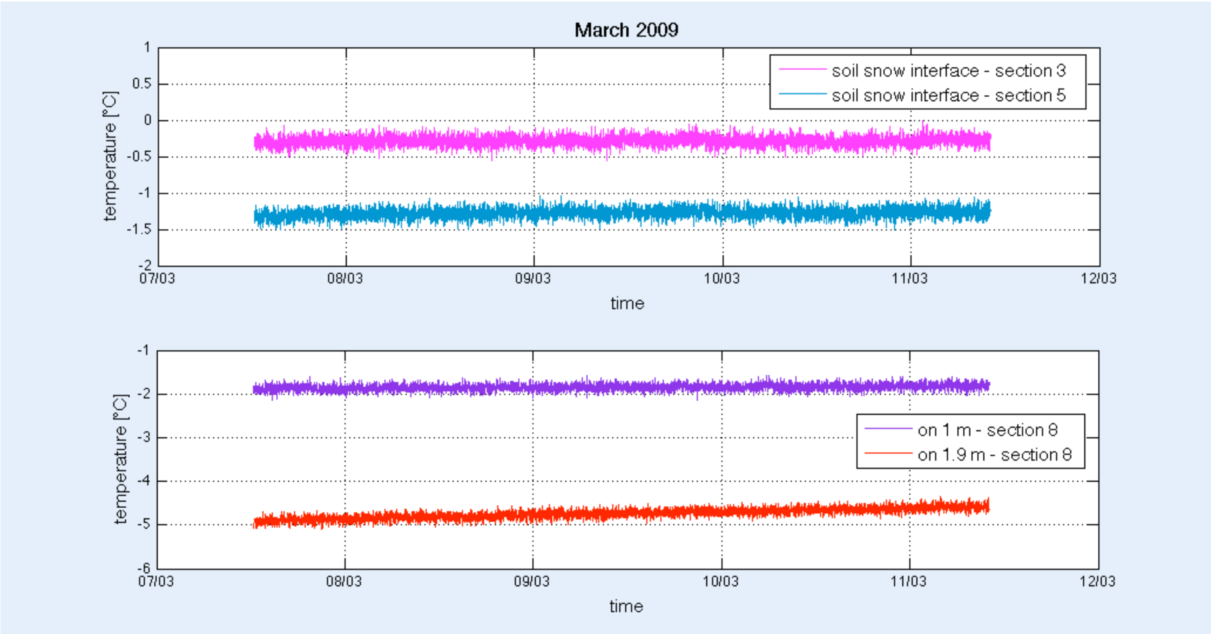

Fig. 80: evolution of DTS temperatures in section 3 and section 5 on the ground and in section 8 at snow depths of 1 m and 1.9 m above the ground, March

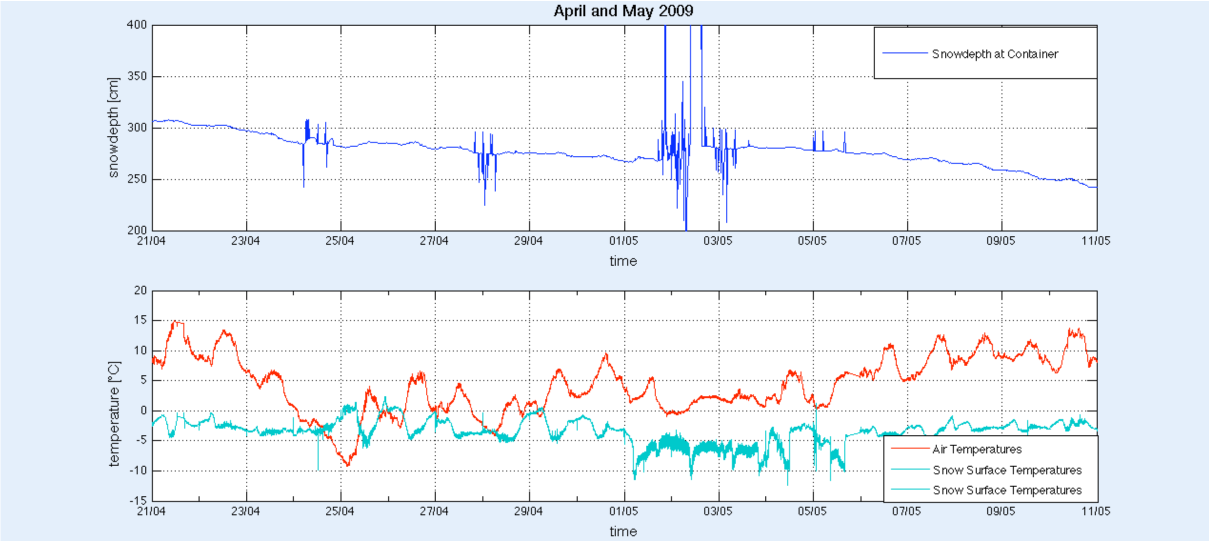

Fig. 81: evolution of snow depths at the container, air- and snow surface temperatures, April and May

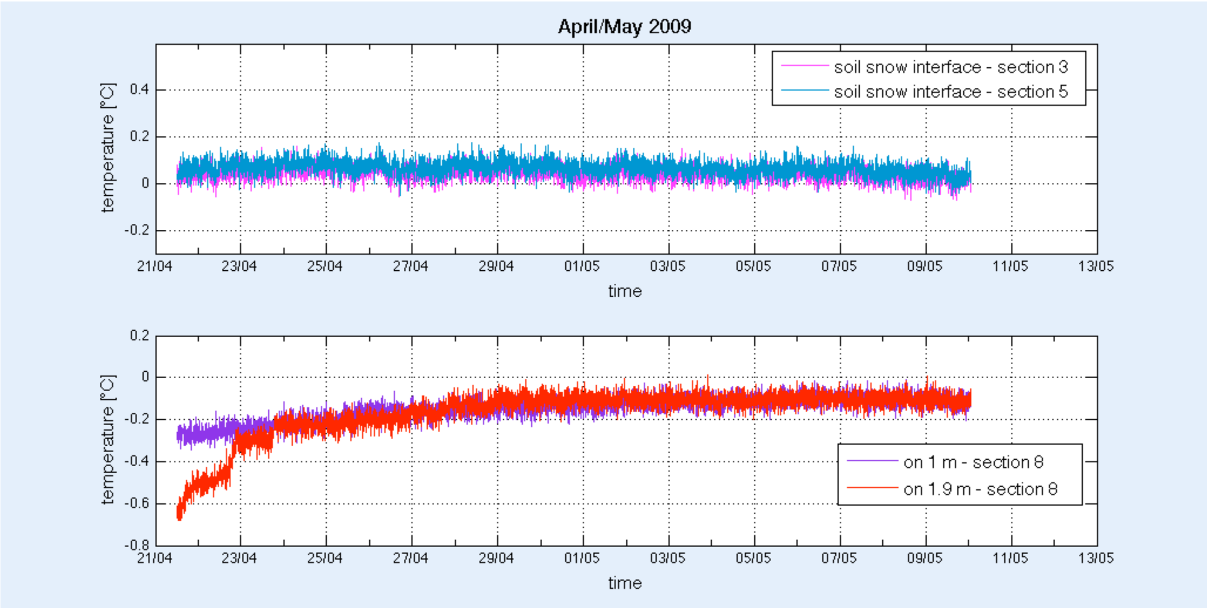

Fig. 82: evolution of DTS temperatures in section 3 and section 5 on the ground and in section 8 at snow depths of 1 m and 1.9 m above the ground, April and May

The figures 83 to 88 document the evolution of the pattern and the range of the spatial ground temperature distribution measured with the DTS system. The temperatures shown on the maps were averaged over the course of 24 hours and were measured at a spatial resolution of 2 m. This corresponds to a spatial repeatability of 0.03 °C or less, a temporal repeatability (instrument caused standard deviation in time in a constant temperature environment) of 0.006 °C (chapter 5.1) and a temperature resolution of better than 0.02 °C (chapter 4.1.2, Fig 20). In all maps same colors represent the same temperature ranges. Therefore temperature patterns and ranges can be compared amongst all days. Absolute temperature values should only be compared among days within one single measurement session, as different measurement sessions were not calibrated to the same reference devices and set-ups (chapter 4.2.1 and 5.1).

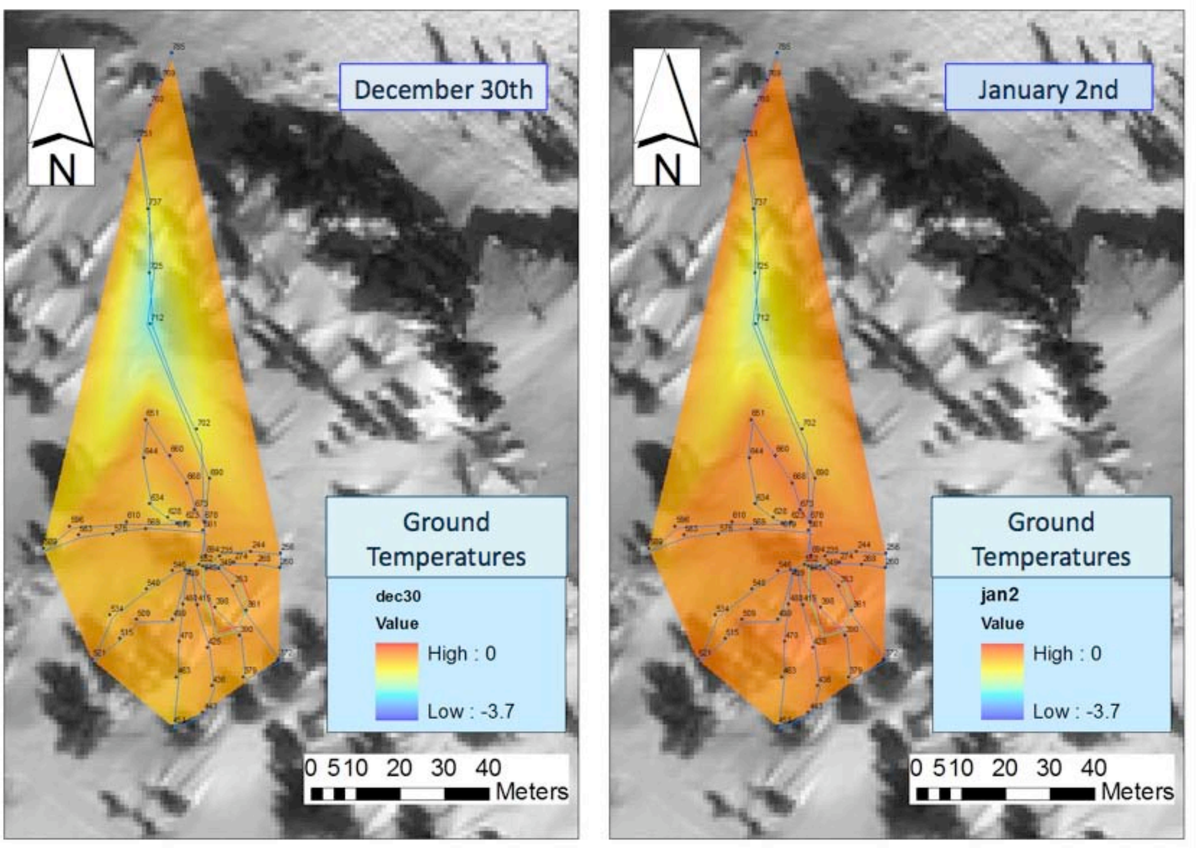

Fig. 83 and 84: spatial temperature distribution at the base of the snow pack on December 30th and January 2nd

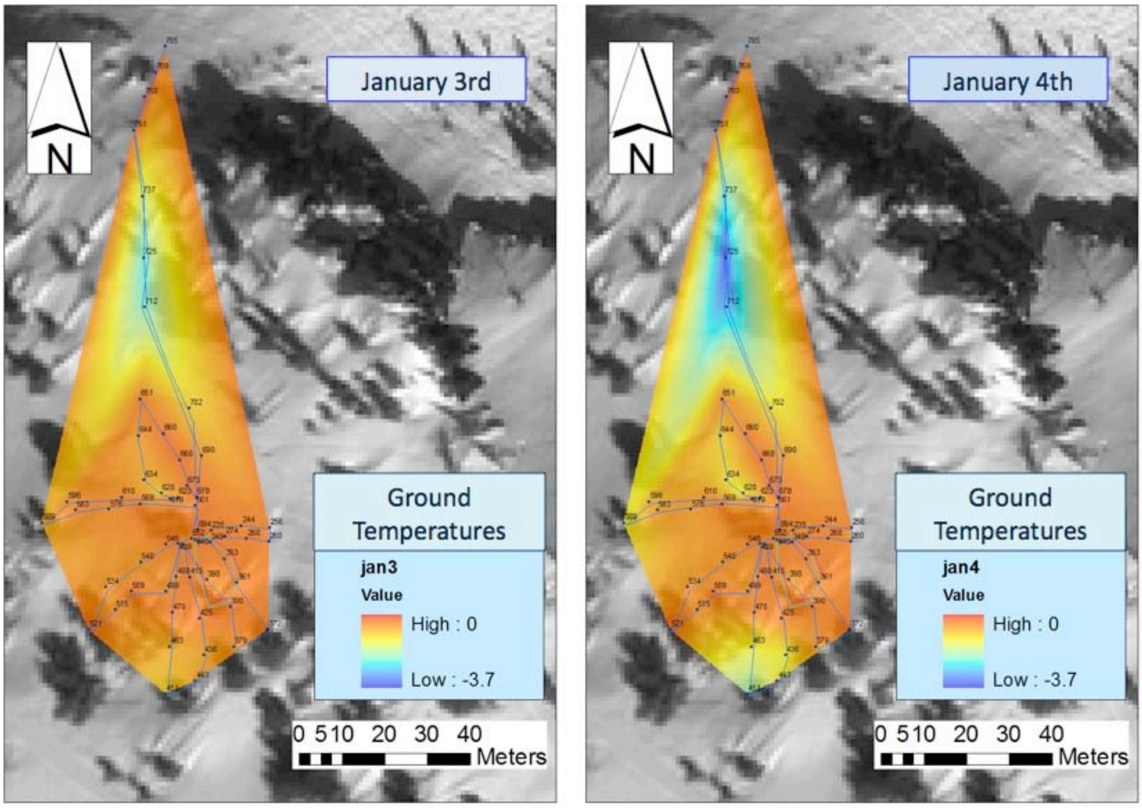

Fig. 85 and 86: spatial temperature distribution at the base of the snow pack on January 3rd and January 4th

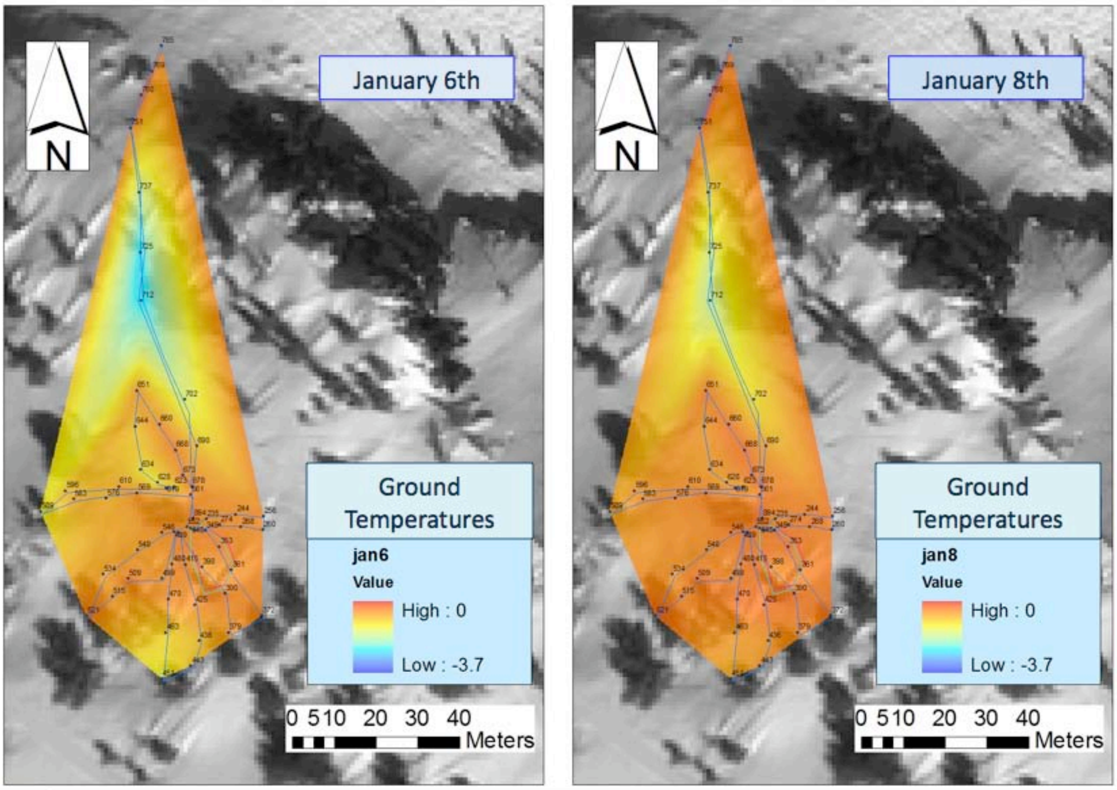

Fig. 87 and 88: spatial temperature distribution at the base of the snow pack on January 6th and January 8th

The maps (Fig. 83 to Fig. 88) show the days in December and January on which ground temperature changes compared to the preceding day were encountered. Ground temperatures became warmer from December 30th to January 2nd; they dropped between January 2nd and January 3rd, reached their coldest values on January 4th and rose again until January 8th. With a delay of about half a day, this evolution corresponds to observed air temperatures at that time. Air temperatures were at +10 °C on January 1st, started to decrease on January 2nd and reached their lowest value of -10 °C on January 3rd. They started to rise again the same day and reached again about +10 °C on January 8th. Snow depths measured at the container at this time ranged from about 1.6 m to 1.3 m (Fig. 75).

The Figures 89 to 92 show the ground temperature distributions observed at the beginning and at the end of the February session and at the beginning and at the end of the March session. No major changes in the pattern of ground temperatures were encountered during the monitored periods in these months. The range of observed temperatures increased from February 5th to February 15th and decreased again until Mach; mainly because of cooler temperatures measured in section 5, where the terrain rose slightly and where the cable went over a small stone ramp (Fig. 58 - section 5, Fig. 67). While snow surface temperatures increased slightly during February measurements, air temperatures were colder around February 15th than they were around February 5th and became warmer again in March (Fig. 77 and 79). Snow depths measured at the container in February ranged from about 2 m to 3 m; in March they ranged from about 3.8 m to 3.5 m (Fig. 77 and 79). It seems that temperatures in section number 5 (Fig. 58), were more influenced by air temperatures than by radiation influences (snow surface temperatures) or by increasing snow depths, which would indicate that the cable was either exposed to air or was buried under a very shallow snow cover.

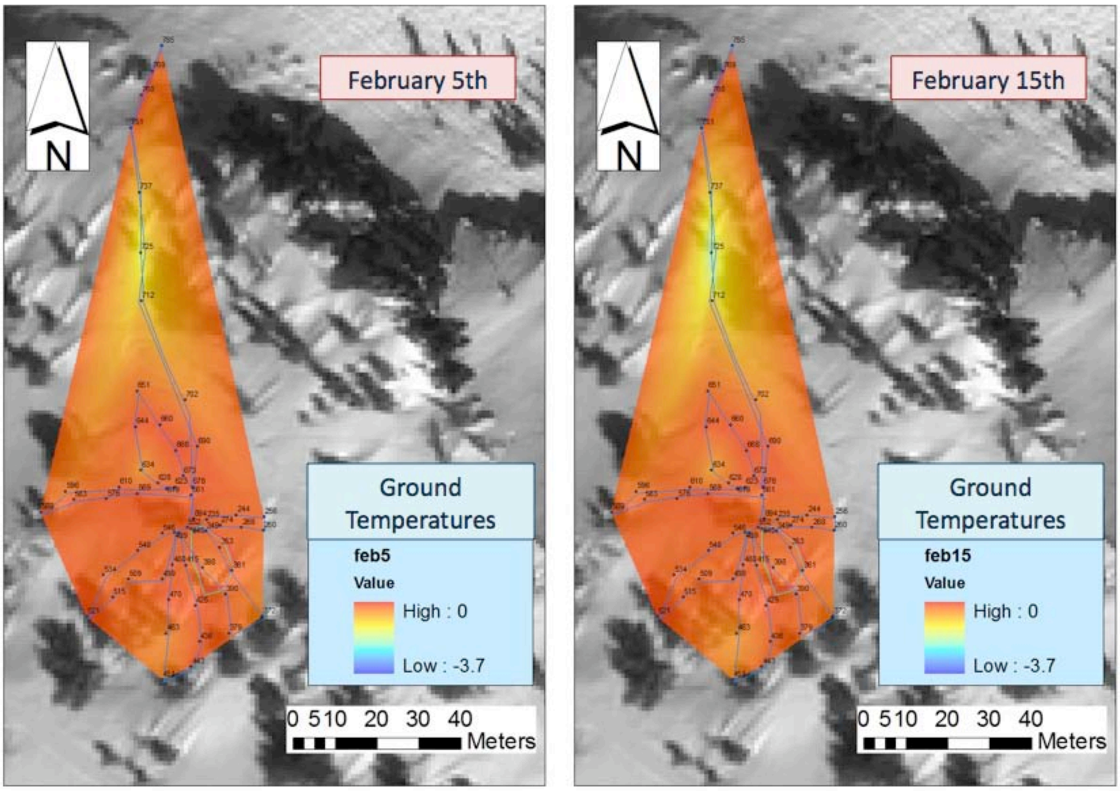

Fig. 89 and 90: spatial temperature distribution at the base of the snow pack on February 5th and February 15th

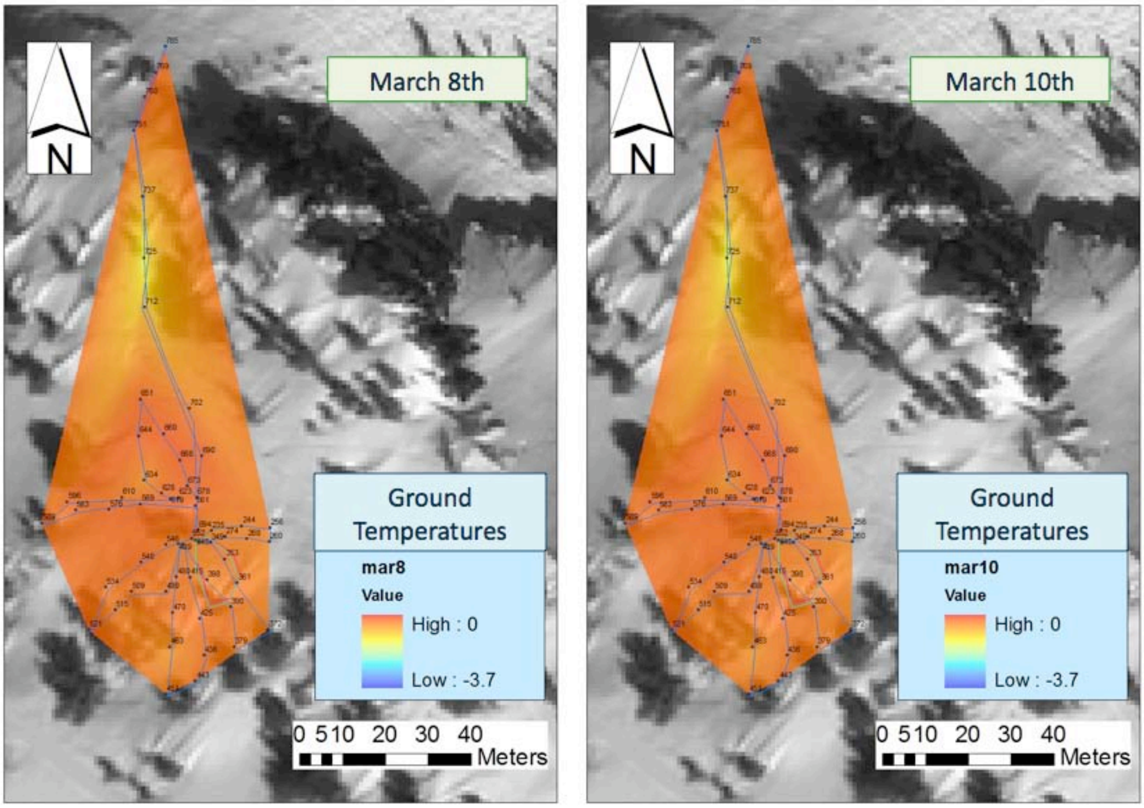

Fig. 91 and 92: spatial temperature distribution at the base of the snow pack on March 8th and March 10th

Figure 93 summarizes the mean values, the ranges, the variances and standard deviations, and the coldest temperatures observed along the entire 660 m of fiber-optic cable deployed on the ground. These values were calculated from temperatures that were averaged over the course of 24 hours and are shown for each full day of measuring. The days in April and May were excluded, as those temperature traces had been corrupted by a step loss error (chapter 4.2.3.3). In December and January the range and variability of ground temperatures in space varied strongly; they increased and then decreased again, corresponding to air temperatures at that time. In February the range and variability of the ground temperatures showed an increase; they decreased again in March. The values shown below were strongly influenced by temperature changes in section 5 (Fig. 58), where the cable went over slightly rising terrain without trees and over a small stone ramp (Fig. 66 and Fig. 67) and where always the coldest temperatures along the cable on the ground were encountered.

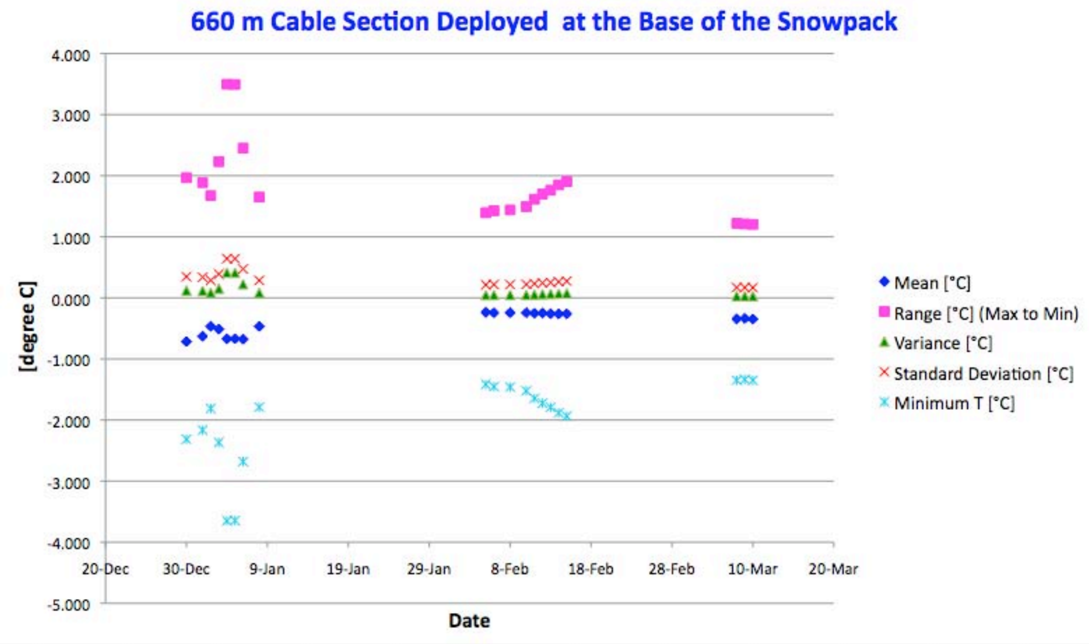

Fig. 93: mean, temperature range, variance and standard deviation and minimum temperatures measured along the 660 m of fiber-optic cable deployed on the ground.

6.3 SNOW PACK TEMPERATURE VARIABILITY

Figure 97 and 98 show temperatures measured along a 40 m transect of the fiber-optic cable on the ground, at the part deployed in December on 1 m of snow, and at the part deployed in February on 1.9 m of snow. All these 40 m - transects were located in the same place, one above the other, in the south east corner of the study field (Fig. 73 and 74, location number 8, chapter 5.2.1 and Fig. 40, chapter 4.2.1).

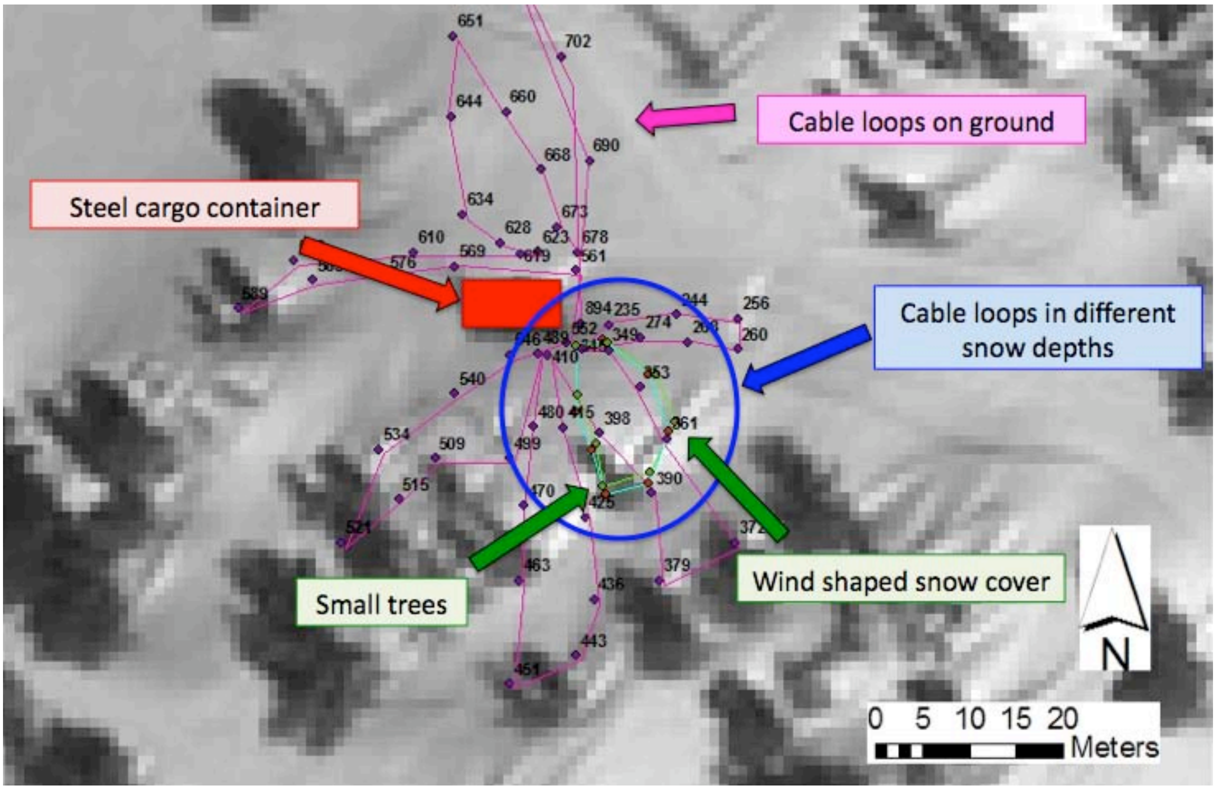

Fig. 94: South East part of the study field, where loops in different snow depths were deployed.

The snow cover at this part of the site was exposed to strong wind drift (Fig. 96). On Figure 95 parts of the two cable loops at about 1 m and at about 1.9 m can be seen, hanging in two small trees. The black spots on the southwest corner of the temperature maps below represent two small trees (Fig. 94 to 105 and Fig. 107 to 117).

Fig 95: cable that was deployed on 1 m and on 1.9 m of snow, hanging in small trees in June.

Fig. 96: snow cover at the southeast section of the site, shaped by wind drift.

Figure 97 shows the evolution of temperatures in different snow depths from December 30th to February 14th. Figure 98 shows their development from February 14th to May 10th. Displayed temperature values were averaged over the course of 24 hours.

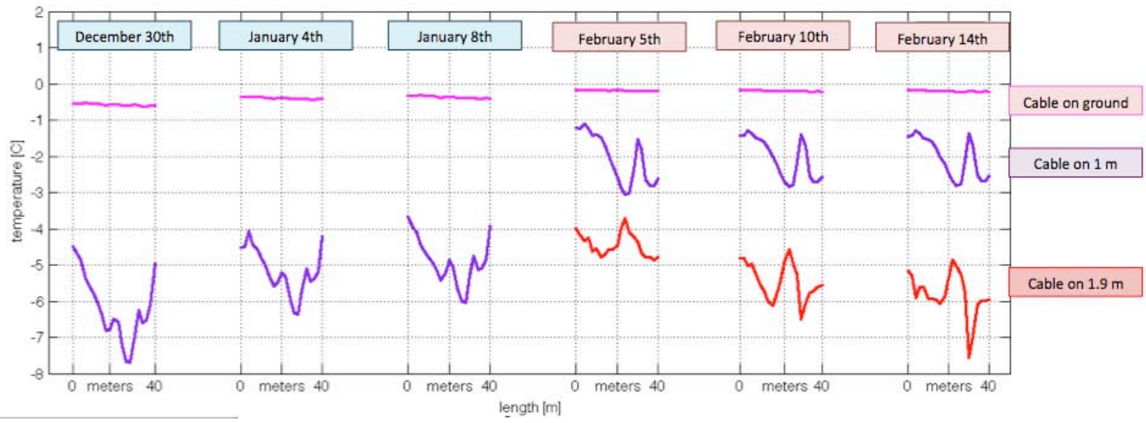

Fig .97: temperatures measured at the ground and in different snow depths along 40 meters of the fiber-optic cable in the south east section of the study field, December through February

Temperatures along the cables deployed in higher parts (on 1 m and on 1.9 m) of the snow pack showed stronger variations in space (more than 2 °C) than those measured on the ground. The temperature gradient between the ground and about 1 m decreased in December. As opposed to ground temperatures in other parts of the site (chapter 5.2.1 and 5.2.2), in this part of the snow pack ground temperatures increased between December 30th and January 4th, and also temperatures higher in the snow pack became warmer during this period. No reaction of snow temperatures on the strongly cooling and then warming air temperatures (Fig. 75) could be detected in this part of the study field. The gradient between temperatures at about 1 m and about 1.9 m above the ground increased throughout February, mainly as the result of decreasing temperatures at 1.9 m at that time; it was smaller in March and decreased strongly until April and May.

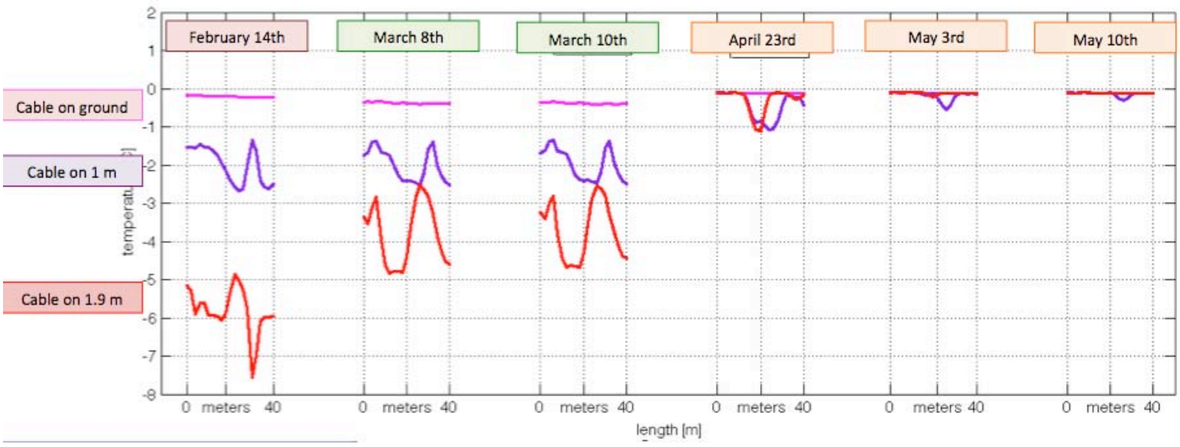

Fig. 98: temperatures measured at the ground and in different snow depths along 40 meters of the fiber-optic cable in the south east section of the study field, February through May

Also for the cable transects (loops) deployed on 1 m and on 1.9 m, snow temperature data that was averaged over the course of 24 hours was imported into ArcGis (www.esri.com) for each point included on the map; and interpolations using the Natural Neighbors tool, which can be found in the Spatial Analyst toolbox, were conducted. The maps below (Fig. 99 to 110 and Fig. 112 to 122) show the observed evolutions of snow temperatures and of their distribution in different snow depths. For the maps of the 1 m- and 1.9 m transects (loops) different color ranges to display temperatures had to be chosen, as absolute temperatures varied too much between different measurement sessions; the distribution of temperatures on a single day would not have been visible at a resolution that would have been necessary to cover the full range of temperatures that were measured throughout the entire season in these snow depths.

Figures 99 to 110 show the temperature distribution observed along the cable that was deployed in December on 1 m of snow. During December/January the distribution of temperatures in this part of the snow pack remained similar; absolute temperatures were getting warmer during this measurement session (Fig. 99 to 101). Snow temperatures averaged over the course of 24 hours from this part of the snowpack did not follow the changes in air temperatures at that time (Fig. 75).

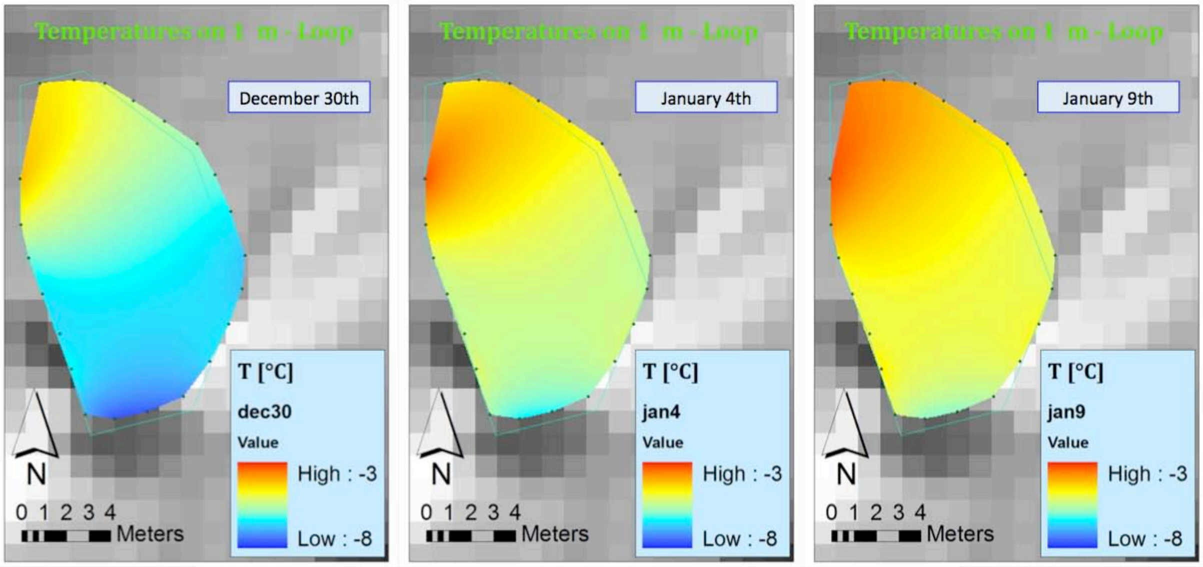

Fig. 99 to 101: Interpolated temperatures measured along a cable loop deployed on 1 m of snow, December 30th, January 4th and January 9th

By February the pattern of the temperatures within the snow pack, at about 1 m above the ground, had changed (Fig. 102 to 104). On February 5th temperatures ranged over a larger span than later in this month. Throughout February (Fig. 105 to Fig. 107) the pattern of the snow temperatures' distribution did not change; with the exception of a spot in the northeast part of the loop, where temperatures at the beginning, on February 5th, were the warmest (Fig. 102) and at the end, on February 15th, were colder than in the surrounding snow (Fig. 106). The temperature range decreased continuously and absolute temperatures increased. In March the temperatures' pattern remained similar to the one observed at the end of February measurements. Snow depths measured at the container increased from about 2 m to about 3 m in February and ranged from about 3.8 m to 3.5 m in March. Snow surface temperatures were around -5 °C at the beginning of February reached a peak of 5 °C on February 10th and cooled off a bit again but remained warmer until the end of measurements (0 °C to -2 °C). On March 8th they ranged around 0 °C. Air temperatures were warmer at the beginning of February measurements (about 5 °C), cooled off to -15 °C on February 10th, rose to 0 °C shortly after that and were at about -10 °C from February 12th to 14th. In March air temperatures were about -4 °C (Fig. 77 and 79).

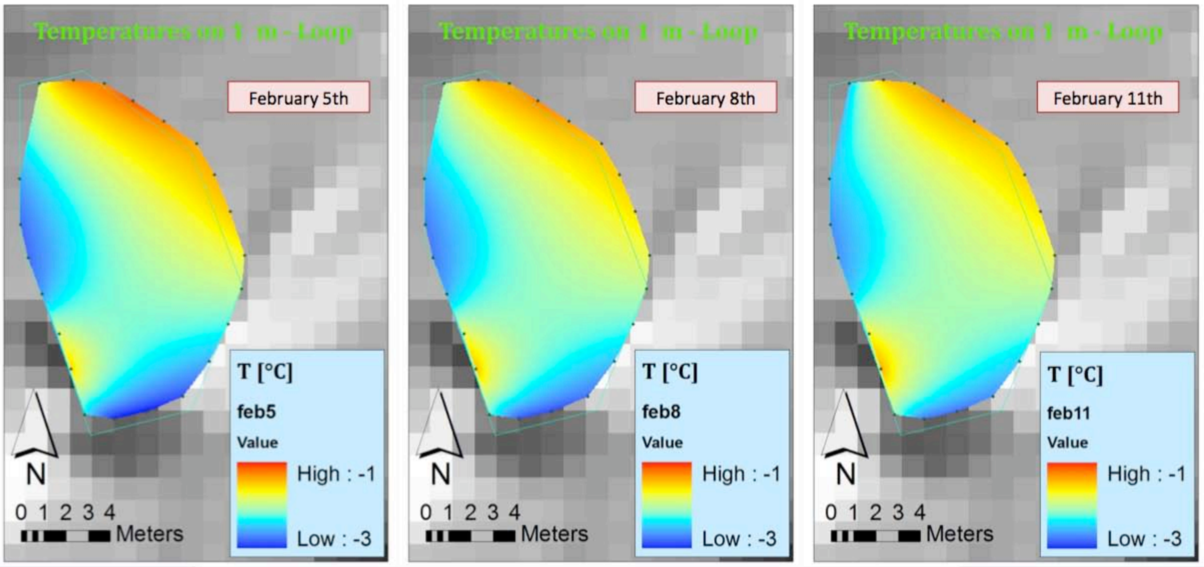

Fig. 102 to 104: Interpolated temperatures measured along a cable loop deployed on 1 m of snow, February 5th, February 8th and February 11th

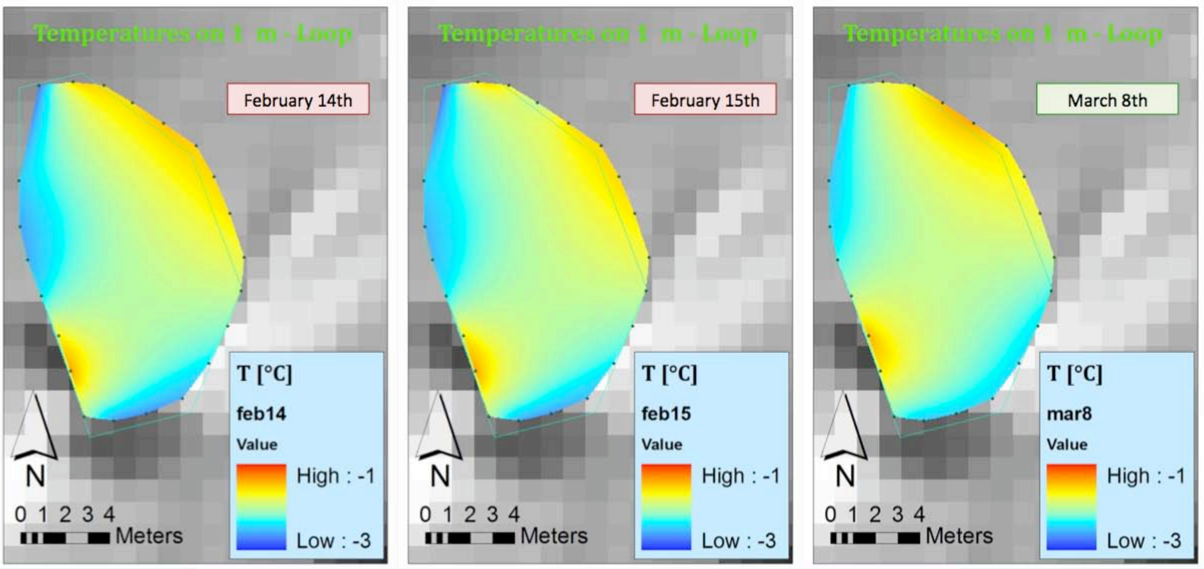

Fig.105 to 107: Interpolated temperatures measured along a cable loop deployed on 1 m of snow, February 14th, February 15th and March 8th

The temperatures measured in this section of the snowpack in February did not react on changing air temperatures at this time.

At the end of April still the same snow temperature distribution as in February and March was encountered. The snow temperature range along the cable kept decreasing and reached a close to isothermal state by May 9th (Fig. 108 to 110). Air temperatures in April and May were warmer than during preceding months (0 to 10 °C). Snow surface- and air temperatures were more variable (diurnal fluctuations). Snow depths were still high, with about 3 m measured at the container (Fig. 81).

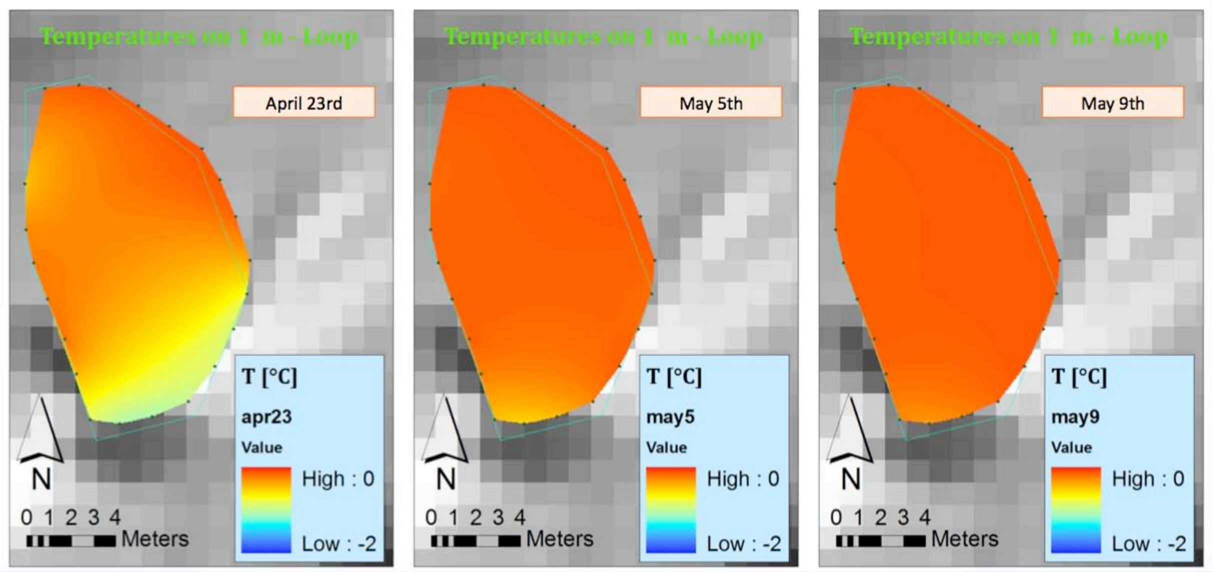

Fig. 108 to 110: Interpolated temperatures measured along a cable loop deployed on 1 m of snow, April 23rd, May 5th and May 9th

Figure 111 summarizes the mean values, the ranges, the variances and standard deviations, and the coldest temperatures observed along the 50 m of fiber-optic cable deployed on 1 m of snow in December. These values were calculated from temperatures that were averaged over the course of 24 hours and are shown for each full day of measuring. The days in April and May could be included, as this section of the cable was not affected by the step loss error (chapter 4.2.3.3). Minimum temperatures, the range of temperatures and their variability over space strongly decreased during December. In February the rate of decrease slowed down but the values still became smaller, though at a declining rate. In March they were relatively constant and similar to the values encountered at the end of the February session. In April and May the temperature range and their spatial variability further decreased, now at an increasing rate. The cable was deployed on the snow when a snow depth of 1 m was measured close to the container.

Snow depths, however, may have been subjected to variations in space as well as in time throughout the winter season.

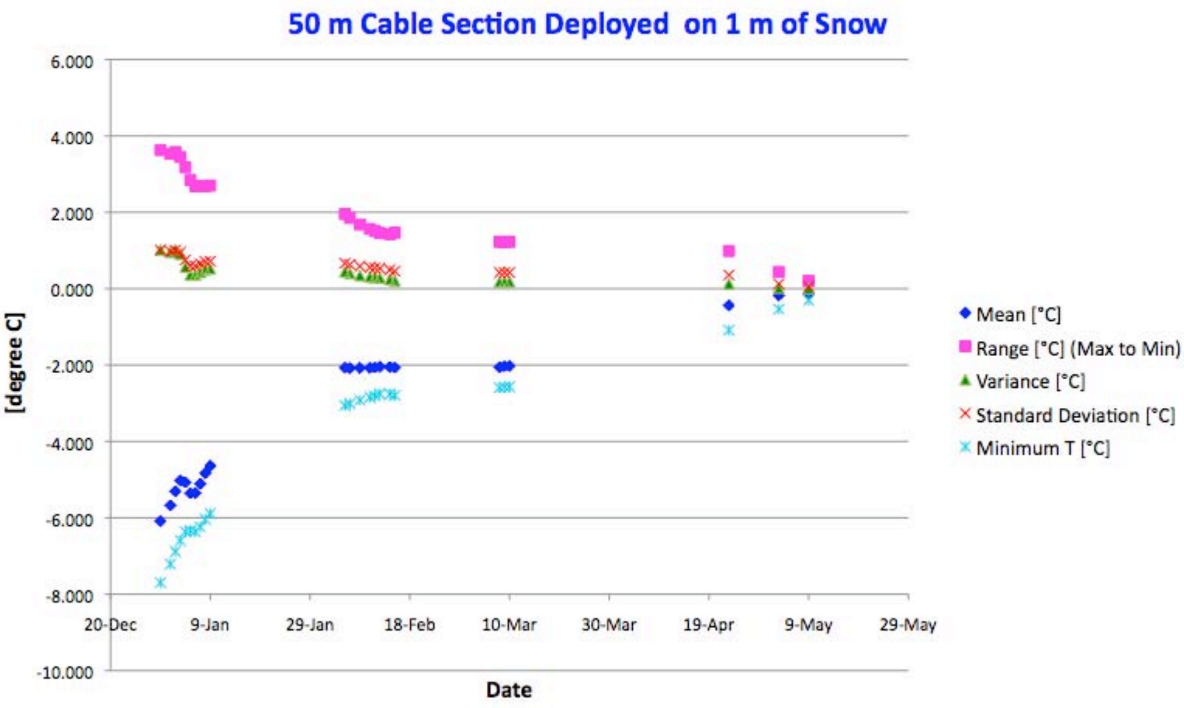

Fig. 111: mean, temperature range, variance and standard deviation and minimum temperatures measured along 50 m of fiber-optic cable deployed on 1 m of snow.

Figures 112 to 122 show the temperature distribution observed along the cable that was deployed on 1.9 m of snow in February. Only within a single measurement session the color ranges represent the same temperatures. At a resolution that would cover the entire range of temperatures observed along the 1.9 m loop from December to May, the spatial temperature patterns would not be visible in temperature maps of a distinct day.

During February the spatial pattern of temperatures along the cable remained constant. Absolute snow temperature values decreased until they reached their minimum on February 14th and increased again on February 15th (Fig. 112 to 122). Air temperatures on February 4th were about 5 °C, they decreased to a minimum on February 10th at about -15° C and warmed up again to 0 °C shortly after that. They quickly dropped again to

-10 °C on February 12th and stayed cold until they increased a little bit on February 15th to -5 °C. Snow surface temperatures ranged around -5 °C from February 5th to February 9th, they reached a peak of 5 °C on February 10th and cooled off again but remained warmer at about 0 °C to -2 °C between February 11th to February 15th (Fig. 77). The short peaks in air temperatures and in snow surface temperatures between February 10th and 11th did not seem to have an impact on measured snow temperatures at about 1.9 m above the ground, that were averaged to a temporal resolution of 24 hours. The general cooling trend of air temperatures from February 5th to February 14th (the short warming around February 10th excluded) and smaller changes on a slightly longer run towards the end of the measurement session (between February 14th and February 15th) however seemed to have an effect (Fig. 116 and 117).

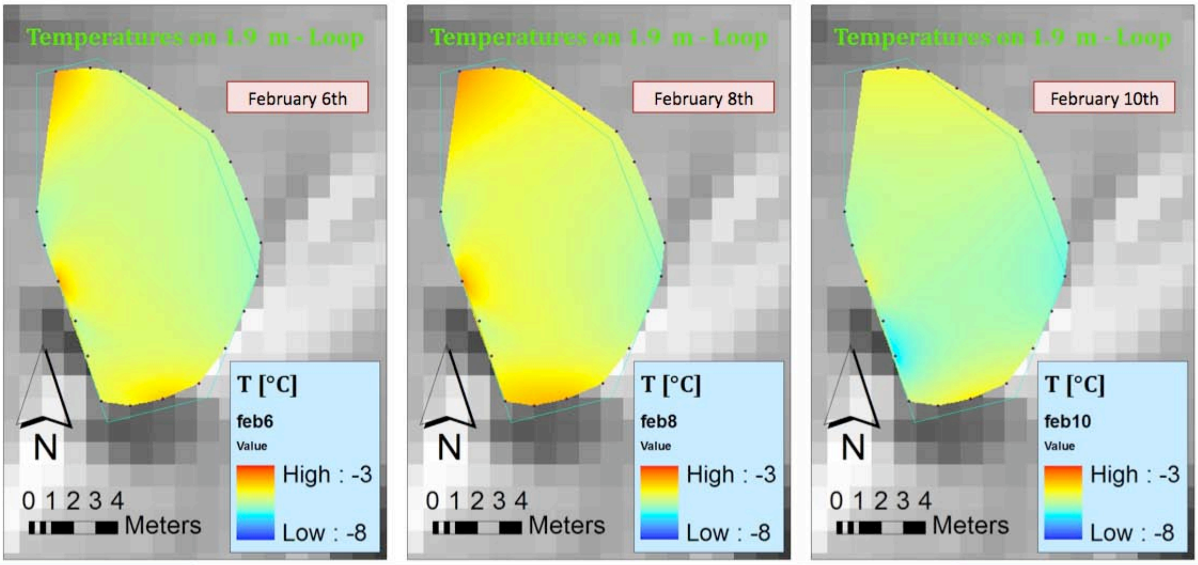

Fig 112 to 114: Interpolated temperatures measured along a cable loop deployed on 1.9 m of snow, February 6th, February 8th and February 10th

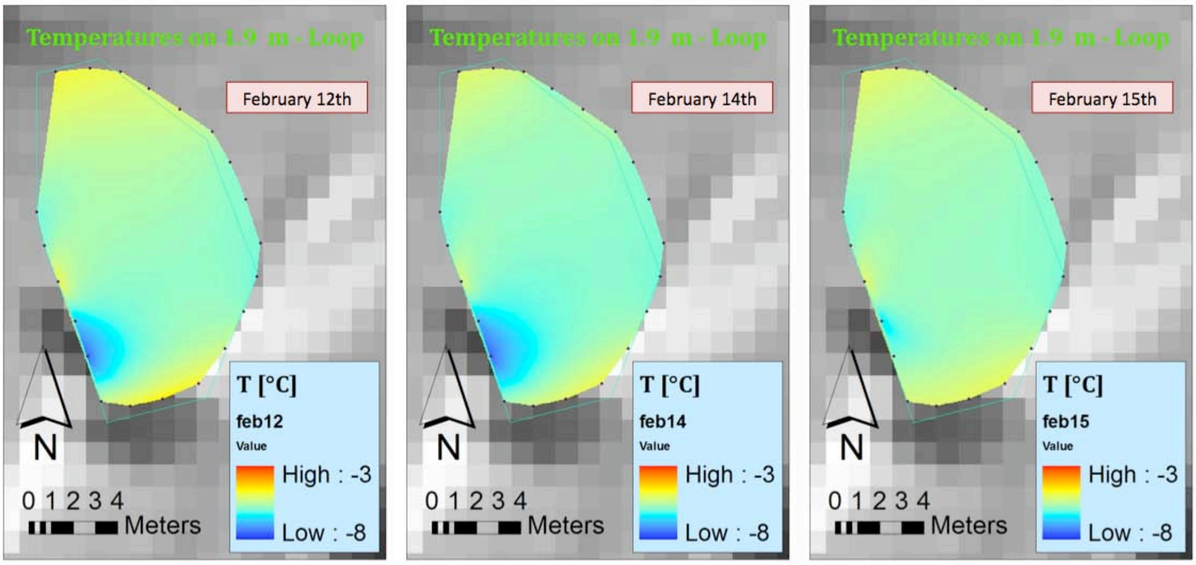

Fig. 115 to 117: Interpolated temperatures measured along a cable loop deployed on 1.9 m of snow, February 12th, February 14th and February 15th

The temperatures measured in this section of the snowpack in February showed a reaction on changing air temperatures at this time.

In general, temperatures measured along the cable deployed on 1.9 meters, increased continuously from the end of February to March and from March to April and May. The distribution of snow temperatures at about 1.9 m above the ground in the snow changed from February to March; and changed again from March to April and May (Fig. 118 and 119, and Fig. 120 to 122). The range of observed temperatures in March was of a similar size as in February and decreased slightly between March 8th and March 10th; it was much smaller by April 23rd. By May 9th this part of the snow pack (about 1.9 m above the ground, south east corner of the study site) had reached an almost horizontally isothermal state.

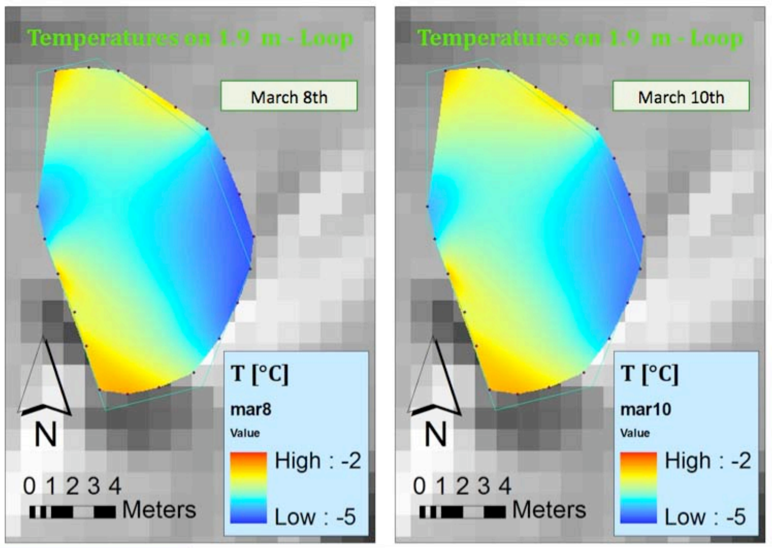

Fig. 118 and 119: Interpolated temperatures measured along a cable loop deployed on 1.9 m of snow, March 8th, and March 10th

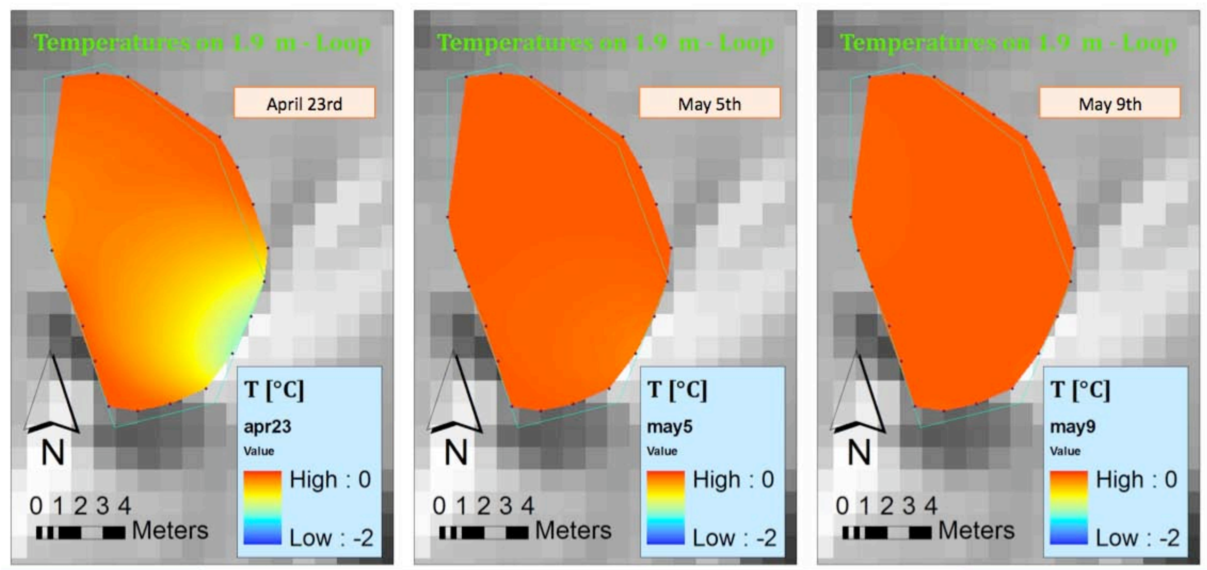

Fig. 120 to 122: Interpolated temperatures measured along a cable loop deployed on 1.9 m of snow, April 23rd , May 5th and May 9th

Figure 123 summarizes the mean values, the ranges, the variances and standard deviations, and the coldest temperatures observed along the 50 m of fiber-optic cable deployed on 1.9 m of snow in February. These values were calculated from temperatures that were averaged over the course of 24 hours and are shown for each full day of measuring. The days in April and May could be included, as this section of the cable was not affected by the step loss error (chapter 4.2.3.3). In February the range and variability of snow temperatures in space varied; they increased after the beginning of February measurements and then decreased again towards the end of the session. They continuously decreased in March, and also from the end of April to the beginning of May, at relatively high rates; then they decreased further, at a slower rate, towards a horizontally isothermal state on May 9th. The cable was deployed on the snow when a snow depth of 1.9 m was measured close to the container. Snow depths, however, may have been subjected to variations in space as well as in time throughout the winter season.

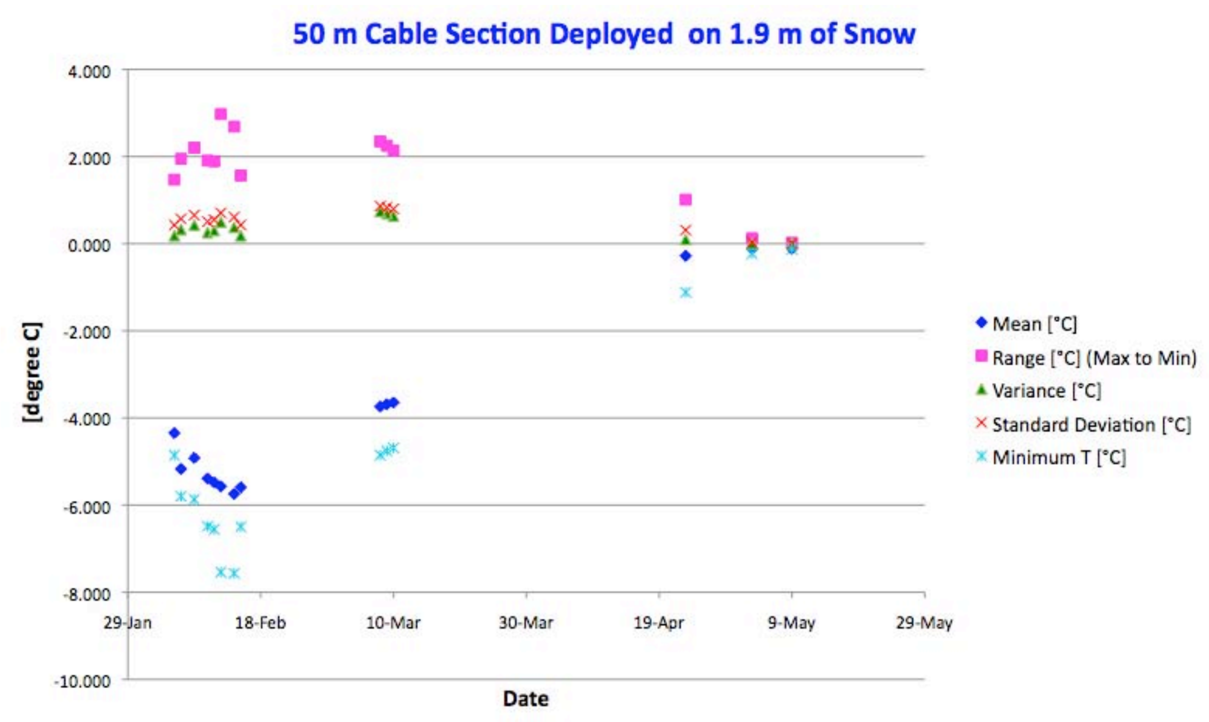

Fig. 123: mean, temperature range, variance and standard deviation and minimum temperatures measured along 50 m of fiber-optic cable deployed on 1.9 m of snow.

Figure 124 compares the evolution of the variances of DTS measured snow temperatures along cable transects in different snow depths. The variances were calculated along the cable segments, for snow temperatures that were averaged over the course of 24 hours. They are shown for the two cable loops that were deployed on 1 m and on 1.9 m of snow, and for a ground loop that was located on the ground below them (Fig. 94; location number 8 - chapter 5.2.1 and Fig. 39 - chapter 4.2.1). Further the variance of temperatures measured along the entire 660 m ground loop of fiber-optic cable is displayed.

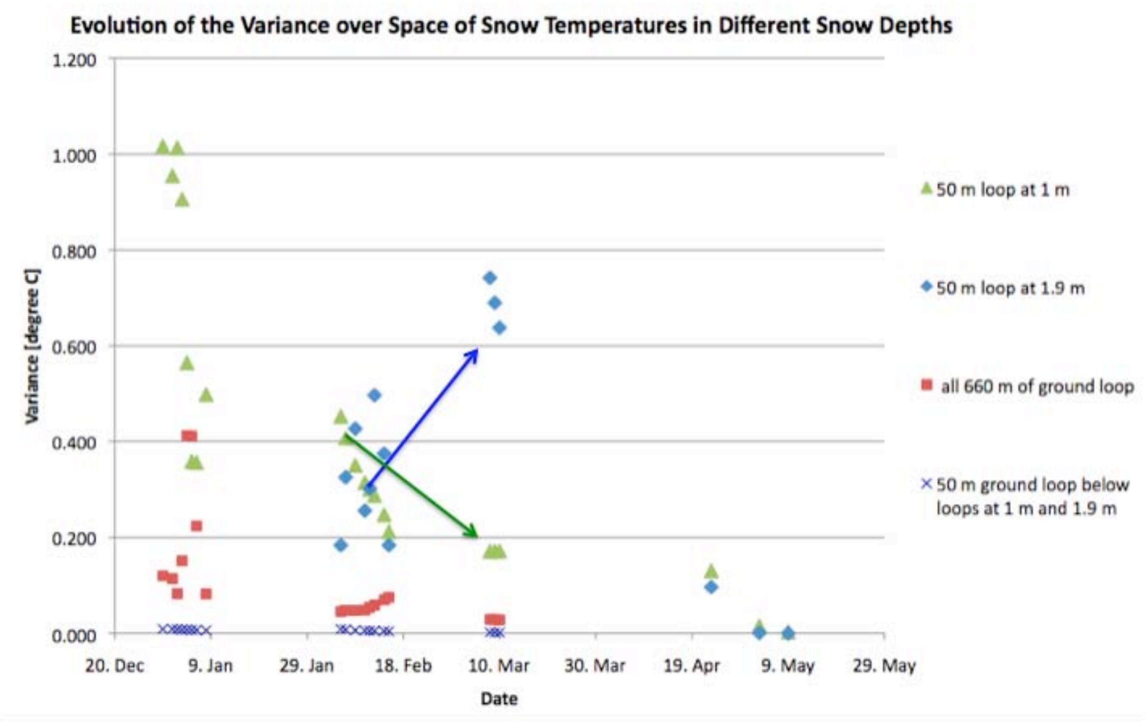

Fig. 124: variance of DTS measured snow temperatures along cable transects in different snow depths

Ground temperatures spatially varied only slightly along the section of cable that was deployed below the two other loops. The variance along this cable segment was slightly larger during December/January and decreased from February through March. Ground temperatures across the entire site did vary to a much larger extent. The variance of ground temperatures across the entire study field in space was largest in December/January and itself varied strongly during this time; it was smaller in February but increased towards the end of this measurement session and was decreasing again in

March. This could probably be explained by strongly varying snow depths across the terrain and the influence of air temperatures on ground temperatures at locations with a significantly shallower snow cover.

Higher in the snow pack temperatures varied strongly in space along the cable loops. Along the loop on 1 m of snow the temperature variability was largest and was highly variable during December/January. It decreased from February to March as opposed to the variability of snow temperatures measured along the 1.9 m loop, which varied strongly in February and increased significantly until March. During this time in February air temperatures decreased and snow depths and snow surface temperatures increased (chapter 5.2.2, Fig. 77). In both snow depths the spatial variability decreased in April to reach their minimum and an almost horizontally isothermal state in May. At the end of the season the variability of snow temperatures in space decreased at a quicker rate at 1.9 m above the ground than at 1 m.

7. CONCLUSIONS

7.1 STUDYING SNOW TEMPERATURE VARIABILITY

The evolution of snow pack temperatures and temperature gradients, their variability in space and in time and the evolution of their variability in time, are of interest in snow- and avalanche research. The snow's temperature settings provide insight in the evolution and variability of many snow properties, which are driven by its temperatures, including the formation of weak layers, their persistence or stabilization. As a snow cover's properties can vary on small spatial and temporal scales, also avalanche dangers can change significantly over small distances (smaller than a single slope) and over short times. Field observations and modeling results are only available for a limited number of points in space or at a limited temporal resolution. When information about avalanche dangers is used to assess risks in the field, spatial and temporal extrapolations with respect to terrain and weather variables become necessary. The degree of spatial variability of snow properties for a given slope is currently unknown, or how it changes over time or in relation to environmental factors of the specific slope. No guidance is available to support, for example, backcountry travelers to extrapolate information from point observations to variable terrain (Hendrikx et al., 2009). A profound understanding of a snow pack's variability and its driving processes (meteorological processes) and influencing parameters (terrain effects) could help improve risks assessments for temporary avalanche protection, in skiing resorts and in the backcountry.

Various field studies were carried out to investigate the variability of alpine seasonal snow covers. Stability tests, temperature profile probes and models were employed to derive data at increased spatial distributions on different scales and to track the evolution of measured properties over several days. Mainly conclusions were limited due to a lack of either highly temporally or highly spatially distributed data. Recent findings, however, indicated that the properties of a snow pack as well as the patterns and character of their variability vary in time, and vary differently in different locations. It could be shown that a snow pack's fracture propagation propensity varies in space and in time, and that also the pattern of its spatial distribution was temporally variable (Hendrix et al., 2009). Further it was found that an index representing the long-term influences of air temperatures on an alpine seasonal snow pack correlated to its layer hardness and that this correlation again was variable in space and in time (Kozak et al., 2003). It was shown that topographic variables including the rate of change in slope and aspect, the elevation, the canopy density and the solar radiation input at a given sample spot were influencing the maximum and average temperature gradients in a snow cover (Deems, 2002) and that, within one slope of the same exposition and a similar incline, temperatures varied by 5 °C to 10 °C as a result of different snow depths (Teufelsbauer, 2009). In the field studies conducted by Hendrix at al. (2009) and by Deems (2002) the amount of data and therefore also possible further conclusions were limited due to the lack of human and financial resources that would have been needed to conduct regular measurements, at a higher frequency and spatially and temporally distributed at the same time (Deems, 2002, Hendrikx et al., 2009). Stability measurement methods as used by Hendrikx et al. (2009) irreversibly destroyed the structure of the snow cover and could not be conducted several times at the same location (Hendrikx et al., 2009). Due to a lack of highly spatially and temporally distributed temperature data within the snow pack Teufelsbauer's two-dimensional snow pack temperature model could not be calibrated in a two-dimensional mode yet (Teufelsbauer, 2009). Hendrikx et al. (2009) called for more data to document spatial and temporal variability of the snow pack in a large number of different locations, settings and environmental conditions, to derive typical correlation lengths for a specific scenario or environment.

7.2 INSTRUMENT PERFORMANCE

Raman spectra fiber optic distributed temperature sensing is a method that allows measuring temperatures continuously in time and simultaneously at a large number of sample spots located along a fiber-optic cable. The DTS system installed on Mammoth Mountain during the winter 2008/2009 could provide spatially and temporally distributed temperature data in snow, with a spatial resolution of 2 m and a temporal resolution of 5 min or better. Measurements could be taken along a cable of 2 km in length, continuously over the course of one to several weeks. For this experimental set up (a cable of 2 km length and measurement intervals of 2 m and 5 min) the temperature resolution that could be achieved with the instrument used in Mammoth Mountain was 0.05 °C (for a five minute averaging interval) or better than 0.02 °C (for a 24 hours averaging interval).

The absolute accuracies that can be achieved with this method strongly depend on the quality of the calibration set-up and -technique at the site. Preferably two, or more, ice-slush baths should be used, equipped with a precision calibrated temperature device as a reference. In snow environments this can prove to be difficult, especially when measurements over longer time spans are planned, as the ice-slush baths would freeze. Therefore on Mammoth Mountain a section of the snow pack was chosen as calibration environment. Poor thermal contact between the calibration coil and a reference device caused an offset error during one measurement session. As a second reference section within the snow was available this mistake could be corrected during data post-processing. Temperatures within the snow pack stratified (temperature gradient), also within the calibration section. An error was introduced in the DTS data due to this stratification and absolute snow temperatures remained unknown.

Relative accuracies of a spatial repeatability (spatial standard deviation over a constant temperature section) of 0.06 °C and a temporal repeatability (temporal standard deviation over a constant temperature section) of 0.04 °C could be achieved, for measurements with a spatial measurement interval of 2 m and a temporal measurement interval of 5 min. For measurements averaged over the course of 24 hours the spatial repeatability was 0.03 °C or better and the temporal repeatability was about 0.006 °C.

To measure temperatures with a high absolute accuracy a well-known constant temperature environment is necessary. A portion of the snow should only be chosen for calibrations, if the calibration cable coils can be buried deep enough in a snow pack to be not subjected to steep or strongly varying snow temperature gradients. The coils should be deployed horizontally on, or above, flat terrain and should take as little vertical space as possible, to limit influences from temperature stratification in the snow. Close thermal contact to the reference device has to be ensured.

The initially derived DTS data on Mammoth Mountain included large errors resulting from instrument noise (instrument drift). The instrument noise (drift) corresponded to changes in ambient air temperatures at the instrument box; it was larger when ambient air temperatures varied stronger and decreased with a decreasing variability of air temperatures. The drifting started right after the beginning of measurements. Thanks to two reference sections – the calibration section and another section of coiled cable that was deployed on the ground, together with a reference device – the instrument drift errors could be successfully corrected.

An unexpected step loss was encountered along the measured temperature trace. Usually step loss errors are corrected automatically when an instrument is configured to take measurements in a double-ended mode. In April and May this routine failed and post-processing corrections would have been necessary. Two sections of knowingly the same temperature would have been needed to correct for the loss error. As only known temperature environments before the part of the cable, which was affected by the loss, were available, the temperatures in April and May had to be excluded from parts of the data analysis. Care should be taken when planning the experimental set-up of a DTS system, that enough cable sections for possibly necessary loss- and drift corrections during data post-processing are available. Preferably several sections along the cable, at least one at its beginning and one at its end, should be monitored by external devices; and/or different parts of the fiber-optic cables should be deployed in the same location to ensure that they are at the same temperature (different parts along the cable deployed in the same location in reality). For drift corrections at least one external reference temperature device is necessary.

During cable deployment, especially on the ground, its course should be checked for possible sharp terrain features. It has to be kept in mind, that under the load of a snow pack such sharp features can penetrate the cable and may lead to signal losses. The losses can lead to a noisier signal and, accordingly, cause smaller relative data accuracies. In some cases they can even cause corrupt temperature traces, as was shown in April and May, 2009, on Mammoth Mountain.

The horizontal position of the cable in Mammoth was georeferenced with a GPS device. The meter marks that were provided on the cable claddings could be successfully used for orientation. They were useful reference points for note taking and positioning.

Tracking the exact vertical position of the cables is more difficult and was not attempted on Mammoth Mountain. Distributed measurements of the underlying terrain and of the snow cover on which cable loops in different snow depths were deployed, would be necessary to reveal detailed information about the cable loop's positioning. Further the settling of the snowpack would have to be tracked.

After they had been corrected for instrument drift in Mat Lab, DTS temperatures could be imported into Microsoft Excel (http://office.microsoft.com) and ArcGis (www.esri.com) for further analysis.

7.3 SNOW TEMPERATURE VARIABILITY – CASE STUDY

During a single measurement session the evolution of the patterns of temperature distributions, as well as the distribution of their absolute values, could be compared. Between different months (measurement sessions) absolute temperatures could only be compared to a very limited extent because they had been referenced to different external devices and because the absolute values of distinct measurement sessions remained unknown as a result of inaccurate offset calibrations.

When an instrument box is set up at a measurement site several times, care should be taken during instrument configuration to ensure that the box is set-up and calibrated exactly the same way each time. Only then results from different sessions can be compared with adequate accuracy.

Temporal and spatial variations in temperatures and the evolution of their spatial distribution at the base of the snow pack and in two different snow depths, at 1 m and at 1.9 m above the ground, could be successfully monitored, at a high spatial resolution and continuously in time.

Temperature variations, as small as 0.2 °C, could be detected. On the ground, variations in a range of more than 1 °C were resolved; along the cables deployed on 1 m and on 1.9 m of snow, spatial variations were larger than 2 °C. In some parts of the site these temperature variations seemed to correspond to terrain features (canopy cover, changing slope aspect, rising terrain or rock outcrops); in other parts temperatures varied but no clear terrain characteristics that might have caused a temperature anomaly could be identified. In these parts strongly varying snow depths that were differently distributed as a result of wind drift, seemed to be the reason for the temperature variability. Also, in some locations snow temperatures remained constant, even though temperature changes would be expected as a result of variations in the subjacent terrain.

Changes over time of the range of observed temperatures across the study field, as well as in their pattern, were resolved. How patterns and ranges of spatial snow temperature distributions changed, again was variable in space. In some parts of the study field the temperature distribution remained similar throughout almost the entire sampling time; in other parts it changed between the different months. In some spots the range of observed snow temperatures responded quickly to changing air temperatures, in other locations only changes on the longer term, corresponding to warming or cooling of snow surface temperatures, was observed. The spatial variability of temperatures evolved differently in different snow depths at the same part of the site and over the same period of time. In February the spatial variability of temperatures in the snow pack decreased at 1 m above the ground but increased at 1.9 m above the ground.

In agreement with Deems (2002) these results indicate that topographic variables are having an influence on the distribution of snow- and snow soil interface temperatures, but are not the only driving force controlling their distribution and evolution. Accordant to Teufelsbauer's results (2009) it seemed that the distribution of snow depths above the fiber optic cable was, besides terrain features, the major other driving force of temperature distributions at the site on Mammoth Mountain. Snow depths were only measured at two points of the study field but were likely to vary significantly across the entire site. Terrain features themselves were very likely to have influenced the snow's precipitation pattern and distribution at the site.

7.4 DTS SYSTEMS IN AVALANCHE RESEARCH

The DTS system on Mammoth Mountain proved to be able to measure snow temperatures at the base of a snowpack and in different snow depths in a highly spatially and temporally distributed manner. Provided the shelter and power supply that was available at the Cooperative Snow Study Site on Mammoth Mountain, it successfully rendered temperatures with a good temporal and spatial resolution (relative accuracy), also in an alpine snow environment. Only the calibration for absolute temperatures turned out to be problematic in a cold environment, as ice-slush baths could not be used.

The horizontal cable positions could be georeferenced with GPS measurements referring to meter marks provided on the fiber optic cable. Accurate vertical positions of cables deployed in the snow pack were harder to derive, as the loops were deployed on snow, which might have been subjected to spatial variations in snow depth and to settlement during the proceeding winter season.

The method renders large amounts of data. Several locations could be covered at the same time step and could be simultaneously and continuously monitored. Diurnal temperature fluctuations as well as temperature changes over the course of several months can be observed. Snow temperatures and their evolution in different snow depths and in various spots across a site can be monitored.

The fiber-optic cables, along which temperatures are measured, are relatively cheap and can be used several times. They are insensitive against the cold temperatures and cable claddings protect the fibers against water influences. The cables can be installed at a site at any time before measuring and can remain in the study field between distinct measurement sessions.

The fact that temperatures are measured along a cable leaves a lot of room for different experimental set-ups. Cables can be laid out across snow or terrain at any desired geometry, as long as bend radii smaller than 2.5 cm are avoided. It is possible to deploy only parts of a cable for one measurement session and to keep the rest of it in reserve to be laid out later, for example, on a new snow layer after following snowfall events.

Strain stresses, to which the fiber-optic cables could be subjected to in snow packs in avalanche prone terrain, can cause step losses, which may lead to erroneous measurements and to increased data noise. Overstuffed cables that are more strain resistant are available, though protection is only provided to an elongation of about 1 %. When strain stresses on the fiber-optic cable are expected, measurements should be taken in a double-ended mode, which allows the DTS instrument box to automatically correct the temperature output for step losses. The increased data noise, however, also remains with double-ended measurements and would negatively affect data accuracy. The data from Mammoth Mountain was affected by a step loss, which might have caused slightly increased data noise but the measurements still rendered data of a good relative accuracy. The magnitude of strain stresses on fiber-optic cables that were deployed in a slope (of snow or any other material) and according effects on the quality of temperature measurements taken with a DTS system have not been studied so far.

Further, once deployed and before they are snowed in by the next significant snow fall, the cables could be dislocated by strong winds, which are also very likely to occur in avalanche prone terrain.

Instrument boxes are expensive. Models that can operate at low temperatures are available. DTS instruments though are sensitive to condensing environments. Shelter and power supply have to be provided for the instrument boxes, which could prove to be difficult at remote sites in avalanche starting zones. The handling of DTS instruments and DTS systems requires a high level of expertise and experience.

DTS systems are an interesting tool, which is unique in its ability to measure temperatures in a larger number of locations, simultaneously and continuously, over long time periods. Advantages are that the cables are cheap and that they allow flexible experimental designing and redesigning. Disadvantages of the method are, that the instrument boxes are expensive and that experimental design, including calibration, quality control, data handling and –analysis, require a high level of expertise and experience. Another clear advantage of the method, compared to measurements of temperatures that are based on a large number of different sensors, is that one single instrument measures the temperatures of all spots. Therefore a good comparability in space and in time, between the temperatures measured at the single data points is provided, throughout one measurement session, and also between different measurement sessions if they are based on a good calibration.

Snow temperatures are having a strong influence on a snow cover's stability behavior, though in a very complex manner. Distributed temperature measurements alone cannot allow assessing the distribution of the snow's strength. In combination with other distributed measurements or with physical and numerical snow cover models, however, they could provide further insight in the snow's thermal properties and their dependence on terrain features and on meteorological influences.

This knowledge could allow drawing conclusions about the differences in the evolution of a snow cover's properties (metamorphism) in different locations and could support avalanche researchers, avalanche- safety services and committees and backcountry travelers in their decision making in variable, avalanche prone terrain.

In snow- and avalanche research temperature measurements with this method, could contribute to a better understanding of the variability of snow cover (thermal) properties and how they relate to terrain features and meteorological variables, as well as how they are influenced by interactions of the two.

PART D: REFERENCES AND APENDICES

8. REFERENCES

Adams, J.: Risk, University College London, London, 1995.

Bartelt, P., Lehning, M.: A physical SNOWPACK model for the Swiss avalanche warning, Part I: numerical model, Cold Regions Science and Technology, 35, 3, 123-145, 2002.

Bergmeister, K., Suda,, J., Hübl, J., Rudolf-Miklau, F.: Schutzbauwerke gegen Widlbachgefahren – Grundlagen, Entwurf und Bemessung, Beispiele, Ernst&Sohn – Verlag fuer Architektur und technische Wissenschaften GmbH & Co.KG, Berlin, Germany, 2009.

Birkeland, K.W.: Spatial and Temporal variations in snow stability and snowpack conditions throughout the Bridger Mountains, Montana. Ph. D. thesis, Department of Geography, Arizona State University, 1997.

Birkeland, K.W., Landry, C.C.: Changes in spatial patterns of snow stability through time, Proceedings of the 2002 International Snow Science Workshop, Penticton BC, Canada, 482-490, 2002. http://www.fsavalanche.org/NAC/techPages/articles/02_ISSW_spatial_var_time.pdf

Brun, E., Martin, E., Simon, V., Gendre, C., Coleou, C.: An energy mass model of snow cover suitable for operational avalanche forecasting, Journal of Glaciology, 35 (121), 333-342, 1989.

Brun, E., David, E., Sudul,M., Brunot, G.: A numerical model to simulate snow-cover stratigraphy foroperational avalanche forecasting, Journal of Glaciology (128), 13-22, 1992.

Bründl, M., Rhyner, J., Steiniger, M., Stucki, T., Amman, W.: Recent developments in avalanche risk management in Switzerland, WSL Swiss Federal Institute for Snow and Avalanche Research SLF, Davos, Switzerland, 2003.

Camponovo, C., Schweizer, J.: Rheological measurements of the viscoelastic properties of snow, Ann. Glaciol., 32, 44-50, 2001.

Colbeck, S.C., Jamieson, J.B.: The formation of facetted layers above crusts, Cold Regions Science and Technology, 33 (2-3), 247 – 252, 2001.

Deems, J.S.: Topographic effects on the spatial and temporal patterns of snow temperature gradients in a mountain snow pack, Master Thesis, Montana State University, Bozeman, Montana, 2002.

Durand, Y., Giraud, G., Brun, E., Mérindol, L., Martin, E.: A computer-based system simulating snowpack structures as a tool for regional avalanche forecasting, J. Glaciol., *45*(151), 469–484, 1999.

Freifeld, B.M., Finsterle, S., Onstott, T.C., Toole, P., Pratt, L.M.: Ground surface temperature reconstructions: Using in situ estimates for thermal conductivity acquired with a fiber-optic distributed thermal perturbation sensor, Geophysical Research Letters, Vol. 35, L14309, doi: 10.1029/2008GL034762, 2008.

Gerland, S., Winther, J., Sand, K.: In-situ snow temperature monitoring at an Arctic tundra site: A comparison of manual and automatic measurements, Mem. Nat. Inst. Polar. Res., Spec. Issue, 54, 261-269, 2001.

Gowar, J.: Optical Communication Systems, Second Edition, Prentice Hall International, UK, 1993.

Hägeli, P.T.: Scale Analysis of Avalanche Activity on Persistent Snow pack Weaknesses with Respect to Large-Scale Backcountry Avalanche Forecasting, (Ph.D. Thesis, University of British Columbia), Canada, 2004.

Harvey, S., Zweifel, B.: New Trends of Recreational Avalanche Accidents in Switzerland, WSL Swiss Federal Institute of Snow and Avalanche Research SLF, Davos, Switzerland, 2008.

Henderson, R.D., Day-Lewis, F.D., Harvey, C.F.: Investigation of an aquifer-estuary interaction using wavelet analysis of fiber-optic temperature data, Geophysical Research Letters, Vol. 36, L06403, doi:10.1029/2008GL036926, 2009.

Hendrikx, J., Birkeland, K., Clark, M.: Asessing changes in the spatial variability of the snow pack fracture propagation propensity over time, Cold Regions Science and Technology, 56, 152-160, 2009.

Hoes, O.A.C., Schilperoort, R.P.S., Luxemburg, W.M.J., Clemens, F.H.L.R., van de Giesen, N.C.: Locating illicit connections in storm water sewers using fiber-optic distributed temperature sensing, Water Research, 43 (2009) 5187-5197, 2009.

Hubbart, J., Link, T., Campbell, C., Cobos, D.: Evaluation of a low-cost temperature measurement system for environmental applications, Hydrologic Processes, 19, 1517-1523, 2005.

Hübl,J., Kienholz, H., Loipersberger, A. (Hrsg.): DOMODIS: Dokumentation alpiner Naturereignisse [Documentation of Mountain Disasters], Internationale Forschungsgesellschaft INTERPRAEVENT, Klagenfurt, Austria, 2006.

Inaudi, D.: Application of civil structural monitoring in Europe using fiber optic sensors, Prog. Struct. Engn Mater. 2000; 2: 351-358, 2000.

Inaudi, D., Glisic, B.: Distributed Fiber optic Strain and Temperature Sensing for Structural Health Monitoring, IABMAS'06 The Third Int'l Conference on Bridge Maintenance, Safety and Management, Proto, Portugal, 2006.

Jordan R.: A one-dimensional temperature model for a snowcover, CRREL Spec. Rep., 1991.

Kozak, M.C., Elder, K., Birkeland, K., Chapman, P.: Variability of snow layer hardness by aspect and prediction using meteorological factors, Cold Regions Science and Technology, 37, 357-371, 2003.

Kulterer, K.: Gefahrenzonenplan: Einfluss von Stuetzverbauungen Anhand der Lawinen Hohentratten- und Alpenlahner, Diplomarbeit am Institut fuer Alpine Naturgefahren, in Zusammenarbeit mit dem Forsttechnischen Dienst fuer Wildbach- und Lawinenverbauung, Sektion Kaernten, Austria, 2004.

Lehning, M., Bartelt, P., Brown, R.L., Russi, T., Stöckli, U., Zimmerli, M.: Snowpack Model Calculations for Avalanche Warning based upon a new Network of Weather and Snow Stations, Cold Reg. Sci. Technol*.,* 30, 145-157, 1999.

Lehning, M., Bartelt, P., Brown, B., Fierz, C., Satyawali, P.: A physical SNOWPACK model for the Swiss avalanche warning, Part II: Snow microstructure, Cold Regions Science and Technology, 35, 3, 145-167, 2002a.

Lehning, M., Bartelt, P., Brown, B., Fierz, C.: A physical SNOWPACK model for the Swiss avalanche warning, Part III: meteorological forcing, thin layer formation and evaluation, Cold Regions Science and Technology, 35, 3, 169-184, 2002b.

Lowry, C.S., Walker, J.F., Randall, J.H., Anderson, M.P.: Identifying spatial variability of groundwater discharge in a wetland stream using a distributed temperature sensor, Water Resources Research, Vol. 43, W10408, doi: 10.1029/2007WR006145, 2007.

Lundquist, J.D.: Using inexpensive temperature sensors to monitor the duration and heterogeneity of snow-covered areas in complex terrain, Civil and Environmental Engineering, University of Washington, Seattle, submitted to Water Resources Research, special Measurements Method Issue, 2008.

Lundquist, J.D., Rochford, C.: Distributed temperatures in the snow zone: spatial patterns and innovative measurement techniques, http://faculty.washington.edu/jdlund/home/Lundquist_WSC2007.pdf, 2007.

Landry, C., Birkeland, K., Hansen, K., Borkowski, J., Brown R., Aspinall, R.: Variations in snow strength and stability on uniform slopes, Cold Regions Science and Technology, 39, 205-218, 2004.

Logan, S., Birkeland, K.W., Kronholm, K., Hansen, K.: Cold Regions Science and Technology, 47 (1-2), 148-158, 2007.

Mayr, P.: Weiterentwicklung und Evaluierung Mobiler Messtechnik zur Erfassung von Temperatur- und Festigkeitsentwicklung in der Schneedecke, Diplomarbeit, Universitaet fuer Bodenkultur BOKU, Vienna, 2006.

McClung, D.M.: The Elements of Applied Avalanche Forecasting, Part 1 – The Human Issues, Natural Hazards 25: 111-129, Kluwer Academic Publishers, Netherlands, 2002a.

McClung, D.M.: The Elements of Applied Avalanche Forecasting, Part 2 – The Physical Issues and Rules of Applied Avalanche Forecasting, Natural Hazards 26: 1131-146, Kluwer Academic Publishers, Netherlands, 2002b.

McClung, D., Schaerer, P.: The Avalanche Handbook, The Mountaineers, Seattle, Washington, 1993.

McClung, D., Schweizer J.: Effect of snow temperature on skier triggering of dry snow slab avalanches, 1996. http://www.avalanche.org/~issw/96/art25.html, acessed March 10th 2010.

McClung, D., Schweizer J.: Skier triggering, snow temperatures and the stability index for dry-slab avalanche initiation, Journal of Glaciology, 45 (150), 190-200, 1999.

Mock, C.J., Birkeland, K.W.: Snow Avalanche Climatology of the Western United States Mountain Ranges, Bulletin of the American Meteorological Society, Vol. 81, No. 10, 2000. http://journals.ametsoc.org/doi/abs/10.1175/1520-0477%282000%29081%3C2367%3ASACOTW%3E2.3.CO%3B2, accessed April 12th 2010.

Moffett, K.B., Tyler, S.W., Torgersen, T., Menon, M., Selker, J.S., Gorelick, S.M.: Environmental Science and Technology, Vol. 42, No. 3, 2008.

Mueck, C.: Der Lawinenwinter 2007/2008 – Bilanz und Unfallanalyse, Medieninformation der Tiroler Landesregierung, Amt der Tiroler Landesregierung, Innsbruck, Austria, 2008.

Munter, W.: 3x3 Lawinen – Risikomanagement im Wintersport, Verlag Pohl & Schellhammer, Edition VIVALPIN, Garmisch-Partenkirchen, Germany, 2003.

Peck, D., Seebacher, P.: Distributed Temperature Sensing Using Fiber Optics, Presented to the 2000 Electricity's Engineering Association, Annual Conference, Auckland, New Zealand, 2000.

Powell, D., Klieforth, H.: Weather and Climate, Sierra East – Edge of Great Basin, pp 70 – 93, University of California Pres, Berkley and Los Angeles, California, USA, 2000.

Prokop, A.: The Application of Terrestrial Laser Scanning for Monitoring Natural Hazards. 11th Congress INTERPRAEVENT 2008, 26. - 30. Mai 2008, Dornbirn, Austria, 2008

Prokop, A., Schirmer, M., Rub, M., Lehning, M. Stocker, M.: A comparison of measurement methods: terrestrial laser scanning, tachymetry and snow probing for the determination of the spatial snow-depth distriubtion on slopes. ANN GLACIOL, 49, 210-216, 2008

Rhyner, J.: Lawinenwarnung Schweiz – Komponenten eines bewaehrten Systems, Forum fuer Wissen, 2007, 11-18.

Rudolf-Miklau, F.: Naturgefahren-Management in Oesterreich, Vorsorge – Bewaeltigung – Information, LexisNexis Verlag ARD Orac GmbH & Co KG, Wien, 2009.

Schweizer, J., Jamieson J.B., Schneebeli M.: Snow avalanche formation, Reviews of Geophysics, 41 (4), 1016, doi:10.1029/2002RG000123, 2003.

Schweizer, J., Kronholm, K., Jamieson, J.B., Birkeland, K.W.: Review of spatial variability of snow pack properties and its importance for avalanche formation, Cold Regions Science and Technology, 51(2-3):253-272, 2008.

Selker, J.S., Thevenaz, L., Huwald, H., Mallet, A., Luxembourg, W., van de Giesen, N., Stejskal, M., Zeman, J., Westhoff, M., Parlange, M.B.: Distributed fiber optic temperature sensing for hydrologic systems, Water Resources Research, 42, W12202, doi:10.1029/2006WR005326, 2006.

Smith, G. (Ed.): Sierra East – Edge of the Great Basin, University of California Pres, Berkley and Los Angeles, California, USA, 2000.

Smolen, J.J., van der Spek, A.: Distributed Temperature Sensing, A DTS Primer for Oil & Gas Production, Smolen Associates, Texas, and Shell International Exploration and Production B.V., The Netherlands, 2003.

Techel, F., Pielmeier, C.: Wet snow diurnal evolution and stability assessment. In: Schweizer, J., Van Herwijnen, A. (eds): International Snow Science Workshop. 27. September to 2. October, 2009, Davos, Switzerland, 2009. Proceedings. Bimensdorf, Swiss Federal Institute for Forest, Snow and Landscape Research, 256 – 261, Switzerland, 2009.

Teufelsbauer, H.: Linking laser scanning and snow pack modeling: data processing and visualization, Computers and Geosciences, 35, (7), 1481-1490, 2009.

Tyler, S.W., Selker, J.S., Hausner, M.B., Hatch, C.E., Torgersen, T., Thodal, C.E., Schladow, S.G.: Environmental temperature sensing using Raman spectra DTS fiber-optic methods, Water Resources Research, 45, W00D23, doi: 10.1029/2008WR007052, 2009.

Tyler, S.W., Burak, S.A., McNamara, J.P., Lamontagne, A., Selker, J.S., Dozier, J.: Spatially distributed temperatures at the base of two mountain snow packs measured with fiber-optic sensors, Journal of Glaciology, Vol. 54, No. 187, 2008.

Weir, P.: Snow avalanche management in forested terrain, Land Management Handbook No. 55, Ministry of Forestry of British Columbia, Province of British Columbia, Canada, 2002.

Westhoff, M.C, Savenije, H.H.G., Luxemburg, W.M.J., Stelling, G.S., van de Giesen, N.C., Selker, J.S., Pfister, L., Uhlenbrook, S.: A distributed stream temperature model using high resolution temperature observations, Hydrology and Earth System Sciences, 11, 1469-1480, 2007.

Whitney, S.: The Sierra Nevada – a Sierra Club Naturalists Guide, Sierra Club Books, San Francisco, 1979.

Wiesinger, T.: Schneetemperaturprofile in einer winterlichen Schneedecke, Master Thesis, Formal- und

Naturwissenschaftliche Fakultaet, University of Vienna, Vienna, Austria, 1988.

Whiteman, C.D., Hubbe, J.M., Shaw, J.W.: Evaluation of an inexpensive temperature datalogger for meteorological applications, Journal of Atmospheric and Oceanic Technology, 17, 77-81, 2000.

Yilmaz, G., Karlik, S.E.: A distributed optical fiber sensor for temperature detection in power cables, Sensors and Actuators, A 125 (2006) 148-155, 2005.

http://www.avalanche-center.org/Incidents/statistics/, accessed March 29th 2010

www.agilent.com, accessed May 10th 2010

http://www.bergrettung.at/uploads/media/LawinenAnalyse2004-05.pdf, accessed March 30th 2010

www.erstespur.de, accessed March 21st 2010

http://www.fos-s.be, accessed May 15th 2010

1. http://www.fos-s.be/website/foss/assets/files/productdownloads/distributed_temperature_system_dts.pdf, accessed May 10th 2010

http://imgi.uibk.ac.at/iceclim/snowmodelling, accessed April 20th 2010

http://lawine.tirol.gv.at/uploads/media/05_Die_Arbeit_der_Lawinenkommissionen.PDF, accessed April 1st 2010

http://www.lios-tech.com, accessed May 10th 2010

http://www.nasa.gov/pdf/186123main_SnowPitProcedures.pdf, accessed April 20th 2010

http://www.noezsv.at/wastun/schneechaos_lawinen/schutz_vor_lawinen.htm, accessed March 30th 2010

http://www.slf.ch:

1. http://www.slf.ch/forschung_entwicklung/lawinen/lawinenschutz, accessed March 29th 2010
2. http://www.slf.ch/forschung_entwicklung/risikomanagement/warn_informationssysteme/index_DE?-C=&, accessed March 29th 2010
3. http://www.slf.ch/forschung_entwicklung/lawinen/entstehung/projekte/schneedeckenstabilitaet/index_DE?duration=&start=0&person=&topicid=&, accessed March 21st 2010
4. http://www.slf.ch/praevention/lawinenunfaelle/index_DE, accessed May 10th, 2010
5. www.slf.ch/lawineninfo, accessed March 19th 2010

http://salzburg.orf.at/stories/429882/, accessed March 30th 2010 www.sensornet.co.uk:

1. http://www.sensornet.co.uk/technology/distributed-temperature-sensing/, accessed May 10th 2010

http://www.sensornet.co.uk/technology/distributed-temperature-sensing/sentinel-dts-range, accessed May 16th, 2010

www.sensortran.com, accessed May 10th 2010

www.tec21.ch/pdf_anzeigen.php?pdf=tec21_0820063199.pdf, accessed March 29th 2010

http://www.tourismuspresse.at/presseaussendung/TPT_20071213_TPT0005t, accessed March 30th 2010

9. APPENDICES

9.1 APPENDIX A – Matlab Routines for DTS Data

Parsing together ddf. – files, derived from double-ended measurements that include the DTS temperature information:

```
function DEParseDDF(dirname,Dstart,Dstop,outfile)
% SEParseDDF: "Double-Ended Parse DDF (files)" function to Parse the
files
%              created by DTS (Distributed Temperature Sensor).
%
% USAGE: DEParseDDF(dirname,Dstart,Dstop,outfile) where
%        dirname = name and path of directory containing DDF files
%            (make sure to include the trailing '\' (windows) or '/'
(mac))
%        Dstart = begin (in meters)
%        Dstop = and end, or min and max points on the DTS trace to be
%            processed
%        DayOffset = from DTS time to local time in decimal days
%        outfile = output filename
%
% Example: DEParseDDF('ddf_files/',0,2016,'DTS_Trial.mat')
%
% INPUTS: (variables) dirname,Dstart,Dstop,outfile
%         (files)   *.ddf
%         (functions)   SEReadDDF.m
%
% OUTPUT: (file) outfile.mat, containing the following (variables):
%           datetime = date and time of each measurement
%           distance = measurement points along fiber (in meters)
%           tempC = temperature of fiber (degrees C)
%           Stokes = raw Stokes (dimensionless) amplitude along fiber
%           AntiStokes = raw AntiStokes (dimensionless) amplitude
%           Stokes2 = raw Stokes amplitude for reverse data
%           AntiStokes2 = raw AntiStokes amplitude for reverse data
%
% VERSION NOTES:
%        1. (9/16/2007):  Designed to read Single-Ended Measurements
from
%             a Sensornet Sentinel (or Halo) DTS
%        2. (9/16/2007):  function DEReadDDF is called as part of
function
%        3. (7/22/2008):  dirname and Distances=[Dstart Dstop] are
included
%           in the call so that program is generic.  An output filename
is
```

```
%           added so that multiple runs can be processed in the same
dir.
%
% WRITTEN BY:  Scott Tyler, 9/16/2007
% LAST REVISED BY:  Christine Hatch, 8/11/2008
%
Distances=[Dstart Dstop]; % distances where measurements are valid;
% dirname='ddf_files/';  % can enter path manually here
files=dir(dirname); % the first 2 file names are . and .. so delete
files(1:2)=[];
nf=length(files);
ktime=0;
DayOffset=0; % Use this if measurements were not taken in the correct
time
for f=1:nf   % only apply to .ddf files in the folder
    ddf=strfind(files(f).name,'.ddf');
    if ~isempty(ddf)
        ktime=ktime+1;
        [t,d,T,S,A,SR,ASR]=DEReadDDF([dirname
files(f).name],DayOffset,Distances);
        datetime(ktime)=t;
        datestr(t)
        if ktime==1
            fdist=d;
        elseif ~isequal(fdist,d)
            error('distance vector d not same as first distance
vector')
        end
        tempC(:,ktime)=T;
        Stokes(:,ktime)=S;
        AntiStokes(:,ktime)=A;
        StokesR(:,ktime)=SR;
        AntiStokesR(:,ktime)=ASR;
    end
end
distance=d;
if ~issorted(datetime)
    warning('datetime not sorted - can fix this but let me know if it
happens')
end
saveline=strcat(['save ',outfile,' datetime distance tempC Stokes
AntiStokes StokesR AntiStokesR']);
eval(saveline);
```

Subroutine called by the preceding routine (DEParseDDF) - reading the ddf. – files into MatLab:

```
% DEReadDDF: "Double-Ended Read DDF (files)" function to Read the files
%              created by DTS (Distributed Temperature Sensor).
%
% USAGE: Called internally by DEParseDDF
%
% Example: [t,d,T,S,A,SR,ASR]=DEReadDDF([dirname
files(f).name],DayOffset,Distances);
%
% INPUTS: (variables) filename,DayOffset,Distances
%         (internal variables) t (times), d (distances), T
(temperatures),
%               S (Stokes), A (Anti-Stokes), SR (Stokes reverse), ASR
%               (Anti-Stokes reverse)
%         (files)   *.ddf
%
% OUTPUT: (variables):
%           datetime = serial date number (# decimal days since
1/1/1900)
%           distance = measurement points along fiber (in meters)
%           tempC = temperature of fiber at distances (degrees C)
%           Stokes = raw Stokes (dimensionless) amplitude along fiber
%           AntiStokes = raw AntiStokes (dimensionless) amplitude
%           Stokes2 = raw Stokes amplitude for reverse data
%           AntiStokes2 = raw AntiStokes amplitude for reverse data
%
% VERSION NOTES:
%        1. (9/16/2007):  Designed to read Double-Ended Measurements
from
%           a Sensornet Sentinel DTS
%
% WRITTEN BY:  Scott Tyler, 9/16/2007
% LAST REVISED BY:  Christine Hatch, 8/11/2008

%
function
[datetime,distance,temperature,Stokes,AntiStokes,Stokes2,AntiStokes2]=.
..
    DEReadDDF(filename,DayOffset,Distances)
%
fid=fopen(filename,'r');
C=textscan(fid,'%s','BufSize',100000); % read entire file into cell
array
fclose(fid);
%
% date is the string in form yyyy/mm/dd immediately following 'date'
% time is 2 positions after that
k=find(strcmp(C{1,1}(:),'date'));
if isempty(k)
    error('date not in file')
end
d=C{1,1}(k+1);
t=C{1,1}(k+3);
%
% convert date to serial date number
```

```
dv=datevec([datestr(datenum(char(d),'yyyy/mm/dd'),1) ' ' char(t)]);
DN=datenum(dv);
datetime=DN+DayOffset;
%
% find the beginning of the actual data, following 'anti-Stokes'
heading
k=find(strcmp(C{1,1}(:),'anti-Stokes'));
if isempty(k)
    error('anti-Stokes heading not in file')
end
% find the beginning of the actual data, following 'reverse anti-
Stokes' heading
junk=find(strcmp(C{1,1}(:),'anti-Stokes'));
k=junk(end);
if isempty(k)
    error('second anti-Stokes heading not in file')
end
% convert the actual measurements from strings to numbers
x=str2double(C{1,1}(k+1:end));
% convert to a matrix, where column 1 is distance, 2 is temp, 3&4 are
% Stokes and anti-Stokes
lcheck=length(x)
if mod(length(x),6)~=0
    error('number of measurements should be divisible by 6, check
file')
end
y=reshape(x,6,length(x)/6);
y=y';
distance=y(:,1);
t=distance>=min(Distances) & distance<=max(Distances);
y(~t,:)=[];
distance=y(:,1);
temperature=y(:,2);
Stokes=y(:,3);
AntiStokes=y(:,4);
Stokes2 = y(:,5);
AntiStokes2 = y(:,6);
```

9.2 APPENDIX B – Configuration Files

Configuration files of two measurement days during the February session:

A new configuration file was created automatically by the instrument box for each day of measuring.

February 2nd, 2009

```
DTS Sentinel unit serial number:  SN308033
Multiplexer serial number:  multiplexer serial number
Hardware model number: HL4
Software version number:    Halo DTS v1.0
internal lead length   585.78
gamma 512.80
default diff loss term 0.42
default (ngS + ngR)/2  1.47700
default (ngA + ngR)/2  1.47740
offset reference start -541.00
offset reference stop  -138.00
internal reference start    -37.00
internal reference stop     -4.00
assumed T internal     25.00
installation     mmsa
comments   04/02/09 2coils in bag with snow buried for calibration Jeff
Dozier laid out a coil on 02/04/09
save data   1
repetition time (s)    300
continuous  1
number of repetitions  1
number of channels     4
CHANNEL:   channel 2 reverse
channel active    1
range in points   1304
sample length     2.0292
moving average in points    1
Stokes length correction    1.00000
range 5002.604345030051260000000000000000000
temperature offset calculation    0
fixed T offset calibration value  1.0000
offset reference type  0
offset reference start (m)  0.00
offset reference stop (m)   0.00
offset temperature source   0
fixed temperature for offset0.00
temperature slope calculation     0
fixed T slope calibration value   1.0000
temperature slope calculation     0
first slope reference start 0.00
first slope reference stop  0.00
first slope ref temperature source      0
```

```
first slope ref fixed temperature 0.00
second slope reference type 0
second slope reference start0.00
second slope reference stop 0.00
second slope ref temperature source    0
second slope ref fixed temperature     0.00
differential loss correction1
paired channel   1
direction  1
fibre end point  2009.28
spatial averaging (m) 2.0291895085961826300000000000000000
measurement time (s)   150
number of zones  0
CHANNEL:   channel 2
channel active   1
range in points  1304
sample length    2.0292
moving average in points    1
Stokes length correction    1.00000
range 2060.2795575655864000000000000000000
temperature offset calculation    0
fixed T offset calibration value  0.9788
offset reference type  1
offset reference start (m)  972.63
offset reference stop (m)   1029.45
offset temperature source   0
fixed temperature for offset-1.40
temperature slope calculation     0
fixed T slope calibration value   1.0000
temperature slope calculation     0
first slope reference start 0.00
first slope reference stop  0.00
first slope ref temperature source     0
first slope ref fixed temperature 0.00
second slope reference type 0
second slope reference start0.00
second slope reference stop 0.00
second slope ref temperature source    0
second slope ref fixed temperature     0.00
differential loss correction1
paired channel   0
direction  0
fibre end point  2009.28
spatial averaging (m) 2.0291895085961826300000000000000000
measurement time (s)   150
number of zones  0
CHANNEL:   channel 3
channel active   0
range in points  2754
sample length    2.0292
moving average in points    1
Stokes length correction    1.00000
range 5002.6043450300512600000000000000000
temperature offset calculation    0
fixed T offset calibration value  1.0000
offset reference type  0
offset reference start (m)  0.00
offset reference stop (m)   0.00
offset temperature source   0
fixed temperature for offset0.00
```

```
temperature slope calculation     0
fixed T slope calibration value   1.0000
temperature slope calculation     0
first slope reference start 0.00
first slope reference stop  0.00
first slope ref temperature source      0
first slope ref fixed temperature 0.00
second slope reference type 0
second slope reference start0.00
second slope reference stop 0.00
second slope ref temperature source     0
second slope ref fixed temperature      0.00
differential loss correction0
paired channel   4
direction  0
fibre end point  NaN
spatial averaging (m)  2.029189508596182630000000000000000
measurement time (s)   10
number of zones  0
CHANNEL:   channel 4
channel active   0
range in points  2754
sample length    2.0292
moving average in points     1
Stokes length correction    1.00000
range 5002.604345030051260000000000000000000
temperature offset calculation    0
fixed T offset calibration value  1.0000
offset reference type  0
offset reference start (m)  0.00
offset reference stop (m)   0.00
offset temperature source   0
fixed temperature for offset0.00
temperature slope calculation     0
fixed T slope calibration value   1.0000
temperature slope calculation     0
first slope reference start 0.00
first slope reference stop  0.00
first slope ref temperature source      0
first slope ref fixed temperature 0.00
second slope reference type 0
second slope reference start0.00
second slope reference stop 0.00
second slope ref temperature source     0
second slope ref fixed temperature      0.00
differential loss correction0
paired channel   4
direction  0
fibre end point  NaN
spatial averaging (m)  2.029189508596182630000000000000000
measurement time (s)   10
number of zones  0
```

February 20th, 2009

```
DTS Sentinel unit serial number:  SN308033
Multiplexer serial number:  multiplexer serial number
Hardware model number: HL4
Software version number:    Halo DTS v1.0
internal lead length  585.78
gamma 512.80
default diff loss term 0.42
default (ngS + ngR)/2  1.47700
default (ngA + ngR)/2  1.47740
offset reference start -541.00
offset reference stop  -138.00
internal reference start    -37.00
internal reference stop     -4.00
assumed T internal    25.00
installation     mmsa
comments   04/02/09 2coils in bag with snow buried for calibration Jeff
Dozier laid out a coil on 02/04/09
save data   1
repetition time (s)    300
continuous 1
number of repetitions  1
number of channels     4
CHANNEL:   channel 2 reverse
channel active    1
range in points  1304
sample length    2.0292
moving average in points     1
Stokes length correction     1.00000
range 5002.60434503005126000000000000000000000
temperature offset calculation     0
fixed T offset calibration value  1.0000
offset reference type  0
offset reference start (m)  0.00
offset reference stop (m)   0.00
offset temperature source   0
fixed temperature for offset0.00
temperature slope calculation     0
fixed T slope calibration value   1.0000
temperature slope calculation     0
first slope reference start 0.00
first slope reference stop  0.00
first slope ref temperature source      0
first slope ref fixed temperature 0.00
second slope reference type 0
second slope reference start0.00
second slope reference stop 0.00
second slope ref temperature source     0
second slope ref fixed temperature      0.00
differential loss correction1
paired channel   1
direction   1
fibre end point  2009.28
spatial averaging (m)  2.02918950859618263000000000000000000
measurement time (s)   150
number of zones  0
CHANNEL:   channel 2
```

```
channel active   1
range in points  1304
sample length    2.0292
moving average in points    1
Stokes length correction    1.00000
range 2060.279557565586400000000000000000
temperature offset calculation    0
fixed T offset calibration value  0.9788
offset reference type  1
offset reference start (m)  972.63
offset reference stop (m)   1029.45
offset temperature source   0
fixed temperature for offset-1.40
temperature slope calculation     0
fixed T slope calibration value   1.0000
temperature slope calculation     0
first slope reference start 0.00
first slope reference stop  0.00
first slope ref temperature source     0
first slope ref fixed temperature 0.00
second slope reference type 0
second slope reference start0.00
second slope reference stop 0.00
second slope ref temperature source    0
second slope ref fixed temperature     0.00
differential loss correction1
paired channel   0
direction  0
fibre end point  2009.28
spatial averaging (m)  2.029189508596182630000000000000000
measurement time (s)   150
number of zones  0
CHANNEL:   channel 3
channel active   0
range in points  2754
sample length    2.0292
moving average in points    1
Stokes length correction    1.00000
range 5002.604345030051260000000000000000
temperature offset calculation    0
fixed T offset calibration value  1.0000
offset reference type  0
offset reference start (m)  0.00
offset reference stop (m)   0.00
offset temperature source   0
fixed temperature for offset0.00
temperature slope calculation     0
fixed T slope calibration value   1.0000
temperature slope calculation     0
first slope reference start 0.00
first slope reference stop  0.00
first slope ref temperature source     0
first slope ref fixed temperature 0.00
second slope reference type 0
second slope reference start0.00
second slope reference stop 0.00
second slope ref temperature source    0
second slope ref fixed temperature     0.00
differential loss correction0
paired channel   4
```

```
direction	0
fibre end point	NaN
spatial averaging (m)	2.029189508596182630000000000000000
measurement time (s)	10
number of zones	0
CHANNEL:	channel 4
channel active	0
range in points	2754
sample length	2.0292
moving average in points	1
Stokes length correction	1.00000
range	5002.604345030051260000000000000000
temperature offset calculation	0
fixed T offset calibration value	1.0000
offset reference type	0
offset reference start (m)	0.00
offset reference stop (m)	0.00
offset temperature source	0
fixed temperature for offset0.00
temperature slope calculation	0
fixed T slope calibration value	1.0000
temperature slope calculation	0
first slope reference start	0.00
first slope reference stop	0.00
first slope ref temperature source	0
first slope ref fixed temperature	0.00
second slope reference type	0
second slope reference start0.00
second slope reference stop	0.00
second slope ref temperature source	0
second slope ref fixed temperature	0.00
differential loss correction0
paired channel	4
direction	0
fibre end point	NaN
spatial averaging (m)	2.029189508596182630000000000000000
measurement time (s)	10
number of zones	0
```

9.3 APPENDIX C – Instrument and Cable Examples

HALO-DTS – DATA SHEET

The Halo-DTS is Sensornet's revolutionary DTS system that sets new standards in value and performance.

For industrial monitoring applications where reliability, safety and seamless system integration are essential, the compact, low-power, user friendly Halo-DTS is the ideal solution to close your monitoring gap. The system features an inbuilt multiplexing module (with either 2 or 4 channels) enabling up to 4 single ended measurements or 2 double-ended measurements. User configurable zones and alarms functionality are also available for a wide variety of applications. The system is packaged in a standalone unit which contains both the sensing optoelectronics and an onboard PC. The system operates with an intuitive software interface (based on Windows OS), making it a simple-to-use system. The system has been designed with safety in mind and has been tested to some of the industry's most rigorous standards.

Summary of sensing capabilities			
RANGE	CHANNELS	TEMPERATURE RESOLUTION	SAMPLING RESOLUTION
0-4km	2 or 4	See reverse	2m

Operating environment		
OPERATING TEMPERATURE	STORAGE TEMPERATURE	HUMIDITY
0˚C to +40˚C	-15˚C to +65˚C	5% to 95% relative humidity, non-condensing

Power requirements		
AC POWER	DC POWER	POWER CONSUMPTION
100V - 240V, 50Hz - 60Hz	24V or 48V supply option available	40W - 50W maximum

Certification & compliance		
SAFETY	EMC	CE MARK
The Halo DTS has been independently classified to EN 60825-1 (2001-03) as a Class 1M laser product. The DTS (1mW mean power output) is suitable to monitor Zone 0 Hazardous areas according to the European Commission report no. EUR 16011 EN (1994).	EN61326:1997/A1:1998; Conducted Emissions: Class B; Radiated Emissions: Class A**; EN 61000-4-3:1996; EN 61000-4-6:1996; EN 61000-4-4:1995; EN 61000-4-2:1995/A1:1998/A2:2001; EN 61000-4-11:1994; EN 61000-4-5:1995; EN 61000-3-2:1995; EN 61000-3-2:2000; EN 61000-3-3:1995 ** Excluding monitor and keyboard	Accordance with 89/336 EEC EMC Directive Accordance with LVD 72/23 EEC Directive: EN 41003; EN 50178; EN 60065; EN 60825-1; EN 60950; EN 61010-1

Physical dimensions*			
HEIGHT	WIDTH	DEPTH	WEIGHT
87mm (3.4 inches)	435mm (17.1 inches)	445mm (17.3 inches)	9kg (22lb)

*Fits in standard 19 inch rack mounting.

All details are subject to change.

sensornet
Part of the TENDEKA family

T: +44 (0)20 8236 2550
E: enquries@sensornet.co.uk
W: www.sensornet.co.uk

HALO-DTS – DATA SHEET

PRODUCT CAPABILITIES

The Halo DTS offers the most advanced performance and reliable monitoring solution available today.

With Sensornet DTS systems (as with all DTS systems) there is a trade off between temperature resolution, spatial resolution, range and speed of measurement (eg. the more time you allow the DTS to acquire data, the better the temperature resolution).

Using the intuitive calibration wizard the user is able to define the required spatial resolution, measurement time and range – and this will define temperature resolution achieved with the system. The following graph illustrates the temperature resolution achieved for the Halo DTS. The graph shows the measurement times of 15 seconds, 1 minute, 5 minutes, 15 minutes and 60 minutes.

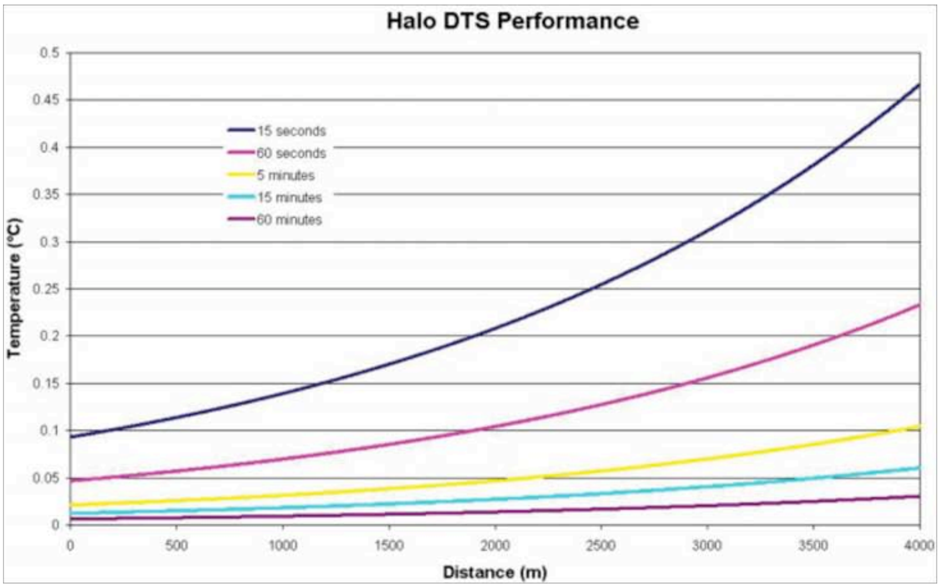

Halo DTS

Communication options available

The Halo DTS has various communication options available:

- Ethernet
- Volt free relay contacts
- OPC
- Modbus
- RS-232

Data storage is onboard. The user is able to copy data to external USB drive. Please contact a Sensornet representative for more information.

BE SURE WITH SENSORNET

Sensornet offers the widest range of DTS to meet your every monitoring requirement, specific to any need, environment and challenge.

You can rely on us to provide the full solution - from system engineering and design, to installation, data interpretation services and global support services. We'll take the time to fully understand your business goals and the unique context and physical circumstances of your asset to provide the best solution to you.

T: +44 (0)20 8236 2550
E: enquries@sensornet.co.uk
W: www.sensornet.co.uk

sensornet
Part of the TENDEKA family

BE THERE

ORYX DTS – DATA SHEET

A POWERFUL REMOTE LOGGING DTS UNIT

The Oryx DTS offers the most advanced and reliable solution for monitoring harsh and remote environments.

The Oryx DTS is a compact Distributed Temperature Sensing (DTS) system designed for harsh environments ideal for monitoring applications from desert to sub-zero conditions.

The Oryx is an autonomous, low powered device allowing the system to be powered by solar or wind power. Combined with satellite, radio link, or fibre communications the Oryx becomes a powerful remote logging DTS unit.

1 Oryx DTS
2 Oryx inside enclosure
3 Oryx with ruggedised laptop

Features	Benefits
• High performance	Industry leading temperature resolution enables accurate data collection
• Wide operating temperature range of -40 to +65°C	Designed for outdoor installation from desert to sub-zero conditions.
• Remote operation	Cost effective as there is no need to be at DTS site for set-up, configuration, updates, or data access.
• Server based data collector and processor	Simple and intuitive user interface provides base-station set-up, communications options for multiple Oryx installations and data visualisation. Proven industrial standard software ensures reliable and continuous operation.
• Non-volatile on-board memory	Ensures high quantity of measurements can be taken. Ideal for "drive-by" collection of data where a communications system would be cost prohibitive. Data stored on-board in event of communications/power failure.
• Ultra low power requirements (12-24V DC)	Enables solar panel / wind power operation. Cost effective performance.
• Optional housing enclosure (IP66 (NEMA 4) or higher)	Weather and dust proof for cost effective deployment.

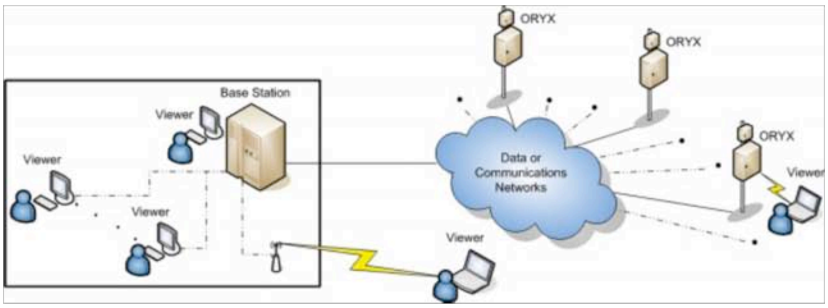

Oryx system setup

sensornet
Part of the TENDEKA family

T: +44 (0)20 8236 2550
E: enquries@sensornet.co.uk
W: www.sensornet.co.uk

ORYX DTS – DATA SHEET

Summary of sensing capabilities

Range	*Channels*	*Temperature resolution*	*Sampling resolution*
0-5 km	2 or 4	See below	1m

Power requirements

Supply	*Power consumption*
Runs on 12 – 24V DC	0.5W stand-by; 18W operating

Communication options

The Oryx DTS is compatible with a wide range of communications options:

- Satellite / Wireless modem
- GSM Modem
- Radio Link
- Direct link to PCs/Laptops
- Serial RS-232
- Wired Ethernet

Certification and compliance

Classified to EN 60825-1 (2007) as a Class 1M laser product.
CE compliant.

BS EN61010-1:2001
BS EN61326-1:2006
BS EN55022:1998
BS EN61000-4-3:2006
FCC CFR47 pt15 (USA)
ICES-003 (Canada)

Performance specifications

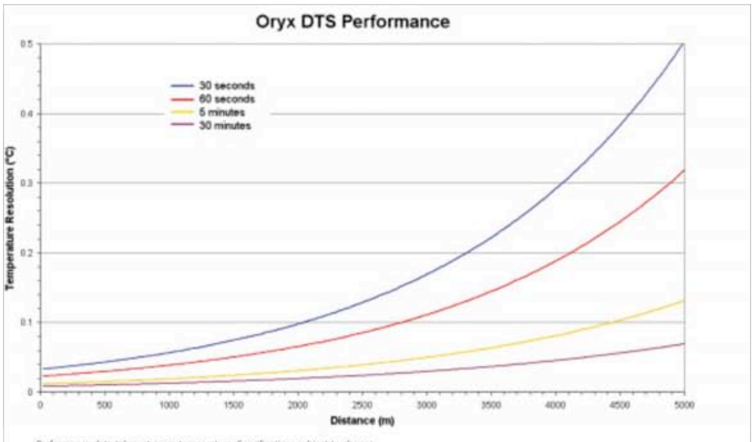

Performance data taken at room temperature. Specifications subject to change.

BE SURE WITH SENSORNET

Sensornet offers the widest range of DTS to meet your every monitoring requirement, specific to any need, environment and challenge.

You can rely on us to provide the full solution - from system engineering and design, to installation, data interpretation services and global support services. We'll take the time to fully understand your business goals and the unique context and physical circumstances of your asset to provide the best solution to you.

T: +44 (0)20 8236 2550
E: enquries@sensornet.co.uk
W: www.sensornet.co.uk

sensornet
Part of the TENDEKA family

BE THERE

SENTINEL DTS™ – DATA SHEET DTS-SR, MR, LR & XR

INDUSTRY LEADING PERFORMANCE

The Sentinel DTS™ is the most technologically advanced distributed temperature sensing system today.

The Sentinel range of DTS units, lead the way in terms of performance in DTS technology, with temperature resolutions as fine as 0.004°C achieved in the field, the fastest measurement speeds available and the greatest coverage of up to 30km from a single channel. The self contained Sentinel DTS surface system operates with an intuitive user interface allowing fast and simple calibration and configuration. The system has been designed with safety in mind and has been tested to some of the industry's most rigorous standards.

Features	Benefits
• High performance	Industry leading temperature resolution as fine as 0.004°C enables interpretation in the most difficult applications.
• Fine spatial resolution	1m spatial resolution allows accurate location of changing temperature events.
• Fast measurement speed	Measurements as short as 10 seconds to enable real time monitoring of transient events, particularly in safety critical applications.
• Intuitive configuration	Intuitive user interface allowing fast and simple calibration and configuration. Double-ended calibration through use of a multiplexer.
• Multiple channels	2, 4, 8 and 16 channel multiplexer modules available to increase system flexibility.
• Alarms functionality	User configurable zones and alarms available to tie in to SCADA systems. MODBUS/OPC/WITSML data formats. Relay contact module also available.
• Remote operation	System can be configured and operated remotely through its Ethernet interface.

Summary of sensing capabilities

Range	*Sentinel DTS Model*	*Description*	*Temperature Resolution**	*Spatial Resolution*	*Sampling Resolution*
0 – 5km	Sentinel DTS-SR	Short Range	<0.01°C	1m	0.5m
0 – 8km	Sentinel DTS-MR	Medium Range	<0.01°C	1m	0.5m
0 – 10km	Sentinel DTS-LR	Long Range	<0.01°C	1m	0.5m
0 – 30km	Sentinel DTS-XR	Extreme Range	<0.05°C	1m (<20km) 2m (>20km)	1m (<20km) 2m (>20km)

*Please see following page for more details regarding the capabilities of the Sentinel product range.

Operating environment

Operating Temperature	*Storage Temperature*	*Humidity*
+5°C to +40°C	-15°C to +65°C	5% to 95% relative humidity, non-condensing

Power requirements

AC Power	*DC Power*	*Power Consumption*
100V - 240V, 50Hz - 60Hz	24V or 48V supply option available	120W maximum

Physical dimensions

*H x W x D**	*Weight*
180 x 435 x 480mm (7.1 x 17.1 x 18.9")	21kg (46lb)

*fits in standard 19" rack mounting.

sensornet
Part of the TENDEKA family

T: +44 (0)20 8236 2550
E: enquries@sensornet.co.uk
W: www.sensornet.co.uk

SENTINEL DTS™ – DATA SHEET DTS-SR, MR, LR & XR

Certification & compliance

Safety

The Sentinel DTS has been independently classified to EN 60825-1 (2001-03) as a Class 1M laser product. The DTS (1mW mean power output) is suitable to monitor Zone 0 Hazardous areas according to the European Commission report no. EUR 16011 EN (1994).

EMC

EN61326:1997/A1:1998; Conducted Emissions: Class B; Radiated Emissions: Class A**; EN 61000-4-3:1996; EN 61000-4-6:1996; EN 61000-4-4:1995; EN 61000-4-2:1995/A1:1998/A2:2001; EN 61000-4-11:1994; EN 61000-4-5:1995; EN 61000-3-2:1995; EN 61000-3-2:2000; EN 61000-3-3:1995 ** Excluding monitor and keyboard

CE Mark

Accordance with 89/336 EEC EMC Directive Accordance with LVD 72/23 EEC Directive: EN 41003; EN 50178; EN 60065; EN 60825-1; EN 60950; EN 61010-1

PRODUCT CAPABILITES

The following graphs illustrate the temperature resolution of each Sentinel DTS with sensing range and measurement time. Further specifications are available from Sensornet on request.

Sentinel DTS-SR Performance

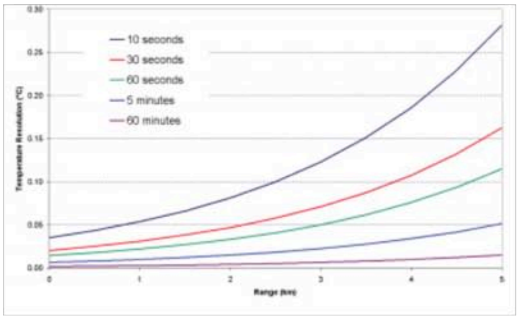

Sentinel DTS-MR Performance

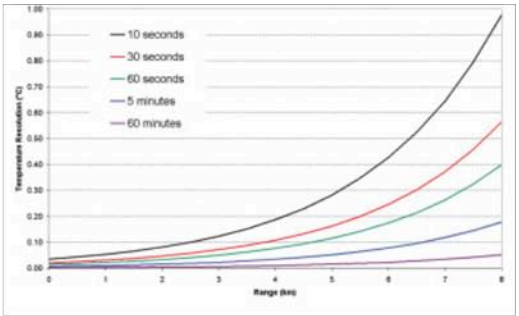

Sentinel DTS-LR Performance

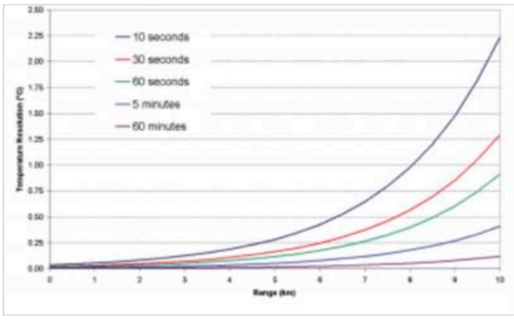

Sentinel DTS-XR Performance

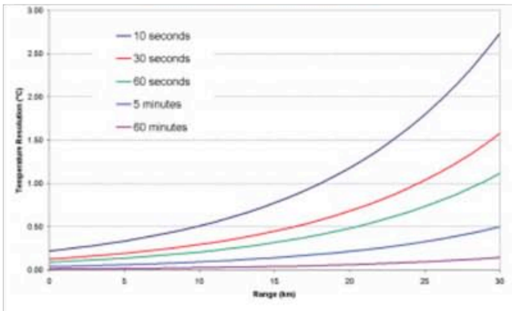

BE SURE WITH SENSORNET

Sensornet offers the widest range of DTS to meet your every monitoring requirement, specific to any need, environment and challenge.

You can rely on us to provide the full solution - from system engineering and design, to installation, data interpretation services, and global support services. We'll take the time to fully understand your business goals and the unique context and physical circumstances of your asset to provide the best solution to you.

T: +44 (0)20 8236 2550
E: enquries@sensornet.co.uk
W: www.sensornet.co.uk

sensornet
Part of the TENDEKA family

BE THERE

Distributed Temperature System DTS

Description

Fast, reliable and cost effective fibre optic temperature sensing for a wide range of indoor and outdoor applications.

- Proven field reliability with industry's lowest maintenance and warranty cost
- Incorporates a hermetically sealed optical block for long life operation
- Only outdoor Distributed Temperature System (DTS) on the market, with the widest operating temperature range and lowest power consumption
- Measurement repeatability throughout the entire operating temperature range
- Remote operation
- Single and dual ended measurement modes for fibre lengths of up to 12km

Temperature over Distance

DTS technology measures a temperature profile along an optical fibre over several kilometres. The DTS system provided from FOS&S, performs measurements down to 1 meter spatial resolution with less than 0,1°C temperature resolution providing thousands of measurement points in a single trace capture. This technology is used in a large range of applications including: power transmission & distribution cable monitoring, pipeline leakage detection and oil well performance monitoring.

The DTS system (indoor and outdoor versions respectively) provide reliable measurements in critical 24/7 monitoring applications. The highly integrated opto-electronic design insures repeatable measurements throughout an extremely wide operating temperature range – enabling worry-free and accurate monitoring!

Permanent monitoring

The instrument design is based on a low power semiconductor laser for maximum life time and a proprietary code correlation concept for high dynamic range and good temperature resolution. Additionally it uses a patent pending single receiver concept, insuring long lasting measurement stability eliminating dual receiver drift effects which could impact the repeatability of the measurement over time.

Fibre Optic Sensing & Sensing Systems – FOS&S
Cipalstraat 14
2440 Geel
BELGIUM

Tel: +32 14 58 11 91
Fax: +32 14 59 15 14
E-mail: sales@fos-s.com
www.fos-s.com

Indoor/Outdoor operation

The industry's largest operating range is enabled by the combination of a highly integrated opto-electric block with a unique fibre reference concept. Laser and detector are temperature stabilised, insuring accurate measurements over the entire temperature range. The components in the heart of the instrument are surrounded by inert gas in a hermetically sealed block, protecting against condensation, dust or moisture – insuring long term operation independent of ambient changes. Additionally the internal reference fibre insures repeatable measurements throughout the largest operating temperature range.

Outdoor installations also benefit from:

- Ultra low power consumption: enables solar panel operation
- Outdoor IP66 (~NEMA 4) housing: weatherproof and watertight
- Transportation & deployment: resistant against highest level of shock and vibrations

Uninterrupted operation

The instrument can be operated remotely as an RTU or online connected to your control room. Regardless your application, the system is independent of the communication infrastructure and continuous monitoring even in cases of network outages, remote locations, and is automatically up and running within 30 seconds after a potential power interruption.
The instrument runs with a proven real time operating system (vxWorks), which is stable and not susceptible to viruses. Additionally it is backed up with a watch dog program.

- LAN interfaces enable remote access with off the self GSM modems
- Open programming interface is fully documented which enables easy integration with customised programs
- No instrument calibration required
- After set up and configuration it continuously measures and logs the traces

Global service & support

Based on more than 20 years of OTDR expertise we have designed the DTS to prevent typical problems encountered in the field. For example, the DTS enclosure allows direct access to the E-2000 fibre optic connectors for replacement if they become damaged or scratched. Replacing a connector is easy and prevents the need to send the instrument back for repair, reducing cost and down time. Additionally, this allows test fibres to be directly spliced to the instrument.

Fibre Optic Sensing & Sensing Systems – FOS&S
Cipalstraat 14
2440 Geel
BELGIUM

Tel: +32 14 58 11 91
Fax: +32 14 59 15 14
E-mail: sales@fos-s.com
www.fos-s.com

FOS&S
Fibre Optic Sensing

Sensing Features

- Compatible with industry standard 50/125 and 62,5/125 multimode optical fibre
- Up to 256 alarm zones, with up to 7 alarm parameters per zone
- Alarm parameters can be set for: maximum; minimum; maximum delta to zone average; minimum delta to zone average and three individual temperature gradients
- Fibre break detection and localisation
- Direct triggering of alarms can be performed with 20 potential-free relay outputs
- DTS Calibration Wizard allows easy calibration of up to 16 fibre segments, accounting for splices, connectors, or variances in fibre characteristics
- Automatic chromatic dispersion correction
- Provides loss trace like an OTDR, easy to understand in dB

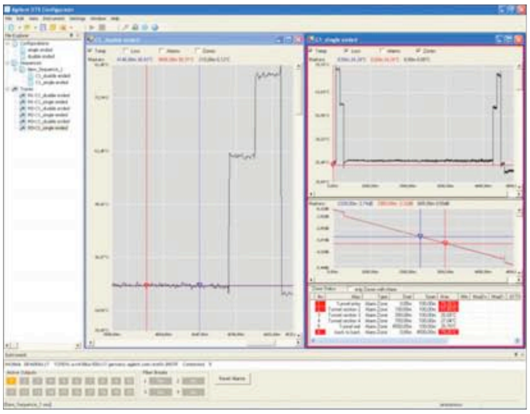

DTS PC software: parameterisation of instrument, visualisation of temperature, loss traces and zone status information.

Dual ended operation mode

A two or four channel DTS offers additionally capability for a dual ended or loop back measurement. It automatically corrects for changes in the Anti-Stokes/Stokes ratio which could result from environmental or mechanical effects (i.e. stress, fibre bends, fusion splices, hydrogen darkening, etc.). This insures accurate temperature measurements over the life of the installed fibre.

Fibre Optic Sensing & Sensing Systems – FOS&S
Cipalstraat 14
2440 Geel
BELGIUM
Tel: +32 14 58 11 91
Fax: +32 14 59 15 14
E-mail: sales@fos-s.com
www.fos-s.com

Temperature Resolution

DTS temperature resolution is a function of several variables including overall measurement distance, spatial resolution setting, and measurement time. Temperature resolution is defined as a standard deviation over distance. Temperature resolution of the DTS instruments:

At various spatial resolution settings | At various measurement timings

2km instrument

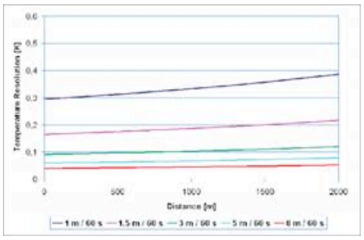

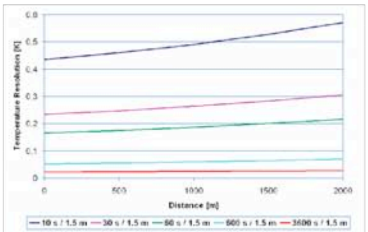

4km instrument

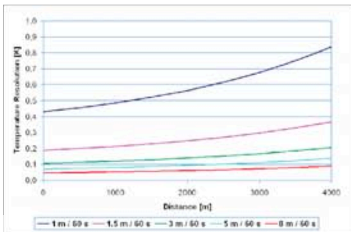

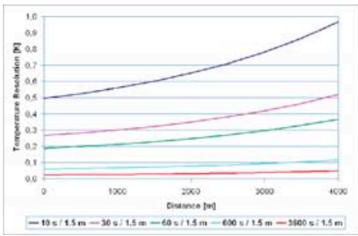

8km instrument

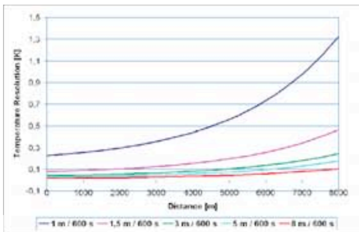

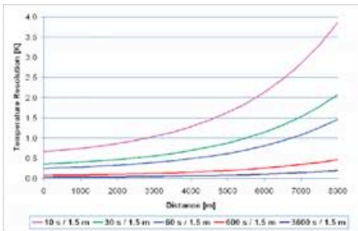

Fibre Optic Sensing & Sensing Systems – FOS&S
Cipalstraat 14
2440 Geel
BELGIUM

Tel: +32 14 58 11 91
Fax: +32 14 59 15 14
E-mail: sales@fos-s.com
www.fos-s.com

12km instrument

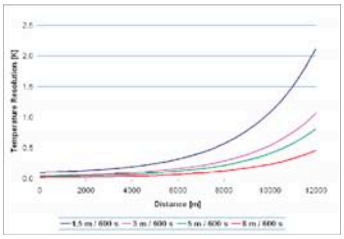

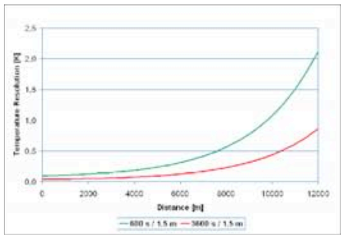

Spatial Resolution

As shown above, the spatial resolution affects the temperature resolution. In some applications, knowing the location of the temperature change can be more critical than resolving the exact temperature. This DTS has excellent spatial resolution as shown in the graph below.

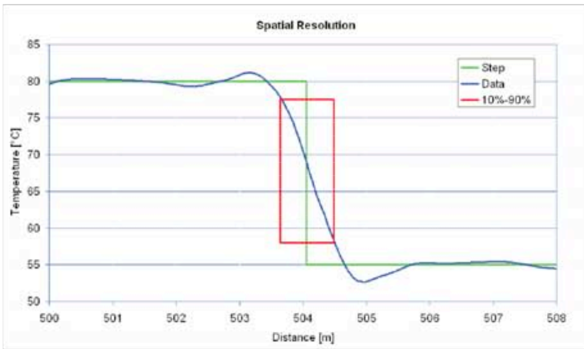

Part of the sensing fibre is at 80°C and part is at 55°C. The temperature step is "resolved" in 0,85m (reflecting 10 to 90% of the actual 25K temperature step).

Fibre Optic Sensing & Sensing Systems – FOS&S
Cipalstraat 14
2440 Geel
BELGIUM

Tel: +32 14 58 11 91
Fax: +32 14 59 15 14
E-mail: sales@fos-s.com
www.fos-s.com

FOS&S
Fibre Optic Sensing

Hot Spot Detection

In some application, the temperature change can be in a very local area. For instance, a localised hot spot could fall well within 1m, the finest spatial resolution setting. As the fibre is a continuous sensor, where no area is unmonitored the DTS system detects even these narrow hot spots as shown in the chart.

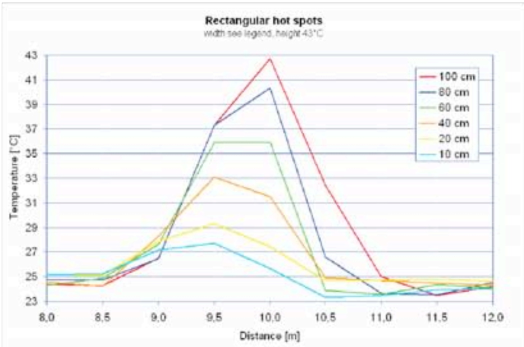

Short pieces of fibre are held into a 43°C hot water bath. Even though the specified spatial resolution is "only 1m" a hot spot of e.g. 10 cm is detected and reflects 12% of the true temperature step, while e.g. 40 cm reflect 45% of the true temperature step.

Measurement stability and repeatability

Measurement repeatability over time and operating conditions is the cornerstone of reliable data collection. Particular attention has been paid to measurement repeatability in the design, manufacturing and testing of the DTS products.

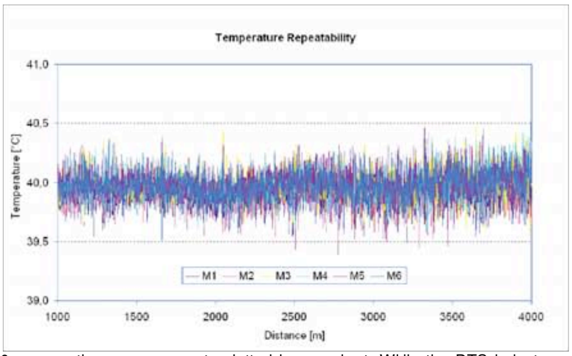

6 consecutive measurements plotted in one chart. While the DTS industry specifies temperature resolution as a "one sigma value" the actual trace has a "peak to peak" noise. The repeatability "filters" out the noise and compares the difference between several measurements.

Fibre Optic Sensing & Sensing Systems – FOS&S
Cipalstraat 14
2440 Geel
BELGIUM
Tel: +32 14 58 11 91
Fax: +32 14 59 15 14
E-mail: sales@fos-s.com
www.fos-s.com

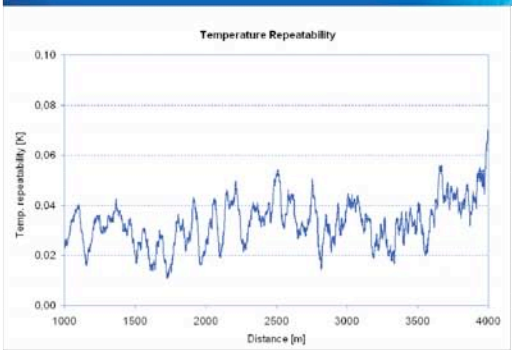

Repeatability of 6 measurements compared to each other. Measurement time 10 min; spatial resolution 1,5 m, curve averaged over 50 m to account for temperature resolution. Specification: 0,10 K temperature repeatability.

Repeatability throughout Operating Temperature Range

As the instrument is exposed to changes in ambient temperature it is crucial for a reliable and worry- free measurement, that the measurement is not only repeatable at constant conditions, but also repeatable throughout the entire operating temperature range. FOS&S is offering the industry's widest operating temperature range with the following repeatability:

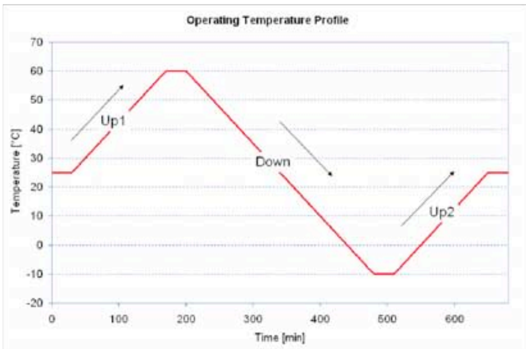

Temperature Cycle: simulated day and night ambient exposure.

Fibre Optic Sensing & Sensing Systems – FOS&S
Cipalstraat 14
2440 Geel
BELGIUM

Tel: +32 14 58 11 91
Fax: +32 14 59 15 14
E-mail: sales@fos-s.com
www.fos-s.com

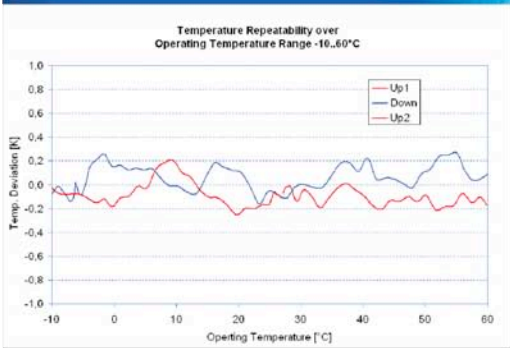

Typical performance of 150 measurements during 12 hour of instrument temperature cycling from -10 to +60°C. Specification: 0,8 K Temperature repeatability through out operating temperature range.

Standard specifications

DTS typical performance specification[1]:	Indoor/Outdoor			
	002	004	008	012
Distance range	2 km	4 km	8 km	12 km
Minimal spatial resolution[2]	< 0.9 m			1.5 m
Minimum sampling interval	0.5 m			1.0 m
Temperature resolution[3] (standard deviation over distance) Measurement time: 10 min Spatial resolution: 1.5 m 1 channel 2 channels 4 channels	Fibre Length 2 km 0.11 K 0.12 K 0.13 K	Fibre Length 4 km 0.15 K 0.16 K 0.17 K	Fibre Length 8 km 0.50 K 0.55 K 0.60 K	Fibre Length 12 km 2.6 K 3.0 K 3.5 K
Temperature repeatability[4] (standard deviation) 1 channel 2 channels 4 channels	 0.10 K 0.11 K 0.12 K			
Temperature repeatability troughout operating temperature range[3] (standard deviation)	0.80 K			
Absolute temperature standard deviation[5]	1.0 K			
Housing & environmental conditions	**Indoor (19'')**		**Outdoor (IP66)**	
Operating temperature range	-10°C to 60°C (2, 4 Channel option: from -5°C)			
Storage temperature range	-40 to 80°C			
Operating humidity range	0% to 95% RH (2, 4 Channel option:: 15% to 85% RH)			

Fibre Optic Sensing & Sensing Systems – FOS&S
Cipalstraat 14
2440 Geel
BELGIUM
Tel: +32 14 58 11 91
Fax: +32 14 59 15 14
E-mail: sales@fos-s.com
www.fos-s.com

FOS&S
Fibre Optic Sensing

	Non condensing	
Max. operating altitude	2000 m (10-30 VDC) 4000 m (10-25 VDC)	
Dimensions (HxWxD)	88x448x364 mm	500x400x150 mm
Weight	9 kg	17 kg

Supplementary information	Indoor/Outdoor
Sensing fibre	
Fibre types	MM 50/125 µm graded index MM 62.5/125 µm graded index
Dynamic range	30 dB (2-way loss)
Sensing temperature range	-273°C to 700°C depending on sensor coating
Interfaces	
Optical connector	E2000; 8° angled
Number of channels	1, 2, 4, depending on channel option
Computer interface	USB, LAN
Relay board (option)	4 input / 20 output
Power rating	10 – 30 VDC (10 – 25 VDC above 2000 m) < 40 W (entire operating conditions)
Other	
Measurement times	From 10 s to 24 h
Available spatial resolution settings	1 m; 1,5 m; 3 m; 5 m; 8 m
Available measurement modes	Single ended Dual ended; incl. fibre break recovery
Internal data storage capability	150 traces total
Power supply (option) operating conditions	0°C to 50°C; non condensing; indoor use only
Recommended calibration period	3 years
Laser class (IEC 60825-1 : 2001)	1 M

[1] For reference fibres J-Fibre "OptiGrade Multimode Fibre 50/125 µm, class 600" (Attenuation: ~0.7 dB/km @ 1300 nm, ~2.4 dB/nm@850 nm; Bandwidth: > 600 MHz·km @ 850 nm & 1300 nm) or equivalent. Fibre within temperature range -5°C to 90°C. Fibre end terminated.

[2]Setting 1 m. First 500 m of the sensing fibre, thereafter add 0.07 m/km to account for chromatic dispersion effects of the sensing fibre. Single ended measurement mode.

[3]Spatial resolution setting: 1.5 m; measurement time: 10 min; intermediate trace update time: 30s. Above 90°C sensing fibre temperature add 0.15%K to temperature resolution value. Sensing fibre spliced to instrument, to remove connector temperature dependency. Single ended measurement mode.

[4] Measurement time: 10 min; curve averaged over 50 m.

[5] After calibration of the sensing fibre at +20°C and +65°C. Average over first 50 m of the sensing fibre.

Fibre Optic Sensing & Sensing Systems – FOS&S
Cipalstraat 14
2440 Geel
BELGIUM

Tel: +32 14 58 11 91
Fax: +32 14 59 15 14
E-mail: sales@fos-s.com
www.fos-s.com

DTS power consumption over operating conditions

Operating Temperature	Power rating
-10°C	16W
0°C	15W
20°C	17W
40°C	25W
60°C	28W

Laser Safety Information

All laser sources comply with 21 CFR 1040.10 except for deviations pursuant to Laser Notice No. 50. Dated 2001 July 26.

Ordering information

Part Number	Description
DTS Indoor	Indoor Distributed Temperature System
DTS Outdoor	Outdoor Distributed Temperature System

Fibre Optic Sensing & Sensing Systems – FOS&S
Cipalstraat 14
2440 Geel
BELGIUM
Tel: +32 14 58 11 91
Fax: +32 14 59 15 14
E-mail: sales@fos-s.com
www.fos-s.com

AFL Telecommunications
A Fujikura Business

Fiber Optic Cable

Flat Drop Cable

Designed for quick installation and ease in handling, AFL Flat-Span Drop Cable serves as the last link for the FTTx networks of today. The design is constructed utilizing proven buffer tube technology with a single tube containing up to twelve fibers. Two diametrically opposed dielectric rods are placed alongside the buffer tube to provide the mechanical properties of the cable. The finished product, with its compact flat profile, acts as a self-supporting aerial solution for those last mile drops to the customer's home or office.

Cable Components

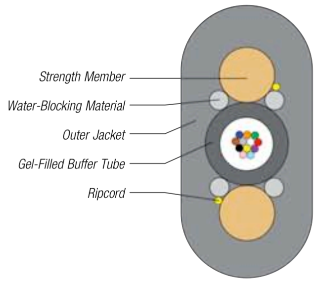

Typical Lengths

REEL SIZE	MAXIMUM LENGTHS (Single-mode)	
	FEET	METERS
30" x 12"	4300	1300
24" x 12"	2600	800

Fiber Information

FIBER TYPE	MAXIMUM ATTENUATION (dB/km)	
	1310nm	1550nm
Single-mode	0.40	0.30

Mechanical Data

PARAMETER	U.S.	METRIC
Fiber Count (max.)	12	12
Cable Dimensions:	.20" x .33"	5.0 mm x 8.5 mm
Linear Weight:	.026 lbs/ft	39 kg/km
Installation Load	300 lbs	1,336 N
Bend Radius, installation	5.9"	15 cm
Bend Radius, post-installation	3.9"	10 cm

Operational/Installation Data

PARAMETER	VALUE		
Operation / Installation Temperature	-40°C to +70°C		
Storage Temperature	-40°C to +75°C		
Loading	NESC		
	Light	Medium	Heavy
Maximum Span Lengths (ft)	400	250	150
Maximum Span Lengths (meters)	122	76	46
Minimum Installation Sag (% of span)	1%	1%	1%

Note: Larger spans can be achieved if necessary with installation sags larger than 1% of span.

www.AFLtele.com or 1.800.235.3423